

Electronic Thesis and Dissertation Repository

9-27-2017 1:00 PM

Meander belt delineation: Developing a predictive model for meander belt width

Julia Howett, *The University of Western Ontario*

Supervisor: Peter Ashmore, *The University of Western Ontario*

A thesis submitted in partial fulfillment of the requirements for the Master of Science degree in Geography

© Julia Howett 2017

Follow this and additional works at: <https://ir.lib.uwo.ca/etd>

Recommended Citation

Howett, Julia, "Meander belt delineation: Developing a predictive model for meander belt width" (2017). *Electronic Thesis and Dissertation Repository*. 4915.
<https://ir.lib.uwo.ca/etd/4915>

This Dissertation/Thesis is brought to you for free and open access by Scholarship@Western. It has been accepted for inclusion in Electronic Thesis and Dissertation Repository by an authorized administrator of Scholarship@Western. For more information, please contact wlsadmin@uwo.ca.

Abstract

The delineation of a meander belt has been recognized in Ontario through land use planning policies as a primary tool for determining the extent a river or stream requires for natural meandering tendencies; thus, providing input to channel restoration projects, development constraints or limits, and regulated areas for species-at-risk. Current delineation procedures utilize site-specific historical migration assessments, or published empirical equations to predict meander belt width. In the case of altered, low order watercourses in southern Ontario, the meander belt width dimension is usually assessed by the application of empirical relations, as the available historic record often lacks the information necessary to conduct meander morphology and migration assessments. There is limited research concerned with the variables controlling meander belt development, and on the precision and reliability of the measurement of belt width. Drawing on a sample population of river reaches in the Credit River watershed, this research project evaluates the current standards of practice for meander belt delineation in southern Ontario, focusing on empirical equations to determine whether the width of the meander belt can be reliably predicted from hydro-geomorphic variables. Results suggest meander belt width is scaled to drainage area, discharge, and bankfull channel width. These results differ from equations commonly used in Ontario assessments suggesting further need for model testing and assessment of the reliability of meander belt width as a planning tool.

Keywords

meander belt width, river corridor management, fluvial geomorphology

Acknowledgements

Above all, thank you to my remarkable research advisor, Dr. Peter Ashmore, for making my Masters experience absolutely incredible, and one which I will always cherish. I am sincerely grateful for your knowledge and constant support and guidance throughout the past two years.

Thank you to Beacon Environmental Ltd. for financially supporting my research. Moreover, thank you Imran Khan for not only educating me with your vast amount of knowledge regarding this research, but also for your friendship and guidance throughout this process.

Thank you to the members of my examination board, Dr. Dan Shrubsole, Dr. Desmond Moser, and Dr. Imtiaz Shah, for your thoughtful discussion and prompt response.

A wholehearted thank you to Lara Middleton for your love, support, and friendship. I doubt I would have made it through this journey without you. Thank you to Sarah Peirce for your support and formatting wizardry. And a big thank you to my other geography mates M. Allen, R. Hilland, C. Irwin, N. Pearce, T. Wiechers. Our weekly intellectual meetings at the GC were integral to my thesis and my Masters experience.

A huge thank you to my parents, Nancy and Peter, for sticking with me through the highs and lows over the last two years, and never turning down the revered opportunity to read through my drafts. Thank you to all my friends and family for their unconditional love and support. You know who you are – I could not have done this without you!

Table of Contents

Abstract	i
Keywords	i
Acknowledgements.....	ii
List of Figures.....	vi
List of Tables	viii
Abbreviations.....	ix
1 Introduction.....	1
2 Review of River Corridor Management and Meandering Channels	3
2.1 General Principles of River Corridor Management.....	3
2.2 Planimetric and Historical Assessment Methods for River Corridor Management	4
2.2.1 Channel Migration Zone.....	5
2.2.2 River Corridor (Vermont).....	6
2.2.3 Freedom Space.....	7
2.3 Limitations of Planimetric and Historical Assessments	8
2.3.1 Summary.....	9
2.4 Meander Belt as a Method of River Corridor Management	10
2.5 Empirically-Based Models for Corridor Prediction.....	14
2.5.1 Limitations of Empirically-Based Models.....	17
2.5.2 Summary.....	18
2.6 Characterization of Meandering Channels.....	19
2.7 Anatomy of Meander Bends	23
2.7.1 Sinuosity	24
2.7.2 Meander Wavelength.....	25
2.7.3 Meander Amplitude	26
2.7.4 Radius of Curvature	27
2.7.5 Limitations of Meander Geometry Measurement.....	27
2.8 Study Rationale and the Case of the Credit River	29
2.9 Research Objectives.....	29
3 Data Sources and the Credit River Watershed.....	31
3.1 The Credit River Watershed	31
3.1.1 Location	31

3.1.2	Physiography.....	33
3.1.3	Hydrology	36
3.1.4	Land Use	40
3.2	Data Sources for Analysis.....	42
3.2.1	Credit River Watershed Orthophotography	43
3.2.2	Credit Valley Conservation Geomorphological Database	43
3.2.3	Credit River Watershed Study Conducted by Aquafor Beech Ltd.	44
3.2.4	Contours.....	44
3.2.5	Provincial Digital Elevation Model	45
3.3	Summary.....	46
4	Site Selection and Measurement of Parameters.....	47
4.1	Site Selection	47
4.1.1	Characteristics of Selected Sites	49
4.2	Field Investigations.....	59
4.3	Desktop Analysis	59
4.3.1	Drainage Area	59
4.3.2	Discharge	61
4.3.3	Other Hydrogeomorphic Parameters Measured or Calculated	61
4.4	Meander Belt Delineation Procedure.....	62
4.4.1	Reach Delineation.....	63
4.4.2	Digitizing Meander Axis.....	64
4.4.3	Digitizing Meander Belt	66
4.5	Summary.....	67
5	Statistical Analysis of Meander Belt Width and Hydrogeomorphic Parameters.....	69
5.1	Correlations Analysis.....	69
5.1.1	Correlations with Meander Belt Width.....	70
5.1.2	Correlations between Hydrogeomorphic Parameters	73
5.2	Regression Analysis Procedures	74
5.2.1	Least Squares Regression	74
5.2.2	Reduced Major Axis Regression	76
5.2.3	Goodness of Fit Statistics.....	77
5.3	Explored relations of meander belt width and hydrogeomorphic variables	78

5.3.1	Mean bankfull channel width.....	78
5.3.2	Discharge	80
5.3.3	Drainage Area	82
5.3.4	Meander Amplitude	84
5.3.5	Discretization of Meander Belt Relations.....	87
5.4	Relations between Hydrogeomorphic Parameters	93
5.4.1	Relations between Drainage Area and Discharge.....	93
5.4.2	Relations with Mean Bankfull Channel Width.....	95
5.4.3	Relations with Meander Amplitude	98
6	Discussion.....	101
6.1	Characteristics of selected watercourses.....	101
6.2	Definition and Measurement of Meander Belt Width	102
6.3	Comparability of Models to Predict Meander Belt Width.....	103
6.3.1	Mean Bankfull Width Relation to Meander Belt Width.....	103
6.3.2	Discharge Relation to Meander Belt Width.....	106
6.3.3	Drainage Area Relation to Meander Belt Width.....	108
6.4	Interpretations	110
6.5	Future Research Perspectives	111
7	Conclusion	113
	References.....	115
	Appendix A – Site Characteristics	120
	Appendix B – Descriptive Statistics for Model Development.....	122
	Appendix C – Field Investigation Form	127
	Appendix D – Correlation Matrix.....	128
	Appendix E – Descriptive Statistics of Regression Analysis	129
	Curriculum Vita	162

List of Figures

Figure 2.1 – Channel migration zone delineation, from Rapp & Abbe (2003).	6
Figure 2.2 – River corridor delineation, adapted from Kline & Dolan (2008).	7
Figure 2.3 – Freedom space delineation, from Biron et al., (2014).	8
Figure 2.4 – Erosion hazard allowances by channel confinement, from MNR (2002).	12
Figure 2.5 – Common features of river meanders, from Hooke (2013).	19
Figure 2.6 – Classification of meander loops, from Brice (1974).	21
Figure 2.7 – Meandering channel pattern classification, from Thorne (1997).	22
Figure 2.8 – Definition of key meander geometry parameters.	24
Figure 2.9 – Configurations for sinuosity index of 1.5, from Hey (1976).	25
Figure 3.1 – Credit River Watershed location in southern Ontario, Canada.	32
Figure 3.2 – Credit River Watershed elevation.	33
Figure 3.3 – Credit River Watershed zones.	35
Figure 3.4 – Credit River Watershed physiography.	36
Figure 3.5 – Water Survey of Canada gauge station locations.	38
Figure 3.6 – Credit River discharge at Orangeville (1967-2015).	39
Figure 3.7 – Credit River discharge at Cataract (1915-2015).	39
Figure 3.8 – Credit River discharge at Boston Mills (1982-2015).	40
Figure 3.9 – Credit River discharge at Norval (1988-2015).	40
Figure 3.10 – Mean annual discharge for Credit River at four main-branch gauge stations.	40
Figure 3.11 – Credit River Watershed land use.	41
Figure 3.12 – Greenbelt boundaries within the Credit River Watershed.	42
Figure 4.1 – Selected sites within the Credit River watershed.	48
Figure 4.2 – Sinuous low-order channel with degree of regular meandering (Reach LC3).	50
Figure 4.3 – Irregular meandering apparent in a medium-sized watercourse (Reach FC1).	51
Figure 4.4 – Larger fluvial system with regular meandering tendencies (Reach CR11).	52
Figure 4.5 – Watercourse which exhibits relative stability from 1954-2013 (Reach HC1).	54
Figure 4.6 – Watercourse which exhibits relative stability from 1954-2013 (Reach BC2).	55
Figure 4.7 – Watercourse which exhibits relative instability from 1954-2013 (Reach LCR1).	57
Figure 4.8 – Watercourse which exhibits relative instability from 1954-2013 (CR9).	58
Figure 4.9 – GIS-based drainage area measurement flow chart.	60
Figure 4.10 – Reach delineation (Reach BC2).	64
Figure 4.11 – Meander axis identification (Reach BC2).	65
Figure 4.12 – Meander belt delineation (Reach BC2).	67
Figure 5.1 – OLS relation of meander belt width and mean bankfull channel width.	79
Figure 5.2 – RMA regression model for meander belt width and mean bankfull channel width.	80
Figure 5.3 – OLS relation of meander belt width and discharge.	81
Figure 5.4 – RMA regression model for meander belt width and discharge.	82
Figure 5.5 – OLS relation of meander belt width and drainage area.	83
Figure 5.6 – RMA regression model for meander belt width and drainage area.	84
Figure 5.7 – OLS relation of meander belt width and meander amplitude.	85
Figure 5.8 – RMA relation of meander belt width and meander amplitude.	86

Figure 5.9 – OLS relation of meander belt width and meander amplitude with the addition of mean bankfull channel width.	86
Figure 5.10 – Discretization of the OLS model for meander belt prediction via mean bankfull channel width using the median of bankfull width at 6.10 m.	88
Figure 5.11 – Discretization of the OLS model for meander belt prediction via discharge using the median of discharge at 9.23 m ³ /s.	88
Figure 5.12 – Discretization of the OLS model for meander belt prediction using drainage area, with the median of drainage area at 25.3km ²	89
Figure 5.13 – Discretization of meander belt width OLS relation to mean bankfull channel width using watershed zones.	90
Figure 5.14 – Discretization of meander belt width OLS relation to discharge using watershed zones.	90
Figure 5.15 – Discretization of meander belt width OLS relation to drainage area using watershed zones.	91
Figure 5.17 – Organization of meander belt width and discharge by Strahler stream order.	92
Figure 5.18 – Organization of meander belt width and drainage areas by Strahler stream order.	93
Figure 5.19 – OLS relation of discharge and drainage area.	95
Figure 5.20 – OLS relation of mean bankfull channel width and discharge.	97
Figure 5.21 – OLS relation of mean bankfull channel width and drainage area.	97
Figure 6.1 – Meander belt width measurement discrepancies.	103
Figure 6.2 – Comparison of OLS meander belt width prediction models using bankfull width.	105
Figure 6.3 – Comparison of OLS meander belt width prediction models using discharge.	107
Figure 6.4 – Comparison of OLS meander belt width prediction models using discharge and bankfull width.	108
Figure 6.5 – Parish Geomorphic (2004) model for meander belt width prediction via drainage area and stream power.	109

List of Tables

Table 2.1 – Concepts of river corridor management.	4
Table 2.2 – Planimetric Procedures for Meander Belt Delineation.	14
Table 2.3 – Empirical Models for Meander Belt Delineation.	16
Table 2.4 – Channel type as defined by sinuosity ratio. Source: <i>Charlton, 2008</i>	24
Table 3.1 – Sources and measurement of data used in statistical analysis.	43
Table 5.1 – Meander belt width and hydrogeomorphic parameter correlation coefficients.	72
Table 5.2 – Correlation matrix for significantly related hydrogeomorphic variables.	74
Table 5.3 – Relations of discharge and drainage area in southern Ontario.	94
Table 5.4 – Regional models for bankfull channel width via drainage area.	96
Table 5.5 – Relations of meander amplitude and channel width.	99
Table 6.1 – Bankfull width models for meander belt width prediction.	105
Table 6.2 – Discharge relations for meander belt width prediction.	107
Table 6.3 – Relations of drainage area and stream power for meander belt width.	109

Abbreviations

Abbreviation	Property	Unit
A	Channel cross-sectional area	m ²
A_P	Meander amplitude	m
D	Mean bankfull channel depth	m
DA	Drainage area	km ²
M_B	Meander belt width	m
P	Sinuosity	Ratio
Q₂	Discharge	m ³ /s
w	Mean bankfull channel width	m
S	Valley gradient	Ratio
ω	Total stream power	W/m ²
Ω	Specific stream power	W/m

Chapter 1

1 Introduction

Policies that restrict land uses and protect stream corridors based on meander belt delineation have been established in many jurisdictions, including Ontario. The concept of river corridor management was formulated to address issues surrounding erosion hazards and sensitive habitats. Rather than viewing a river channel as a liability which requires controls, such as bank hardening and stabilization, watercourses are now viewed as assets which require space for natural processes to occur (Piegay H. , Darby, Mosselman, & Surian, 2005). Of the various concepts of river corridor management and delineation methods that now exist, one of the most commonly used is that of meander belt delineation.

There are varied definitions of a meander belt, some which restrict the definition to a geometrical parameter, and some which more broadly define it as the space a watercourse occupies within the floodplain. The delineation of a meander belt has been identified as a tool for designating a corridor in which meander migration may occur, with the ultimate goal of limiting development encroachment, minimizing the loss or damage of property, and protecting natural areas or sensitive habitats along river systems (Parish Geomorph, 2004; Kline & Dolan, 2008).

In Ontario, for unconfined watercourses, the Ministry of Natural Resources requires a meander belt allowance for development restrictions and species-at-risk legislation as part of the Government of Ontario regulation policies (MNR, 2002). Meander belt delineation is commonly comprised of planimetric and historical assessments of a watercourse which are used to define an area of natural meander migration and associated erosional processes. The issue of meander belt delineation is most prominent for watercourses which have been previously altered and no longer exhibit natural meandering tendencies. For such watercourses, the most common method of

meander belt delineation is through the application of empirical models that predict meander belt width from other watershed or channel characteristics. While research concerned with understanding the mechanics of meandering rivers exists, there is a paucity of research literature focussing on the hydrologic and geomorphic controls of meander belts. Additionally, upon the review of river corridor management techniques and meander belt delineation, it is apparent that there is a lack of consensus on the methods of meander belt measurement to provide basis for these predictive equations. The applicability and accuracy of models which are frequently used to predict meander belt width have not yet been assessed for watercourses in southern Ontario.

The purpose of this research project is to evaluate the current standards of practice for meander belt delineation in southern Ontario, focusing on empirical equations to determine whether these models can reliably predict belt width. Drawing on a sample population of river reaches in the Credit River watershed, this research will add to the database of meander belt literature which is currently limited for watercourses in southern Ontario.

Chapter 2

2 Review of River Corridor Management and Meandering Channels

2.1 General Principles of River Corridor Management

Perceptions of fluvial governance have shifted in regions of Europe and North America from a preventative approach (i.e., bank hardening and protection) to a management approach which focusses on allowing rivers to migrate freely within a delineated space, protecting natural processes and providing safety for infrastructure; hence, the concept of river corridor management. The concept of river corridor management has been said to have originated from the increased awareness of the unsustainable nature and economic cost of engineered bank protections, as well as the key role of channel dynamics and ecosystem services provided by uninhibited watercourses (Thorne, Hey, & Newson, 1997; Piegay H. , Darby, Mosselman, & Surian, 2005). Several types of river corridor management have been developed under a variety of names, as displayed in Table 2.1. The specific definitions and methods of the river corridor concepts vary; however, these approaches are fundamentally parallel in their purpose of predicting areas at risk of future channel erosion and associated conservation to help reduce threats to existing infrastructure, human developments and critical habitats. However, when considering the regions of application for each of the listed management concepts, it may be inferred that there is a regional association with river corridor management, rather than national or universal approaches.

Table 2.1 – Concepts of river corridor management.

Concept	Region of application	Source
River corridor	Vermont	(Kline & Dolan, 2008)
Channel migration zone	Washington	(Rapp & Abbe, 2003)
Area of fluvial freedom	Spain	(Ollero, 2010)
Erodible corridor concept	(n/a)	(Piegay H. , Darby, Mosselman, & Surian, 2005)
Freedom space	Quebec	(Biron, et al., 2014)
Streamway	Oregon & Washington	(Palmer, 1976)
Stream corridor	U.S.A.	(FISRWG, 1998)
Inner river zone	California	(Department of Water Resources (state of California), 1998)
Riparian corridor	United Kingdom	(Thorne, Masterman, & Darby, 1992)
Meander belt	Ontario	(Parish Geomorphic, 2004)

2.2 Planimetric and Historical Assessment Methods for River Corridor Management

The most common approach to delineating a river corridor is through planimetric assessments of a watercourse (Thorne, Hey, & Newson, 1997; Lagasse, Zevenbergen, Spitz, & Thorne, 2004; Piegay H. , Darby, Mosselman, & Surian, 2005). Historical data, including topographic maps and aerial imagery, are used to identify channel geometry variables (e.g., channel sinuosity, meander wavelength, bankfull channel widths), rates of channel mobility (e.g., rates of erosion and floodplain turnover rates), and structures preventing channel migration (e.g., bank protection and infrastructure). Field data, including riparian vegetation, bed and bank substrate, channel dimensions, fluvial features, and mass movements, are used to supplement the remotely-sensed data collected on a watercourse. With this information, the historical dynamics of a watercourse can be assessed in order to predict channel behaviour in the future. Generally, channel mobility is tracked through image overlays of historical aerial photographs, which compare previous

configurations of the watercourse. The product of this data is used to determine the extent of a river corridor. Three examples of river corridor delineation methods, which were selected based on different detailed approaches to river corridor delineation, are described and compared in the sections to follow.

2.2.1 Channel Migration Zone

The concept of a channel migration zone is one example of a river corridor which is delineated using planimetric assessment for channel which are assumed to be actively meandering; thus, having associated erosion hazards. To delineate a channel migration zone, four distinct areas must be identified: the hazard migration zone, avulsion hazard zone, erosion hazard area, and the disconnected migration area (Rapp & Abbe, 2003). This method requires overlays of previous channel configurations (Figure 2.1) to identify rates of erosion and directional movement of meanders, as well as physical characteristics surrounding the watercourse, such as bed stratigraphy, riparian vegetation, and structures which prevent channel migration. The restricting characteristic of this methodology is that the channel must be actively migrating to delineate the river corridor which may not always be the case.

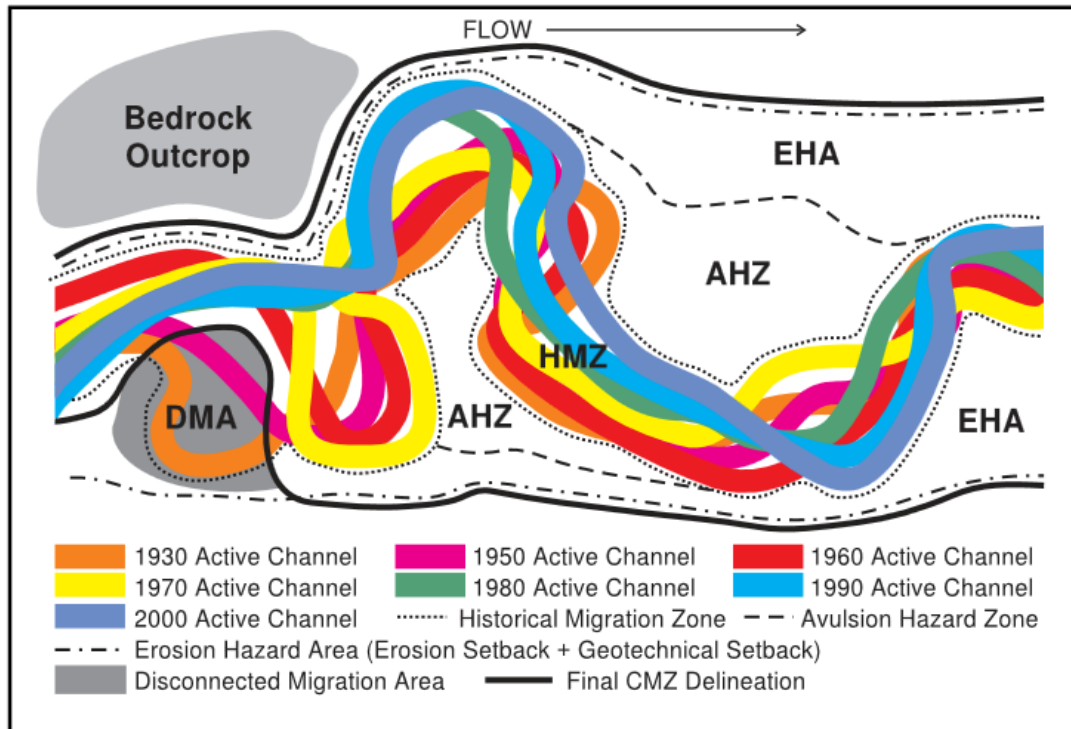


Figure 2.1 – Channel migration zone delineation, from Rapp & Abbe (2003).

(HMZ - Historical Migration Zone, AHZ – Avulsion Hazard Zone, EHA – Erosion Hazard Zone, DMA – Disconnected Migration Area)

2.2.2 River Corridor (Vermont)

The process of identifying a river corridor, as described by the Vermont Agency of Natural Resources (Kline & Dolan, 2008), has been automated using the GIS extension, titled Stream Geomorphic Assessment Tool (SGAT), which identifies the limits of a river corridor in a four-step process. The corridor is created using the product of a space delineated parallel to the watercourse centreline (watercourse corridor), a space parallel to the meander centreline (meander corridor), and a space parallel to the valley wall (Figure 2.2). The GIS extension uses variables such as bankfull channel width, valley wall position, sinuosity, and centrelines to delineate a final river corridor. The automation of the planimetric assessment may offer a more cost and time effective

approach to delineating a river corridor, however the designated corridor which is output from the automation tool may be arbitrary and require further analysis for proper corridor delineation.

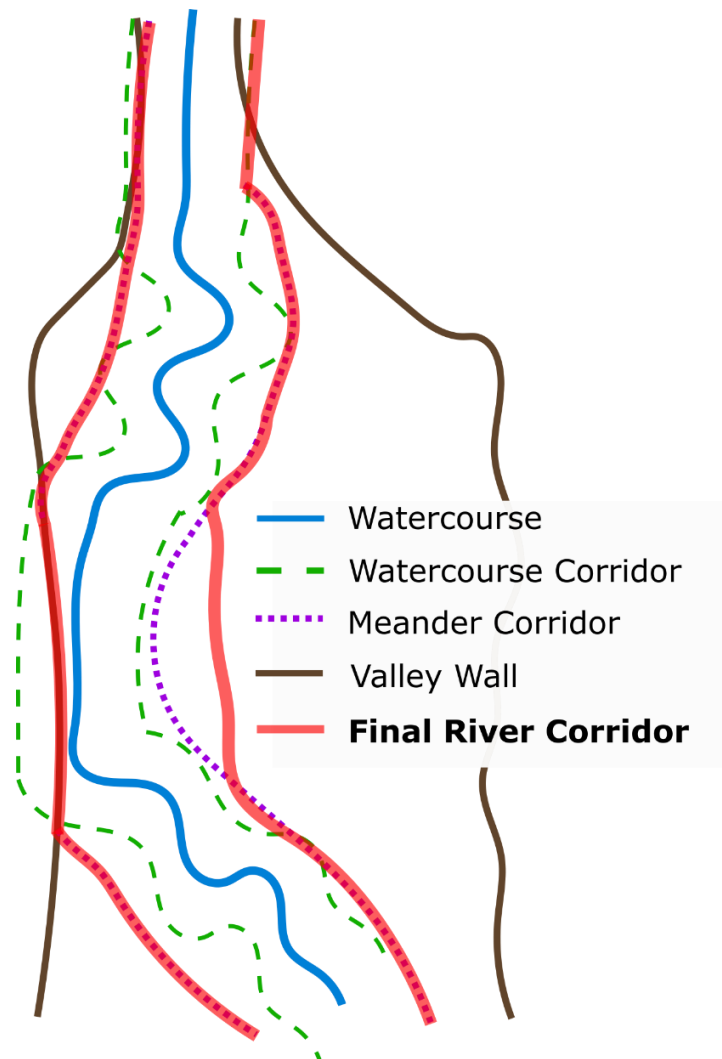


Figure 2.2 – River corridor delineation, adapted from Kline & Dolan (2008).

2.2.3 Freedom Space

Freedom space is a river corridor concept which integrates flooding as well as the erosion and migration processes occurring within a fluvial system into the space permitted for natural river processes to occur (Biron, et al., 2014). The freedom space limits are conceptualized with two distinct spaces: mobility space and flooding space. To delineate the mobility space, historical rates of erosion are calculated using the software Digital Shoreline Analysis System (DSAS). This GIS

extension uses transects across multiple years of channel configurations to generate a quantitative representation of channel migration. The flooding space is determined by identifying distinctive landforms suggesting flood processes, and relating them to the severity of flooding (low, medium, high). Together, the mobility space and flood space are used to delineate three types of freedom space: minimum (L_{min}), functional (L_{func}), and rare (L_{rare}), based on the likelihood of channel migration and flooding (Figure 2.3). Expert practitioners can then determine which freedom space is most necessary for a particular watercourse.

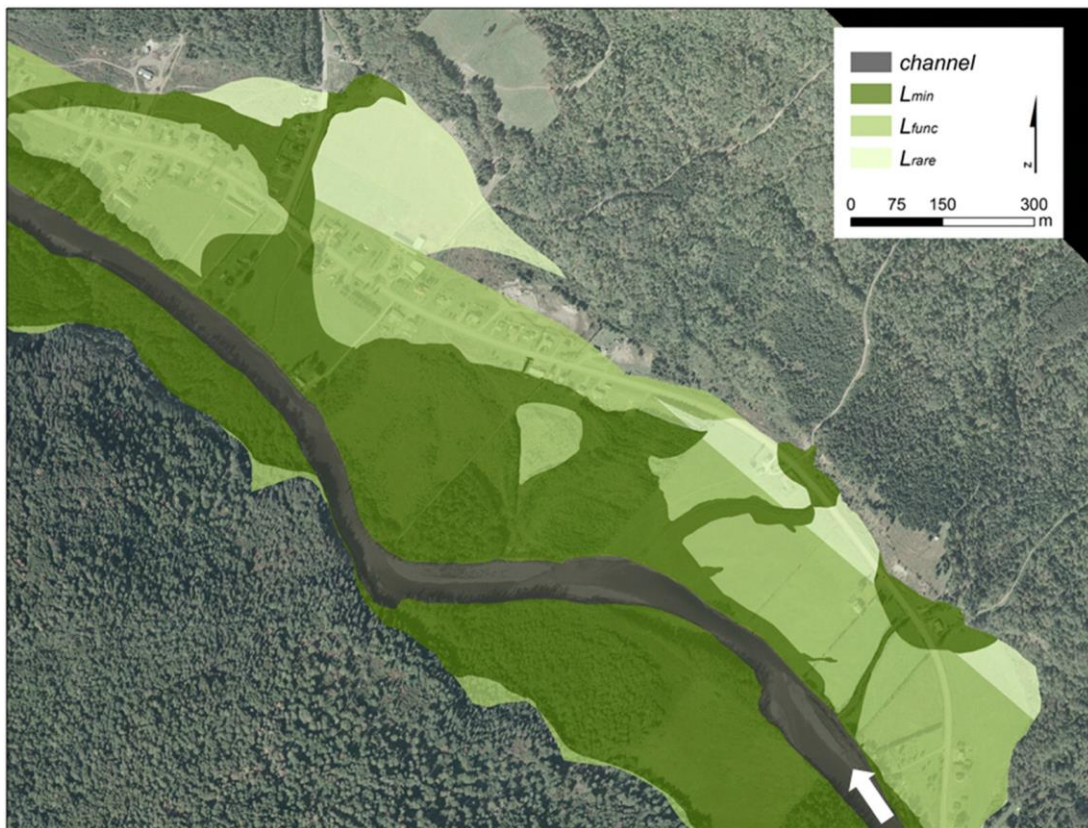


Figure 2.3 – Freedom space delineation, from Biron et al., (2014).

2.3 Limitations of Planimetric and Historical Assessments

There are various limitations associated with the planimetric approach of delineating river corridors. Planimetric assessments are heavily dependent on the mapping medium used to measure

channel features and delineate river corridors. Planimetric analyses are only appropriate if the channel is sufficiently large to be identified clearly on maps or images, and if channel movement can be observed from one survey to another (Piegay H. , Darby, Mosselman, & Surian, 2005; Rapp & Abbe, 2003). This dependency on map or image quality is also largely influenced by the scale of the mapping medium. Although high resolution data may be acquired for more recent years, historical imagery is often subject to lower resolutions, making it difficult to accurately map watercourses. Additionally, the accuracy of the delineated river corridor is dependent on the time span covered by the obtained mapping materials, which are commonly independent of the temporal distribution of flooding and migration activity (Piegay H. , Darby, Mosselman, & Surian, 2005). For migration analyses, this limitation is magnified as high-resolution historical images may be required for delineation. It has been recommended that historical and current imagery have a scale of 1:10,000 or 1:20,000 be used in overlay procedures (Thorne, Hey, & Newson, 1997; Parish Geomorphic, 2004). In some cases, obtaining imagery for current channel configuration may be difficult due to stream size, vegetation cover, or remote locations. Acquiring the necessary data for planimetric assessments can be difficult for many watercourses. Moreover, errors associated with image registration, georeferencing, and feature measurement can be introduced in planimetric analyses, which can jeopardize the accuracy of river corridor delineation which are based on historical migration (Rapp & Abbe, 2003).

2.3.1 Summary

The methods of river corridor management discussed above are a few examples of those approaches grounded in the use of planimetric analysis of historical data (e.g., topographic maps and aerial photography) and field data to develop an understanding of the watercourse dynamics. These concepts differ in the manner in which space is delineated within the final river corridor,

which may be due to the varying locations at which they are applied by prioritizing and emphasizing certain aspects of river migration, and erosion and flooding hazards. Additionally, while some of these methods rely on more simplistic map and image overlays to track previous channel migration, others have adopted more GIS-based or computer-automated programs. Despite the differences in automated or manual delineation, these methods of river corridor management have a common goal of outlining the space a watercourse needs for natural river migration processes to occur, protecting sensitive habitats and mitigating fluvial erosion threats to infrastructure. Nonetheless, these methods are still confined by limitations: the availability of historical data, erroneous conclusions introduced by mapping and measurement techniques, the applicability for altered watercourses, and the repeatability and reliability of the methods when applied to a specific watercourse.

2.4 Meander Belt as a Method of River Corridor Management

Meander belt is a term which is used to describe the space a meandering watercourse occupies within the floodplain. The width of a meander belt is of particular interest as it defines the area that the watercourse occupies or can occupy in the future; thus, providing a quantitative measurement of a river corridor. Jefferson (1902) first coined the term meander belt as, “the width of the belt of meanders between lines tangent along the swings of the river.” For many descriptions of meander belt, this definition is similar. For example, Annable (1996) defines meander belt as the, “greatest lateral width of the meander pattern within the trend of the valley.” Similarly, Ackers and Charlton (1970) define meander belt width as the width between parallel lines which contain the meandering channel. However, there is literature which fails to follow set definition, such as Carlston (1965), who defines meander belt width as the average width of meanders in a river reach, or others such as Williams (1986) who fail to provide a definition of the term. Despite these

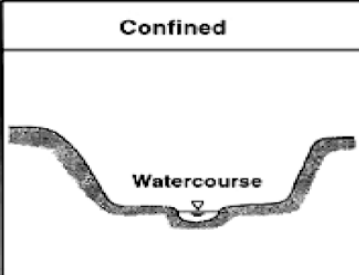
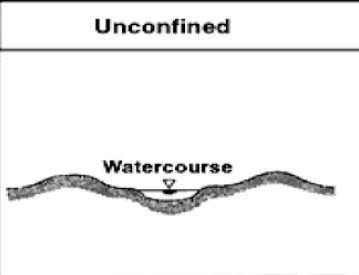
discrepancies in meander belt definition, the term is commonly used throughout literature which focusses on meander geometry and planform.

The Ontario Ministry of Natural Resources' (MNR) Water Resources Section published the *Technical Guide for River and Stream Systems: Erosion Hazard Limits* in 2002. The guide was prepared, "to provide a consistent standardized procedure for the identification and management of riverine erosion hazards in the Province of Ontario," in order to assist in the understanding of regulations in the 1996 Ontario Provincial Policy statement (MNR, 2002). Within the Provincial Policy statement, the discussion of meander belt delineation requirements is scarce, simply stating that development shall be generally directed to areas outside of erosion hazards or the "predicted meander belt of a watercourse," (Section 3, Policy 3.1.1) (Ontario Ministry of Municipal Affairs, 1996). This is reiterated in the Conservation Authorities Act: Ontario Regulation 97/04 where it is stated that a regulation shall prohibit development within the "predicted meander belt of a watercourse" (Government of Ontario, 1990). Meander belt delineation is also discussed in the Endangered Species Act (2007) in relation to Redside Dace (*Clinostomus elongates*), indicating habitat is considered as, "the area encompassing the meander belt width" (Government of Ontario, 2007). Despite the brief discussion of meander belt delineation in Ontario regulatory documents, there is still ambiguity in regards to the circumstances in which a meander belt delineation is unequivocally required.

The most detailed discussion of meander belt delineation is within the MNR (2002) technical guide for erosion hazard limits. The document states three main components of erosion hazards: natural processes of erosion, flooding, and slope stability (MNR, 2002). Fluvial systems are classified in the guide as confined or unconfined. Confined systems are defined as, "ones in which the physical presence of a valley or corridor containing a river or stream channel [...] are visibly discernible

from the surrounding landscape,” (MNR, 2002). This definition differs from that of the more specific and standard geomorphology definition in which confined systems are where, “the channel is bordered on either side by banks that are higher than the highest flood level, or by valley sides,” (Ashmore & Church, 2001). Unconfined systems are defined as, “ones in which a river or stream is present but there is no discernible valley slope that can be detected,” (MNR, 2002). Erosion hazard allowances are varied based on the type of confinement, as seen in Figure 2.4. For unconfined systems, the guide states a meander belt allowance is necessary. However, in many cases meander belts are also delineated by practitioners for confined systems.

River and Stream Systems Landform Classification

	Confined	Unconfined
Watercourse Profile		
Typical Geologic Setting	Valley corridors	Glaciated plains, flat to gently rolling

Hazard Allowances	Confined	Unconfined
Stable Slope	Yes	No
Toe Erosion	Yes	No
Meander Belt	No	Yes
Access Allowance	Yes	Yes

Figure 2.4 – Erosion hazard allowances by channel confinement, from MNR (2002).

The document defines a meander belt allowance as the maximum extent that a water channel migrates (MNR, 2002). It is recommended that the meander belt allowance is calculated by 20 times the bankfull channel width, measured at the largest meander in the reach (MNR, 2002). This

protocol is said to be based on available information, yet lacks reference to any supporting data. The technical guide allows for alternative approaches, in that, “if the proponent determines that the recommended [procedure] is not appropriate for their location, they must provide [...] an analysis of the meander belt width which can be determined through accepted scientific and engineering study,” (MNR, 2002). For those locations where other analyses seem required, the *Belt Width Delineation Procedure* document, prepared by Parish Geomorphic Ltd. (2004) for the Toronto and Region Conservation Authority (TRCA), appears to be the preferred alternative.

The TRCA report (Parish Geomorphic, 2004) was created to recommend a protocol for the delineation of meander belt width for river systems within the TRCA jurisdiction, but is generally adopted by other Conservation Authorities throughout southern Ontario. The document was authored by consulting company Parish Geomorphic. The document references an extensive list of academic literature concerned with meander geometry and morphological assessment. However, as the report was intended for TRCA use and to provide recommendations within set jurisdiction, the contents of the document were not subject to a critical or peer-review process. Nevertheless, the document is used widely across southern Ontario as the primary means of delineating a meander belt. Here, meander belt is defined as the space a watercourse occupies on its floodplain in which all natural channel processes occur (Parish Geomorphic, 2004). There are five core procedures within the report which may be used to delineate a meander belt, of which four are based on the planimetric assessment of a watercourse (*Procedures 1-4*). Each of the procedures follow the same methodology for reach delineation, meander belt axis identification, and historical analyses (where applicable). The procedures differ based on the current and/or anticipated state of the watercourse, demonstrated as the scenario in Table 2.1. *Procedure 1* was designed to establish a general identification of a meander belt, often used for large scale or

planning-level studies. *Procedures 2-4* were designed for an accurate delineation of a meander belt, which requires more detailed analysis of historical and current channel configurations, and anticipated hydrologic scenarios for the watercourse.

Table 2.2 – Planimetric Procedures for Meander Belt Delineation.

Source: Parish Geomorphic (2004).

Procedure	Scenario	Meander Belt Width Calculation
<i>Procedure 1</i>	Preliminary belt width delineation	Tangential lines are drawn along extreme meander bends to generate a preliminary belt width (B). Corrections are made based on channel confinement and incision.
<i>Procedure 2</i>	Change in the hydrologic regime is not anticipated.	If the existing belt width is < 50m: Final Belt Width = Belt Width + D + E
		If the existing belt width is > 50m: Final Belt Width = Belt Width * 1.10 + E
<i>Procedure 3</i>	Change in the hydrologic regime is anticipated. (Increase in duration of flows and in frequency of occurrence).	If the existing belt width is < 50m: Final Belt Width = (Belt Width*1.05) + D + E
		If the existing belt width is > 50m: Final Belt Width = Belt Width * 1.20
<i>Procedure 4</i>	Change in the hydrologic regime is anticipated. (Increase in peak flows and frequency of occurrence).	Final Belt Width = (B + C + D) * adjustment ratio

B = Preliminary Belt Width, C = average bankfull width, D = distance migrated in 100 years (estimated with migration rate), E = distance meander axis shifted in 10-years

2.5 Empirically-Based Models for Corridor Prediction

Knowledge of geomorphic and hydrologic variables which relate to a channel’s ability to migrate within the landscape has permitted the conception of empirical models which predict meander feature dimensions from other meander features or from channel characteristics. These empirical

relations have been adapted and applied as a tool of estimating and predicting meander belt width through the collection of empirical data on watercourses where the related hydrologic and geomorphic variables have been measurable. The models are used primarily as a method of assessing smaller or low-order watercourses lacking the necessary historical mapping materials and watercourses which have been altered and may no longer demonstrate a 'natural' configuration (Parish Geomorphic, 2004), as well as a substitute for time-consuming planimetric analyses. Table 2.3 lists several empirical equations which have been developed to estimate meander belt width (M_B) based on other properties of the river channel and/or watershed.

The most common variables used to predict meander belt width are channel and meander geometry variables, including meander wavelength, radius of curvature, and bankfull channel measurements. Hydrologic parameters are also employed, including stream power and discharge. However, a brief review of the empirical models in Table 2.4 demonstrates large discrepancies among coefficients in equations which relate the same variable to meander belt width. For example, based on these relations, meander belt width ranges from 4.3 to 17.6 times the bankfull channel width. These inconsistencies may be, in part, due to the spatial variability of watercourses, resulting in site-specific empirical equations based on the watercourses from which they were developed. From the empirical equations in Table 2.3, only the models established by Annable (1996) and Parish Geomorphic (2004) were developed on watercourses from the region of southern Ontario. Annable (1996) developed his empirical relations from 47 primarily rural watersheds in southern Ontario. However, he states that the equations display low levels of reliability, as seen by the goodness of fit statistics, and should only be applied as "...first-order approximations of gross-scale channel characteristics related to basin scale studies" (Annable, 1996). Therefore, these relations are not suitable for accurate meander belt width delineations.

Table 2.3 – Empirical Models for Meander Belt Delineation.

Source	Variables	Model	Reliability	Conditions
Ackers & Charlton (1970)	Discharge (Q)	$M_B = 18.50 Q^{0.51}$	S.E. = 0.21	
		$M_B / w = 2.17 Q^{0.19}$	S.E. = 0.23	
		$\lambda / M_B = 2.06 Q^{-0.04}$	S.E. = 0.18	
Annable (1996)	Bankfull discharge (Q_{bf})	$M_B = 56.95 Q_{bf}^{0.45}$	S.E. = 0.34	Rosgen C – type
		$M_B = 16.30 Q_{bf}^{0.88}$	S.E. = 0.29	Rosgen E – type
		$M_B = 131.26 Q_{bf}^{0.29}$	S.E. = 0.01	Rosgen F – type
Bridge & Mackey (1993)	Hydraulic depth (D_H)	$M_B = 59.90 D_H^{1.8}$		
Carlston (1965)	Mean annual discharge (Q_a)	$M_B = 65.80 Q_a^{0.47}$	$r^2 = 0.96$	
Collinson (1978)	Maximum depth (D_{max})	$M_B = 65.60 D_{max}^{1.12}$		
Jefferson (1902)	Bankfull width (w)	$M_B = 17.60 w$		
Lorenz et al. (1985)	Bankfull width (w)	$M_B = 7.53 w^{1.01}$		
Parish Geomorphic (2004)	Total Stream power (ω) Drainage area (DA)	$M_B = -14.827 + 8.319 \ln(\omega * DA)$	$r^2 = 0.739$ S.E. = 8.63	DA < 25 km ²
Ward et al. (2002)	Bankfull width (w) – in feet	$M_B = 4.00 w^{1.12}$		
Williams (1996)	Meander wavelength (λ)			$8 < \lambda < 23,200$ m
	Radius of curvature (Rc)	$M_B = 0.61 \lambda$ $M_B = 2.88 Rc$	$r^2 = 0.98$ $r^2 = 0.96$	$2.6 < Rc < 36,000$ m
	Bankfull width (w)	$M_B = 4.30 w^{1.12}$	$r^2 = 0.92$	$1.5 < w < 4,000$ m
	Bankfull depth (D)	$M_B = 148.00 D^{1.52}$	$r^2 = 0.81$	$0.03 < d < 18$ m
	Standard error (S.E.); Coefficient of determination (r^2)			

For highly modified watercourses, Parish Geomorphic Ltd. derived an empirical equation to predict expected or potential meander belt width from drainage area and stream power of a watercourse (*Procedure 5*). Stream power is a quantitative description of the potential of flowing water to perform geomorphic work as it moves along an energy gradient (Leopold, Wolman, & Miller, 1964). Stream power can be defined by the total stream power (ω), the power per unit length of the channel in watts per square metre, or by specific stream power (Ω), as the power per unit area of the channel in watts per metre. Stream power has been used as a predictor of channel dimensions and channel pattern (Magilligan, 1992; Knighton, 1999), and as a predictor of channel mobility (Bull, 1979; Magilligan, 1992). Therefore, stream power may be a likely control of meander belt width by controlling migration rates and overall channel dimensions. The TRCA report (Parish Geomorphic, 2004) does not provide the supporting data (watercourse locations, river characteristics, statistical methods, etc.) from which the empirical equation was developed. Additionally, incorporating both stream power and drainage area in the relation appears redundant, as drainage area is highly correlated with discharge, and therefore, drainage area may be used, “as a surrogate for discharge in empirical studies of channel morphology” (Knighton, 1999). As stated, the results from the empirical analysis by Parish Geomorphic (2004) are often compared with other meander belt width relations, primarily those of Williams (1986). Alternatively, other relations are employed in lieu of the empirical analysis by Parish Geomorphic, including those of Lorenz et al. (1985) and Ward (2002).

2.5.1 Limitations of Empirically-Based Models

Empirical equations which relate hydrologic and geomorphic watercourse characteristics offer a way to estimate and predict meander belt dimensions, reducing the extensive data needs of planimetric assessments. However, the empirical models which have been developed appear to

exhibit the site-specific nature apparent in planimetric assessments. For instance, Williams (1986) and Ward et al. (2002) both state the application of their respective equations are feasible for meander belt width quantification, despite the large discrepancies among coefficients which relate meander belt width to bankfull channel width. It has been indicated that poor correlations among meander properties is likely due to the strong control of stream bank erodibility and other local factors which control meander size (Leopold & Wolman, 1960; Shahjahan, 1970). This suggests that the relationships developed between meander belt width and channel geometry features may be unique to the specific watercourses for which they were developed, or conversely, do not include all relevant variables for meander belt delineation. Although the site-specific nature of these equations has been acknowledged (Piegay H. , Darby, Mosselman, & Surian, 2005; Shahjahan, 1970), whether it be the type of stream or geomorphic characteristics of the region, empirical relations continue to be applied on watercourses outside of the range of stream size or type for which they were developed.

2.5.2 Summary

Empirical relations offer an opportunity to estimate the size of a river corridor, specifically the width of a meander belt, when planimetric assessments are not feasible. Several empirical equations for the estimation of meander belt width exist which employ both hydrologic and geomorphic variables. Furthermore, empirical relations, such as Williams (1986) and Ward et al. (2002), have been used as part of meander belt width justification, but their validity has not been tested for data from southern Ontario rivers, and the relation by Parish Geomorphic (2004) based on stream power and drainage area seems to have had limited validation and testing.

2.6 Characterization of Meandering Channels

Meandering channels may be characterized as single-thread channels with sinuous planform which is comprised of a series of loops or meander bends (Hooke, 2013). They are differentiated from braided rivers on the continuum of river patterns based on their more stable single-thread configuration which commonly exhibit higher sinuosity values (Leopold, Wolman, & Miller, 1964; Lagasse, Spitz, Zevenbergen, & Zachmann, 2004; Hooke, 2013). Meandering channels commonly exhibit an undulating river bed which alternates between deep and shallow sections, commonly referred to as pool-riffle formations (Leopold, Wolman, & Miller, 1964). This vertical spatial variation along the length of a channel also influences the lateral planform of the channel within meandering systems, as pools are commonly associated with meander bends where erosive forces are concentrated. Figure 2.5 displays the common features of river meanders in an idealized symmetrical meander bend.

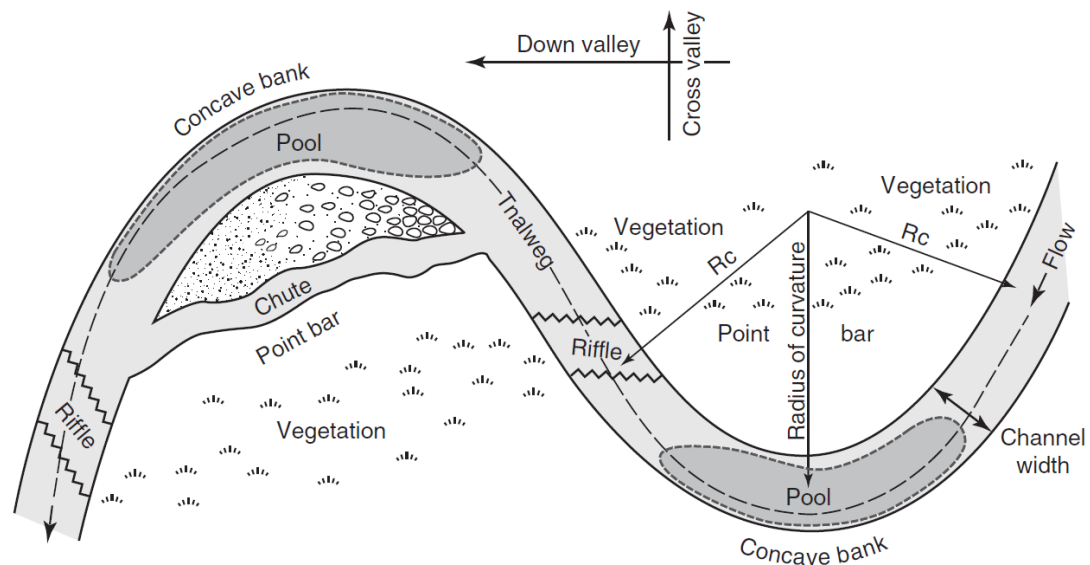


Figure 2.5 – Common features of river meanders, from Hooke (2013).

Unlike the idealized meander shown in Figure 2.5, most meanders appear to be inherently asymmetrical (Carson & Lapointe, 1983). Weihaupt (1989) even suggested that, “no two meander

loops in nature are absolutely identical,” resulting in the inadequacy of the single symmetrical geometric form to describe all meander loops. Despite this notion and the widespread display of asymmetrical meandering tendencies, many initial theories of meandering channels assumed symmetry of meander planform.

Rather than confining the classification of meanders to a simple symmetrical form, a broader range of more complex meander configurations are now utilized. Brice (1974) suggested meander loops be assessed as either simple symmetrical loops, simple asymmetrical loops, or compound loops (Figure 2.6). The evolution of the awareness that meander loops can range in form has also been applied to meandering patterns at larger scales which incorporate several successive meanders. For example, compound patterns have also been described as a second meandering tendency superimposed on another meandering pattern (Parish Geomorphic, 2004).

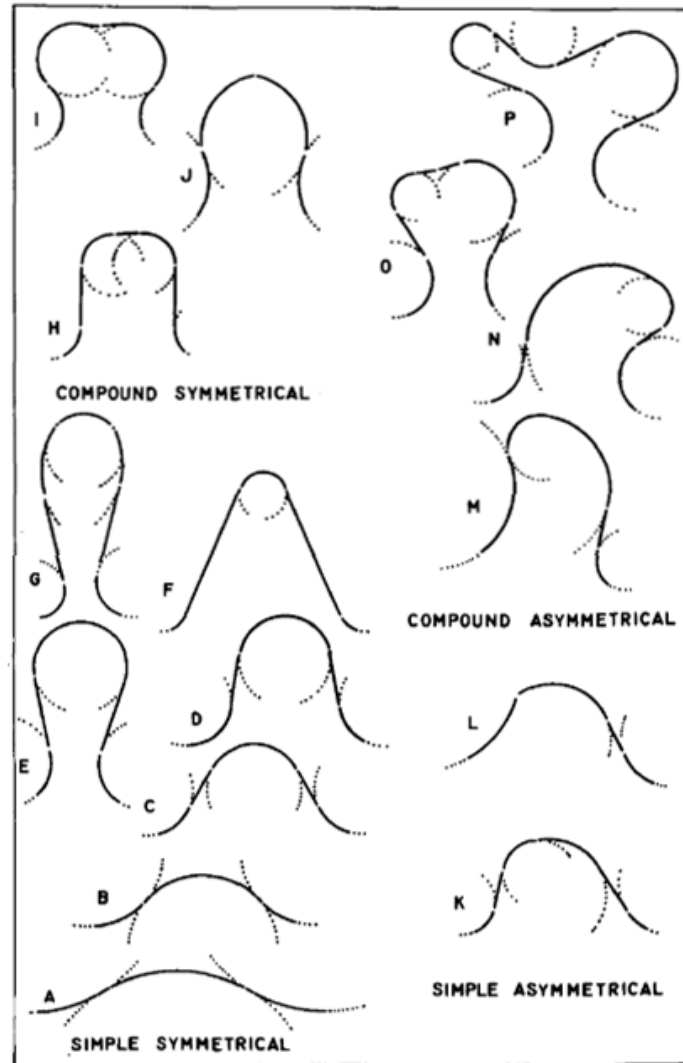


Figure 2.6 – Classification of meander loops, from Brice (1974).

In addition to the irregularity and pattern of a channel, meandering watercourses can be classified and defined by stability: whether they are actively migrating laterally and downstream, or are more relatively stable. A classification method of assessing channel stability was developed by Brice (1975) and further modified by Lagasse et al. (2004); it classifies channels by sinuosity and by variation in channel width (Figure 2.7). Brice (1982) found that channels which do not vary significantly in channel width are relatively stable, while channels which are wider at the apex of meander bends are more active. Lagasse et al. (2004) validated this procedure of qualitatively

assessing channel stability. Combining the width-variability criterion and sinuosity enabled the formation of a classification system for meandering channels. Nevertheless, the numerous forms of meander migration and meander patterns may cause difficulty in placing particular reaches within such classifications.

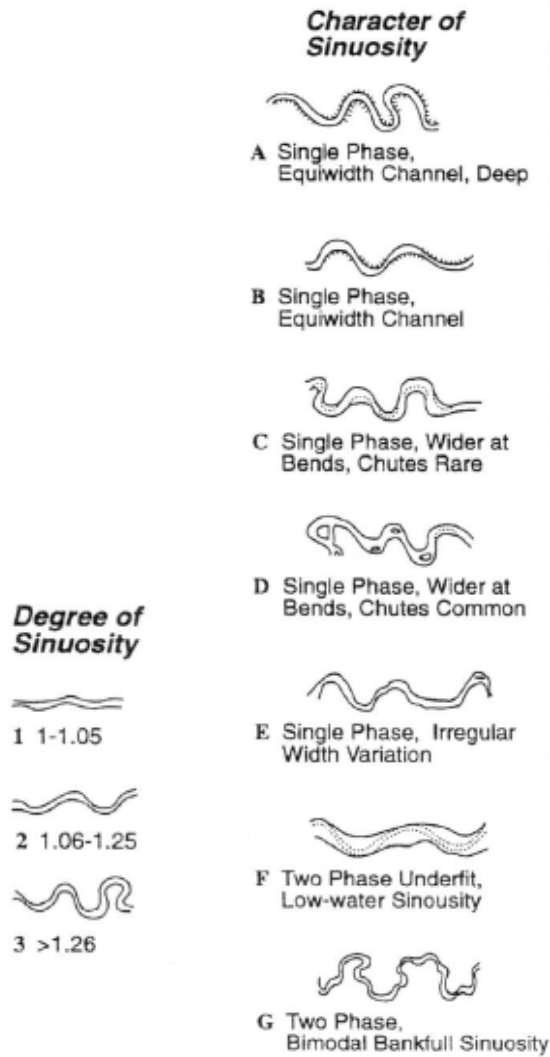


Figure 2.7 – Meandering channel pattern classification, from Thorne (1997), modified from Brice (1975).

2.7 Anatomy of Meander Bends

Meandering channels are often described by their shape, which can be quantitatively measured by a defined set of geometric parameters. Knowledge of meander geometry allows for the classification of watercourses, permitting the identification of similarities among meandering channels and comparisons among states of stability based on meander planform. It has been suggested that meander geometry of a channel is scaled to that of channel width, dominant discharge, stream power or drainage area (Thorne, Hey, & Newson, *Applied Fluvial Geomorphology for River Engineering and Management*, 1997). This follows similar theories of hydraulic geometry developed by Leopold and Maddock (1953), where river dimensions are scaled to discharge or drainage area. This notion offers insight as to which parameters may be most influential of meandering patterns, and thus, which may be most pertinent in meander belt width estimation.

Meander geometry has been reduced to a manageable number of parameters. Ferguson (1975) suggested a three-component pattern continuum framework, in which meandering rivers are characterized by three planimetric properties: the complexity of meandering, the scale of meandering, and the degree of irregularity. Parameters that are commonly used to address this include sinuosity (complexity), meander wavelength (scale), meander amplitude (scale), and radius of curvature of a bend (scale and irregularity) (**Figure 2.8**). Details of these parameters are discussed in the following sections.

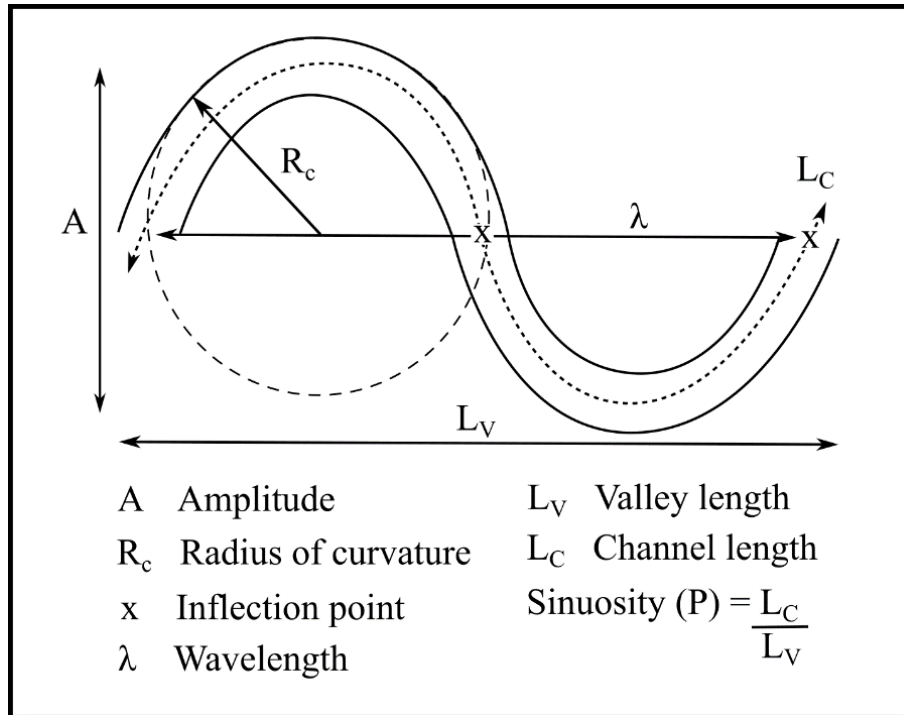


Figure 2.8 – Definition of key meander geometry parameters.

2.7.1 Sinuosity

The sinuosity of a channel has been defined as a measure of the degree of complexity or curvilinearity displayed within a meandering channel (Andrle, 1996). Sinuosity (P) is commonly measured as a ratio between the length along a channel (L_C) to the length of the valley (L_V) within a given reach (**Figure 2.8**). Ratios are frequently compared to a sinuosity index (Table 2.4). The threshold values of the sinuosity index are widely used; however, are arbitrary in nature, as the values are not based on physical differences related to meandering (Charlton, 2008).

Table 2.4 – Channel type as defined by sinuosity ratio. Source: Charlton, 2008.

Sinuosity Ratio	Channel Type
<1.1	Straight
1.1-1.5	Sinuous
>1.5	Meandering

For a given sinuosity value, there are numerous channel configurations which are possible (Figure 2.9); therefore, sinuosity alone does not necessarily distinguish different planforms. This was

confirmed by Hooke & Yorke (2010), who found a relatively constant sinuosity value in a meandering reach despite observing major changes in the shape and length of individual meander bends. Sinuosity is greatly influenced by the scale at which channel parameters are measured.

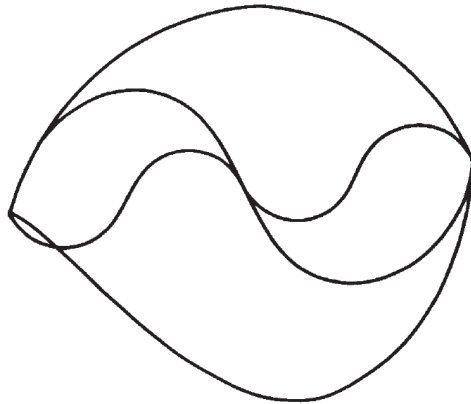


Figure 2.9 – Configurations for sinuosity index of 1.5, from Hey (1976).

Mueller (1968) and Ferguson (1975) proposed hydraulic and topographic sinuosity indexes to account for physical attributes of a watercourse, which incorporates a measurement described as the “air” distance, or shortest distance from the source to the mouth of a watercourse. Additionally, a surrogate of sinuosity was developed by Andrieu (1996) in a method titled the *angle measurement technique*, where a characteristic angle (A_c) defines the maximum degree of complexity. Although this variable is not synonymous with sinuosity, it provides a measure of the scale of complexity while eliminating the scale-dependent nature of sinuosity measurements. Nevertheless, the traditional measurement of sinuosity continues to be employed for the purpose of classifying the scale of complexity apparent in meandering channels.

2.7.2 Meander Wavelength

Meander wavelength (λ) has been defined as a measure of the scale of meandering within a channel by quantifying the spacing of successive meander bends (Leopold & Wolman, 1960; Andrieu, 1996; Lagasse, Spitz, Zevenbergen, & Zachmann, 2004). Therefore, meander wavelength is a measure

of the downstream scale of meandering, rather than a lateral migration measurement. Meander wavelength is determined by doubling the straight-line distance between two successive points of inflection (**Figure 2.8**). However, this measurement is complicated by irregularities in channel pattern. Ambiguity can be introduced when defining points of inflection, particularly in small channels or when irregularities are apparent. Another issue apparent with meander wavelength measurements is the selection of an “average” pair of meanders for assessment which can result in the misrepresentation of a channel (Ferguson, 1975). A detailed characterization of meander wavelengths is that of spectral analysis where a dominant wavelength may be identified (Speight, 1965; Chang & Toebes, 1970; Ferguson, 1975).

There is a well-established relationship between meander wavelength and channel width, dating back to work by Leopold and Wolman (1960), which has allowed for the derivation of empirical equations to estimate meander wavelength. It can be said that meander wavelength bears a relatively constant ratio with channel width, ranging from approximately six to twelve times channel width. Although these equations suggest identifiable underlying tendencies in meander morphology and channel dimensions, they are only approximations of true relations (Williams, 1986). Therefore, care must be taken in applying and relying on such empirical relations to quantify the scale of meandering in a channel.

2.7.3 Meander Amplitude

Meander amplitude is a measure of the lateral extent of a meander (**Figure 2.8**), defined as the lateral distance between tangential lines drawn to the centre of a channel across two successive meander bends (Leopold, Wolman, & Miller, 1964). As meander amplitude is measured on a set of meander bends, in order to describe a channel at a reach scale, a governing meander amplitude or the largest meander amplitude is commonly measured. There is less subjectivity associated with

meander amplitude measurements; however, it has been shown to poorly correlate with other meander geometry or channel characteristic variables (Leopold, Wolman, & Miller, 1964; Williams, 1986). It has been inferred that meander amplitude may be controlled more by local characteristics of the channel, such as the stability of the banks and erosive forces occurring within the watercourse, rather than any hydrogeomorphic principles (Leopold, Wolman, & Miller, 1964).

2.7.4 Radius of Curvature

Radius of curvature (R_c) can be determined by fitting a circle to the centre line or outer bank of the meander bend and measuring the radius of the inscribed circle (**Figure 2.8**). Similar to meander amplitude, radius of curvature is a parameter which is not measured at the reach scale, as are meander wavelength and sinuosity. Brice (1974) inscribed circular arcs on idealized meander loops to indicate the general geometry and symmetry of meanders which assists in understanding and classifying meander shape and evolution. This visual assessment of curve fitting has been enhanced quantitatively by introducing the measurement of radius of curvature of an individual meander bend. This parameter indicates the tightness of an individual meander, and has been employed to represent the state of meander regularity and stability (Geist, 2005; Lagasse, Spitz, Zevenbergen, & Zachmann, 2004). For example, it has been suggested that meanders with larger radius of curvature measurements display greater stability (Hickin & Nanson, 1984; Geist, 2005). The process of fitting a single circle to a simple symmetrical or asymmetrical meander bend can be a relatively straightforward task. However, fitting single circles to complex or compound bends can be difficult and more subjective.

2.7.5 Limitations of Meander Geometry Measurement

Despite the various benefits, there are significant limitations to measuring meander geometry. Perhaps the most substantial issues with meander geometry assessments are the use of topographic

maps and aerial photographs as a medium of measurement, as well as the subjectivity of delineating meander parameters.

Although the introduction of aerial photography has reduced many of the errors associated with topographic maps, issues concerning distortion and scale remain. The scale at which aerial photography is taken greatly affects the accuracy of meander geometry quantification, especially with small watercourses displaying complex and minor meander configurations. Enhancing photographs, specifically those which are historical, can result in the distortion of a channel. The accuracy at which meander geometry is delineated is dependent on the scale and quality of the aerial photographs used; thus, errors will propagate through meander geometry quantification (Ferguson, 1975).

The measurement of geometric meander variables has been proven to be highly subjective. Meander sinuosity is largely dependent on the scale of measurement, and the estimation of the channel and valley lengths can become increasingly difficult with small and complex systems (Andrle, 1996). The precise measurement of meander wavelength is often difficult and subjective, due to scaling issues, channel complexity, and the identification of inflection points (Andrle, 1996; Carlston, 1965; Hooke, 1984). As well as being dependent on the scale of the mapping medium, radius of curvature measurements are significantly influenced by the method of fitting a circle or arc to a meander bend (Lagasse, Spitz, Zevenbergen, & Zachmann, 2004).

Finally, the use of meander geometry to predict meander migration is subject to the assumption of continuity of change (Lawler, 1993). The movement of a meander is assumed to be simple, continuous, and linearly migrating, which fails to account for the sometimes stochastic and episodic nature of meander migration and meander cut-offs (Hooke, 1984).

2.8 Study Rationale and the Case of the Credit River

Current land use management policies and procedures require the application of site-specific planimetric assessments, or empirical equations, to measure or predict river corridor and meander belt dimensions. In the case of small, low-order, or highly modified watercourses, the measurement of meander belt width is driven by the application of empirical relations. However, there is limited documentation regarding the range of meander morphology in the watersheds of southern Ontario, and the principle parameters that control meander belt width have not yet been systematically investigated. Upon analysis of river corridor management techniques and meander belt delineation, it is evident that there is a lack of knowledge and agreement regarding the methods of meander belt delineation, and the controls of meander belt development. Therefore, based on the conclusions of this analysis, the present research aims to shed light on the array of meander morphology within southern Ontario, incorporating empirical data from a selection of watercourses within the region, and to develop an empirical relation for meander belt width prediction and quantification that is both developed for and supported by regionally derived data.

2.9 Research Objectives

The fundamental question driving this investigation is:

What geomorphic and hydrologic variables primarily control meander belt width?

It is anticipated that meander belt width will scale to hydrogeomorphic variables in a similar manner to other meander geometry parameters. In order to assess the presented research question, the project has three primary objectives:

1. Document meander morphology and meander belt width over a range of channel sizes and configurations in a sample of watercourses in the Credit River watershed.

2. Correlate interactions between meander belt width and primary independent variables: stream power, drainage area, discharge, bankfull channel dimensions, and channel configuration.
3. Compare statistical relations of meander belt width prediction developed using the present data set with previously established relations that are currently used in practice in southern Ontario to assess existing policies and procedures.

Chapter 3

3 Data Sources and the Credit River Watershed

3.1 The Credit River Watershed

The Credit River is a tributary to Lake Ontario with a drainage area of approximately 860km² extending northwest to Orangeville, located on the northern shore of Lake Ontario. The watershed has a well documented geomorphological database consisting of channel characteristics and measurements, collected by the Credit Valley Conservation Authority (CVC), which has been made available for the present research. The availability of data made this research feasible within the restricted time limits. The watershed displays landscape diversity, covering several distinct geological settings, many of which are characteristic to southern Ontario. By selecting 46 sites in a fluvial system that includes representative geomorphic and geological settings and range of river types and sizes, the study results will be transferrable to similar landscapes in other watersheds in southern Ontario. The purpose of this chapter is to introduce the Credit River watershed and data sources used in analysis.

The Credit River was selected for two major reasons:

1. Data availability
2. Landscape diversity

3.1.1 Location

The Credit River is located on the northern shore of Lake Ontario and is part of the Great Lakes Basin which drains into the St. Lawrence River. The watershed falls under the Credit Valley Conservation Authority's (CVC) jurisdiction. The watershed, divided into 23 sub-watersheds, stretches from its headwaters in Orangeville, Erin and Mono, through nine municipalities, eventually draining in southeastern Mississauga (Figure 3.1). At the mouth at Port Credit on Lake

Ontario, the upstream drainage is 860km² (Kennedy & Wilson, 2009), with minimum and maximum elevations of approximately 70 and 525 metres above sea level, respectively, giving a total relief of approximately 455 metres (Figure 3.2).

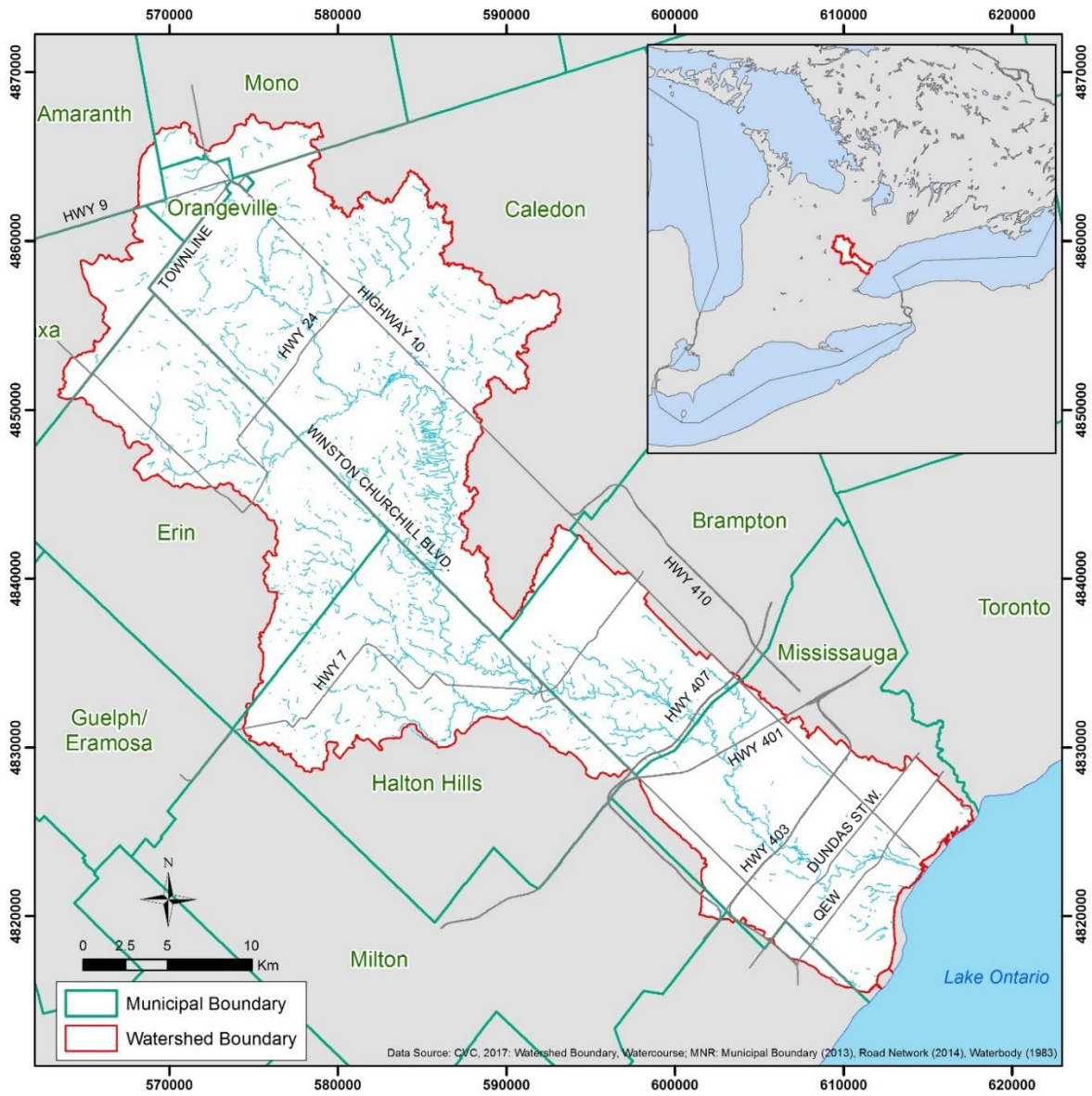


Figure 3.1 – Credit River Watershed location in southern Ontario, Canada.

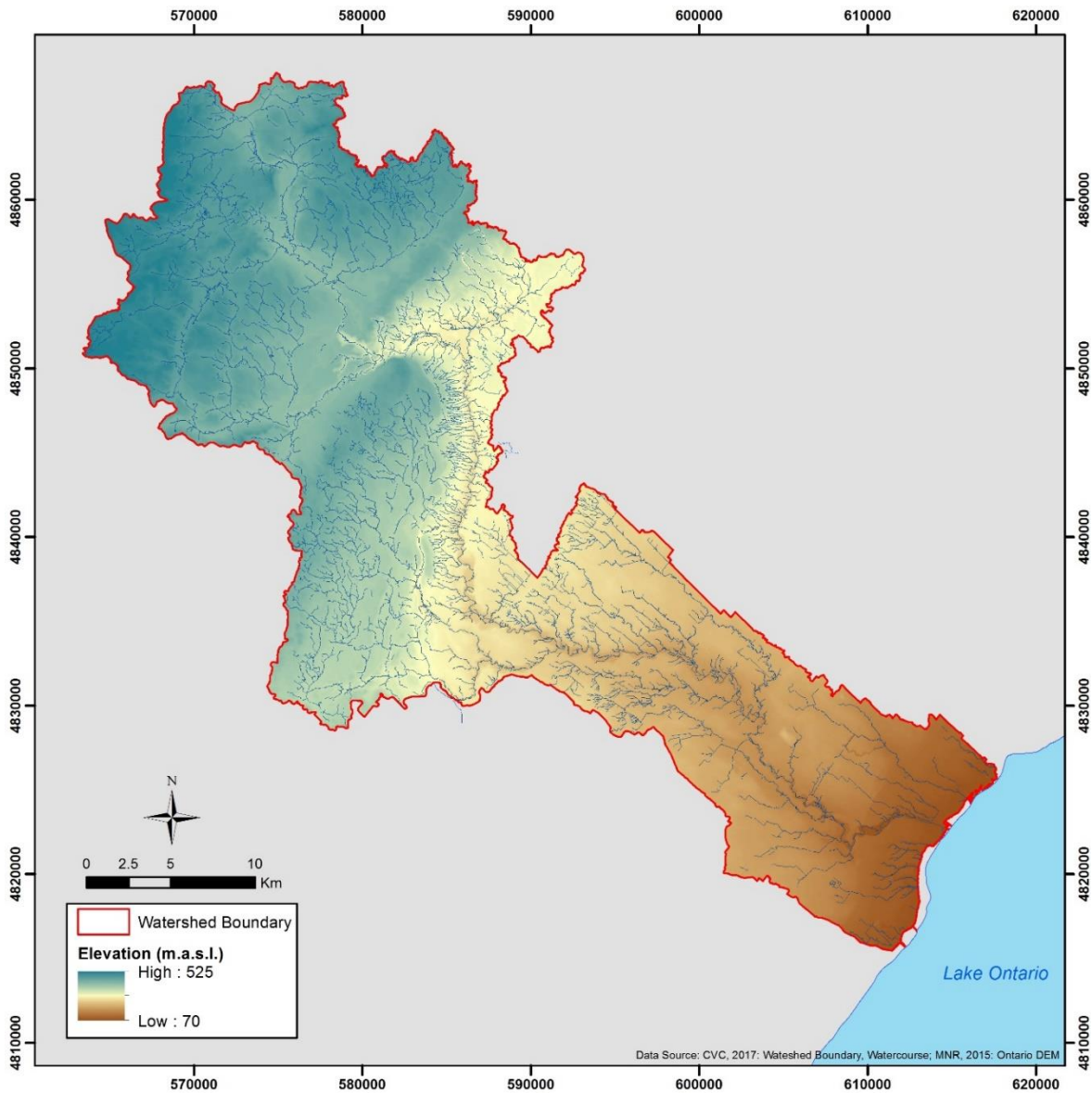


Figure 3.2 – Credit River Watershed elevation.

3.1.2 Physiography

The Credit River watershed can be divided into three distinct physiographic regions, termed by the CVC (2009) as the upper, middle, and lower watershed zones (Figure 3.3). The upper watershed zone, covering 330km² of the entire catchment, can be characterized by hilly areas of till plains, moraines, drumlins, and glacial spillways (Figure 3.4). Tributaries located here are primarily maintained by groundwater recharge, which is permitted by the permeable soils

(Kennedy & Wilson, 2009). The river exits the plateau through knickpoints in the Niagara Escarpment at Cataract and Belfountain, with the main and west branches uniting at the Forks of the Credit. The middle watershed, approximately 300km², is comprised of portions of the Niagara Escarpment, dominated by rock outcrops of dolomitic limestone and shale, and steep terrain. The Oak Ridges Moraine is a prominent feature in the eastern section of the region. The Credit River has built a wide alluvial plain on the Lake Ontario plain downstream of the escarpment, the lower watershed, which is approximately 230km² of the catchment (Kennedy & Wilson, 2009). This relatively flat topographical area, where the valley is cut into till and underlying shale, leads a gentle slope southward towards Lake Ontario (Chapman & Putnam, 1984).

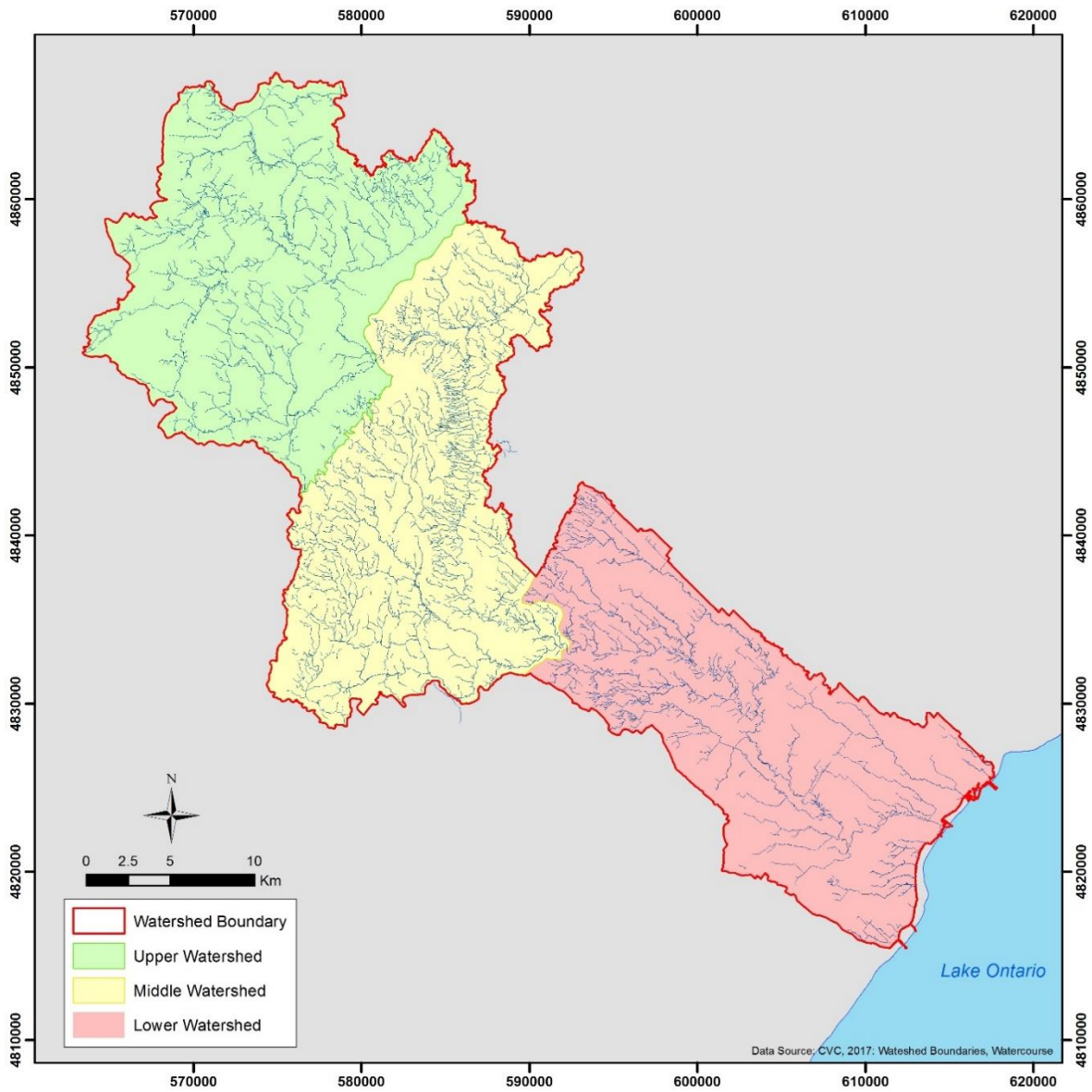


Figure 3.3 – Credit River Watershed zones.

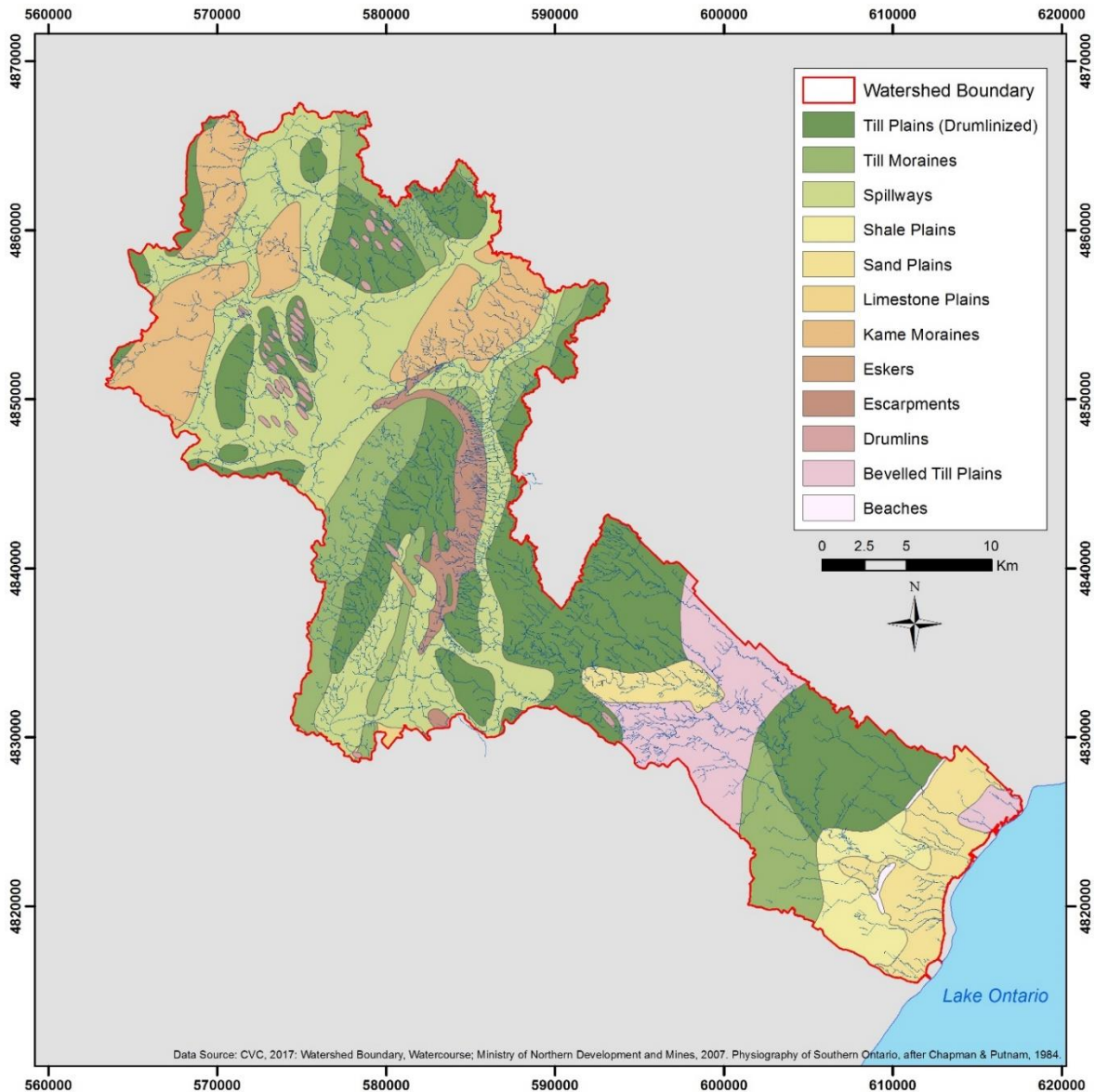


Figure 3.4 – Credit River Watershed physiography.

3.1.3 Hydrology

The Water Survey of Canada operates a total of nine stream-gauges within the Credit River catchment, of which four stream-gauges on the main branch will be addressed in this thesis. From upstream to downstream, the gauges are: 02HB013, “Credit River near Orangeville”; 02HB001, “Credit River near Cataract”; 02HB018, “Credit River at Boston Mills”; 02HB025, “Credit River at Norval” (Figure 3.5). The gauges have been operational since 1967, 1915, 1982 and 1988, respectively, and have confirmed data until 2015. Figure 3.6 to Figure 3.9 demonstrate annual

hydrographs for each gauged station using the historical datasets obtained from Water Survey Canada. A compilation of annual hydrographs from each of the gauges (Figure 3.10) demonstrates very little change in discharge since the time the gauges were installed, with the Norval gauge showing a slight trend with a very low r^2 value. The lack of a trend suggests that using a discharge for a particular time period will not greatly impact the results of model development, for this data set. The hydrographs appear typical for southern Ontario watercourses, and demonstrate little effects of urbanization within the catchment as the seasonality of the annual discharge is apparent.

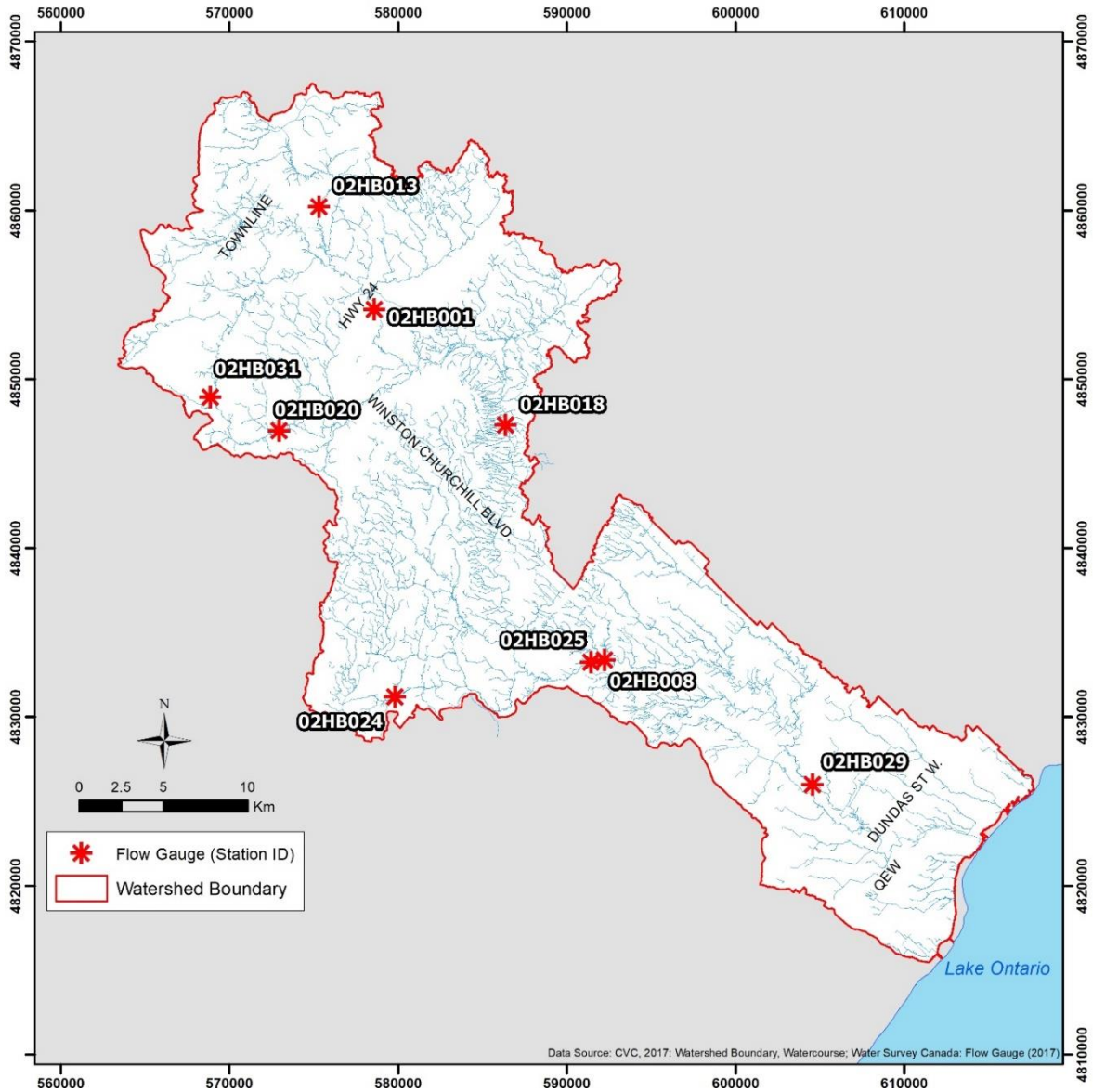


Figure 3.5 – Water Survey of Canada gauge station locations.

Credit River near Orangeville (02HB013); Credit River near Cataract (02HB001); Credit River at Boston Mills (02HB018); Credit River at Norval (02HB025)

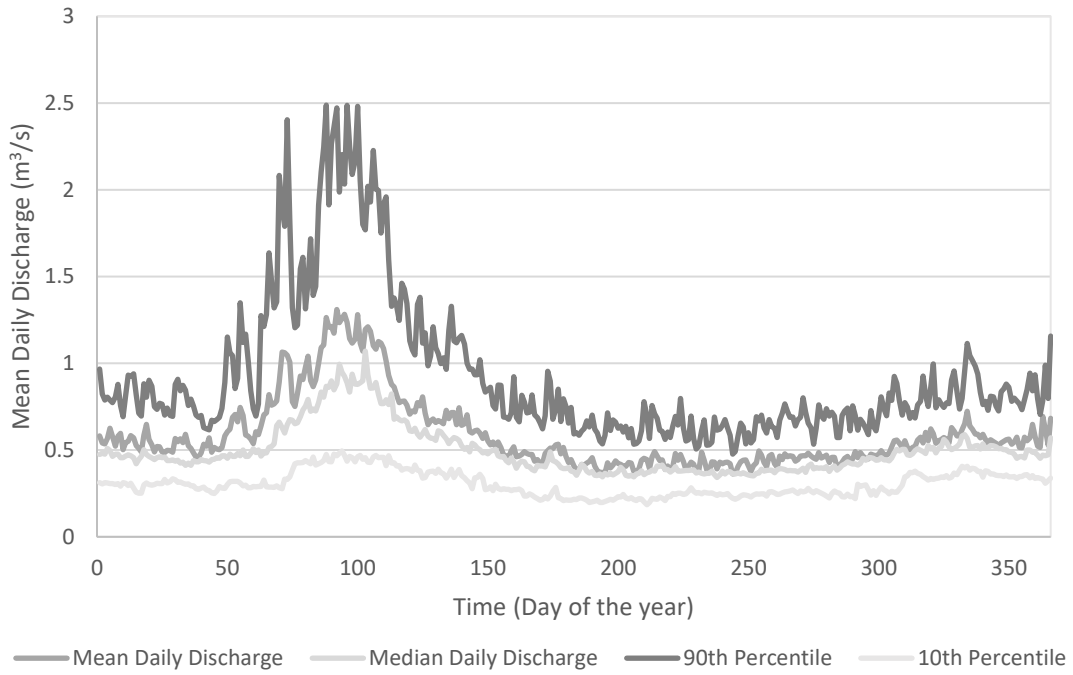


Figure 3.6 – Credit River discharge at Orangeville (1967-2015).

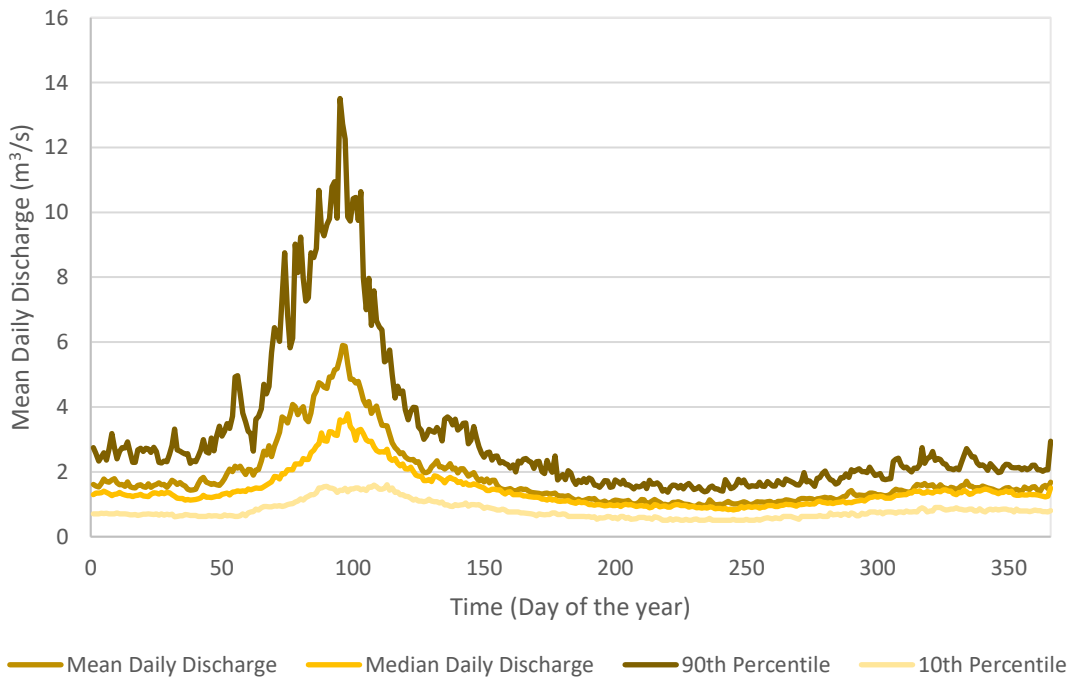


Figure 3.7 – Credit River discharge at Cataract (1915-2015).

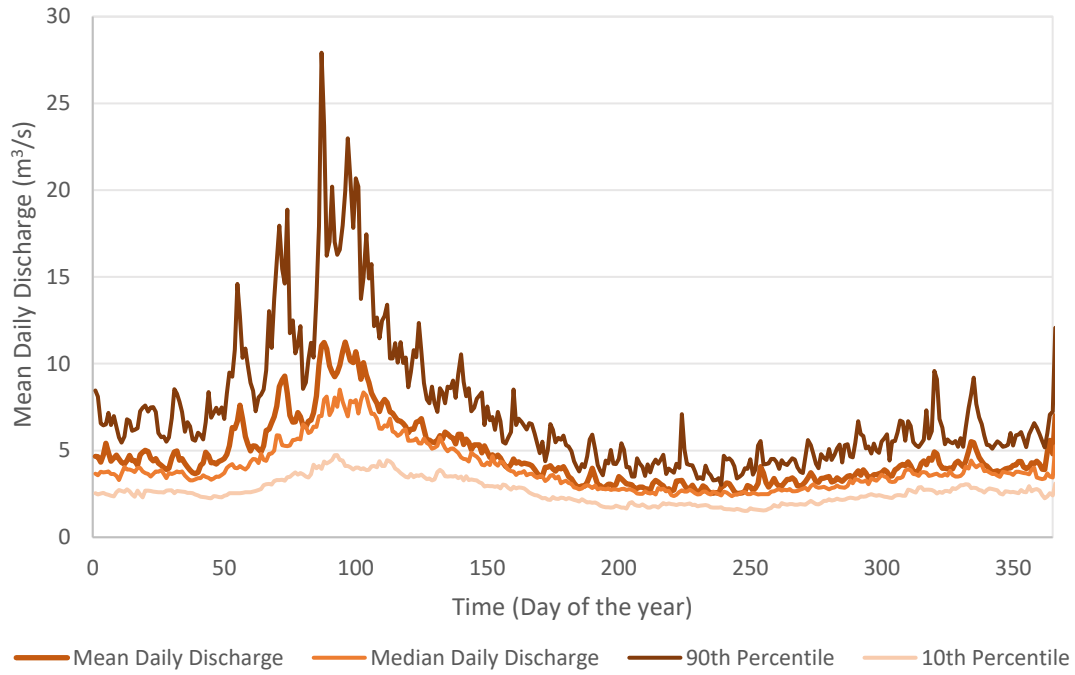


Figure 3.8 – Credit River discharge at Boston Mills (1982-2015).

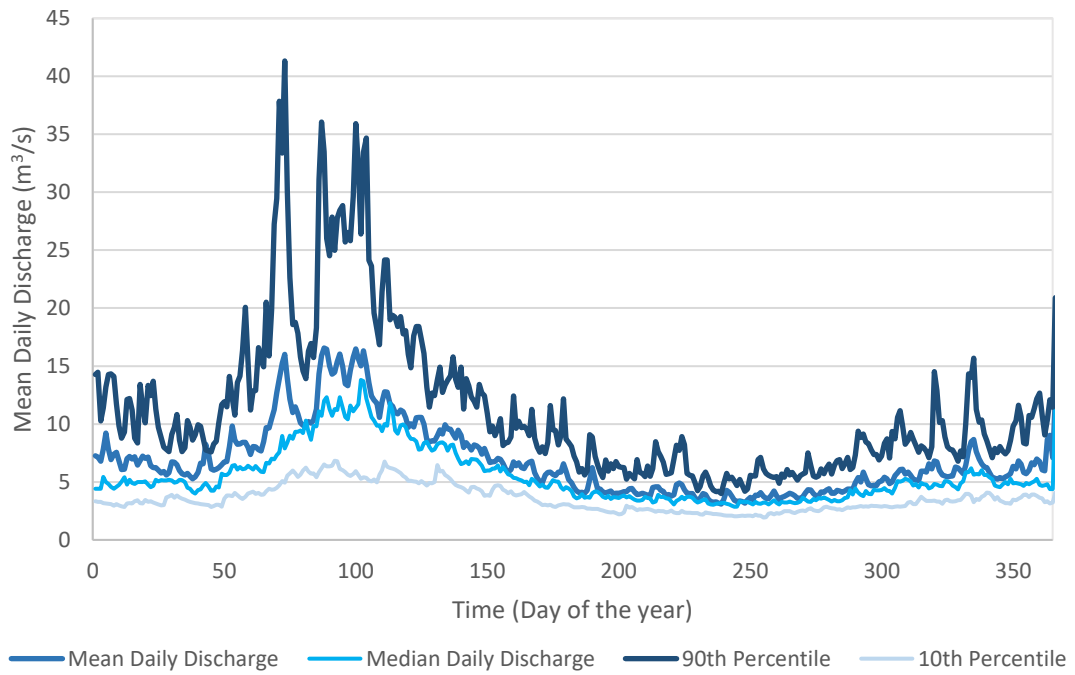


Figure 3.9 – Credit River discharge at Norval (1988-2015).

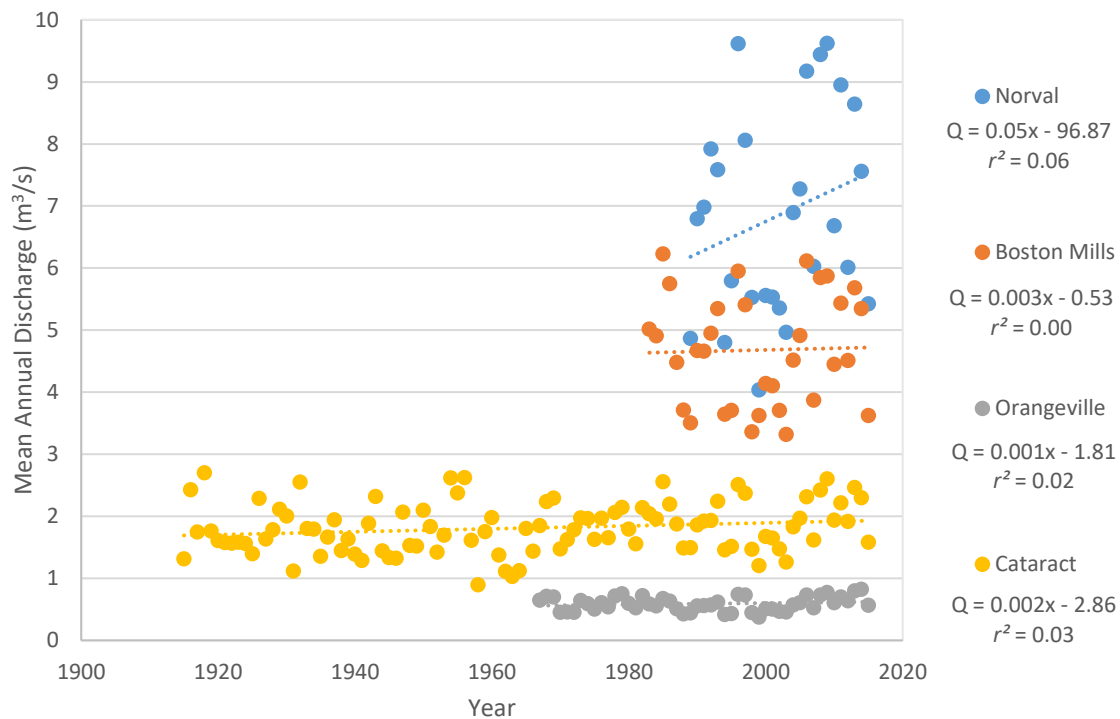


Figure 3.10 – Mean annual discharge for Credit River at four main-branch gauge stations.

3.1.4 Land Use

Land use within the Credit River watershed is primarily agricultural and developed land, which together cover approximately 70% of the basin (CVC, 2009). The lower watershed is heavily developed, covering the majority of Mississauga and western Brampton (Figure 3.11). Approximately 80% of the 750,000 living within the Credit River watershed are located within the lower watershed zone (CVC, 2009). The upper and middle watersheds have remained primarily agricultural and forested. This is, in part, due to the demand for rural estate properties, with 20% of agriculture declared as equestrian farms (CVC, 2009), and due to the Greenbelt Legislation which now protects areas of the Oak Ridges Moraine, Niagara Escarpment, and selected countryside (Figure 3.12) (Kennedy & Wilson, 2009).

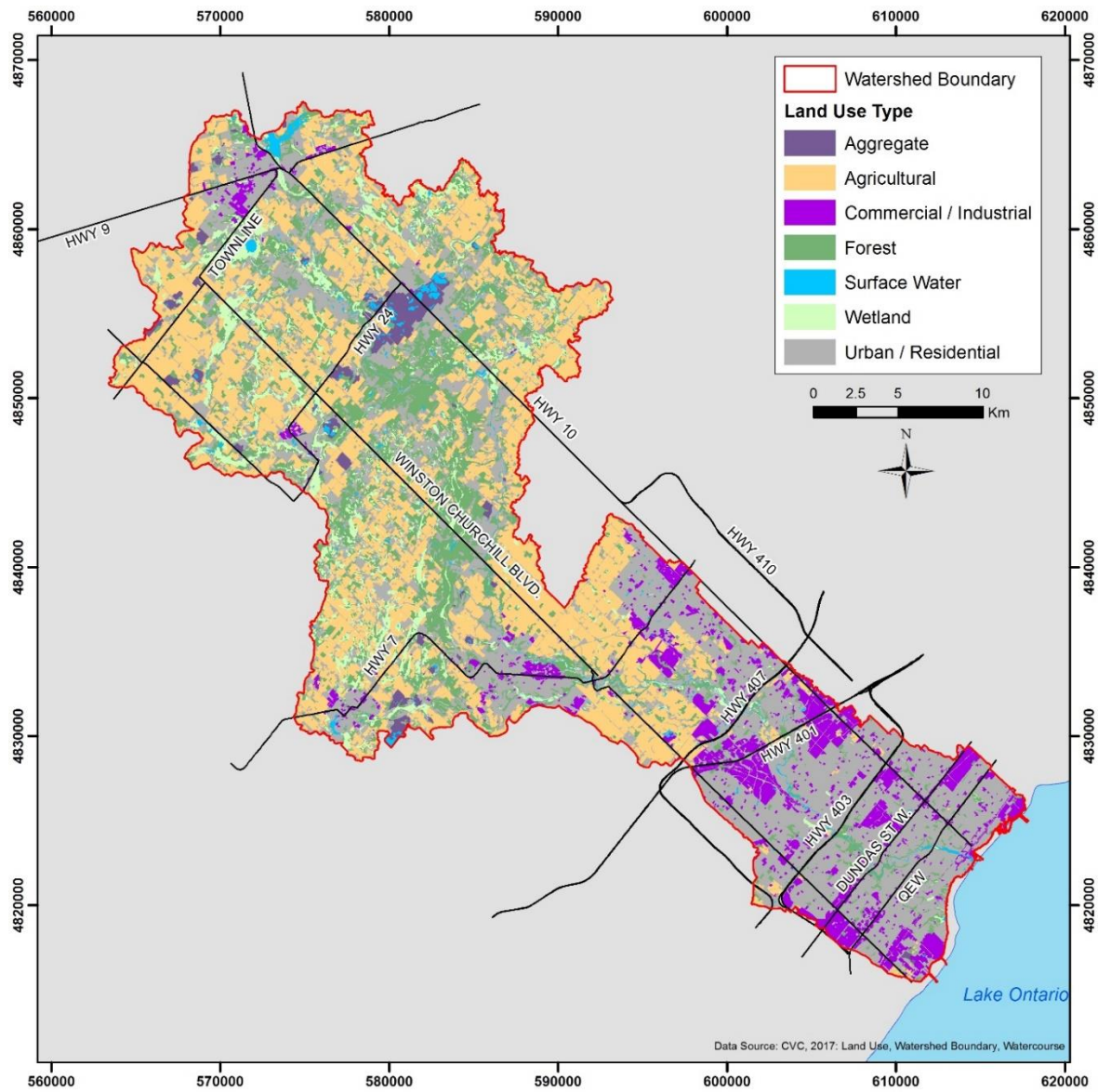


Figure 3.11 – Credit River Watershed land use.

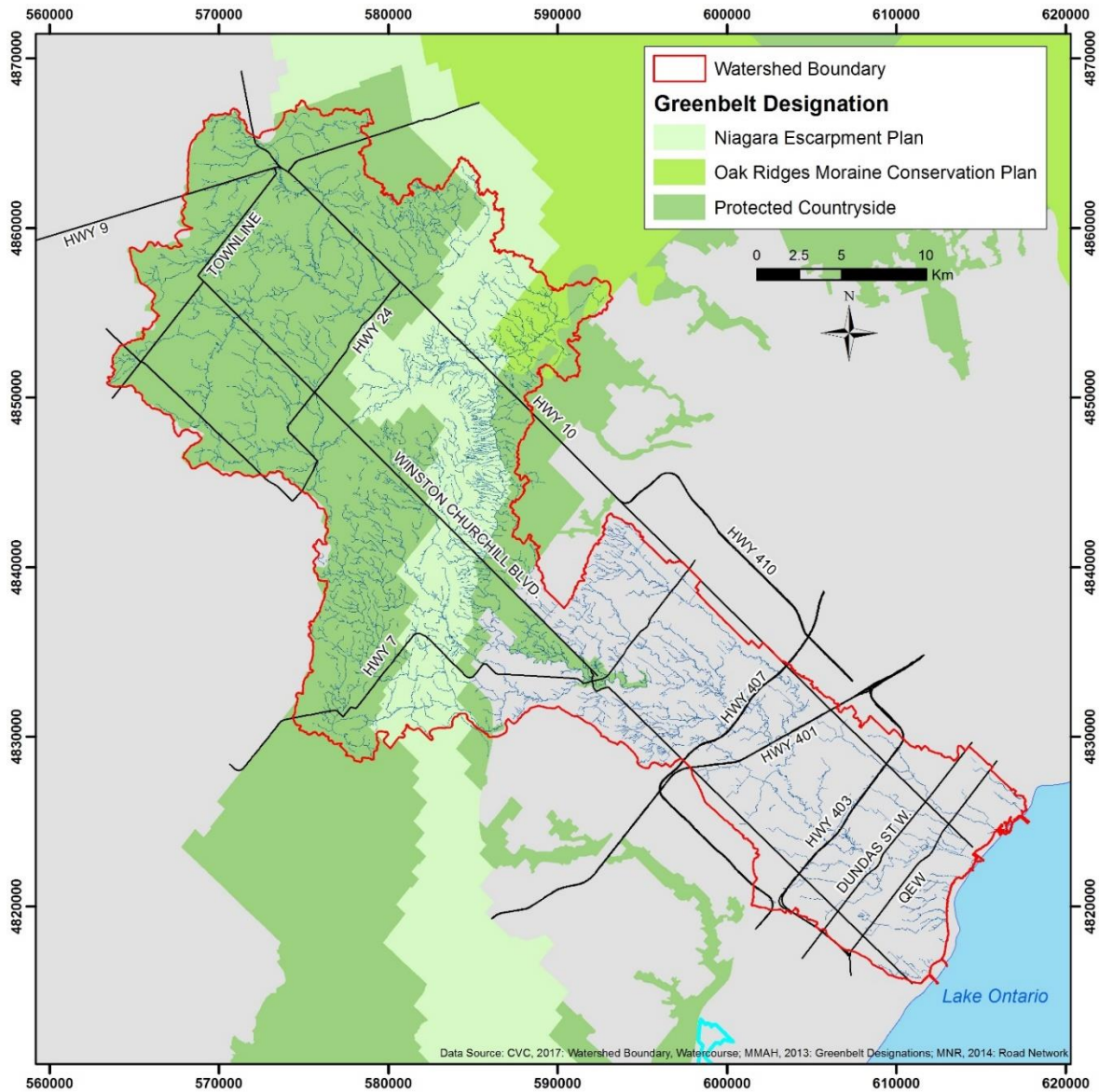


Figure 3.12 - Greenbelt boundaries within the Credit River Watershed.

3.2 Data Sources for Analysis

A large amount of data has been collected within the Credit River watershed by CVC in order to fulfill the Integrated Watershed Monitoring Program (IWMP), which originated in 1999. These data are of value with respect to the objectives of this thesis, and can be used to determine, analyze, and validate the findings of meander belt dimensions for the development of a predictive meander belt width model. Table 3.1 summarizes the data sources and measurement of variables, which

were included in the statistical analysis. Sources of data are described in detail in the sections to follow.

Table 3.1 – Sources and measurement of data used in statistical analysis.

Variable	Measurement	Source
Bankfull channel dimensions (width and depth)	Field investigation	CVC database (validated)
Drainage area	Desktop analysis (ArcGIS software)	CVC database (validated)
Valley gradient	Desktop analysis (ArcGIS software)	Primary data
Discharge	Estimated	OFAT (III)
Stream power (total and specific)	Calculated	Calculated with primary data
Sinuosity	Desktop analysis (ArcGIS software)	Primary data
Amplitude	Desktop analysis (ArcGIS software)	Primary data
Stream Order	Desktop analysis (ArcGIS software)	CVC database

3.2.1 Credit River Watershed Orthophotography

An orthorectified image of the Credit River watershed was obtained from CVC. The 2013 image has a 0.5 metre resolution, and was flown by First Base Solutions on behalf of the Region of Peel and CVC. The orthoimage was used to delineate watercourse centrelines, assess channel planform and conditions, and delineate meander belt widths, as well as several other morphological parameters.

3.2.2 Credit Valley Conservation Geomorphological Database

A geomorphological database of several watercourses has been compiled by CVC as a sector in the IWMP conducted by CVC personnel within the Credit River watershed. Over 80 sites are still currently monitored by CVC; however, some sites have been discontinued, while others were assessed through subwatershed studies, largely conducted by environmental consulting companies. The database includes channel dimensions and conditions, as well as coarse-scaled

information regarding geology, vegetation, and land use surrounding the watercourse. The data obtained from CVC were collected using standard protocols; however, as data collection has occurred over several years, with some measurements dating back to the 1990s, some bias or erroneous measurement is anticipated. Parameters that were used in statistical analysis from the geomorphological database were confirmed or validated through field investigation and desktop analysis. Therefore, the database provided by CVC was used more as a background check of measured variables and in the process of site selection, rather than a direct data source. Meander belt widths were only available for a select number of sites within the database, and were re-measured for all selected sites.

3.2.3 Credit River Watershed Study Conducted by Aquafor Beech Ltd.

Aquafor Beech Limited conducted a watershed study titled, *Estimated Meander Belt Delineation: Credit Valley Watershed*, in 2005, which was presented to CVC. The information from the study was used in the present research to select additional watercourses outside of the CVC monitoring program in order to supplement the number of sites considered. The information provided by the study is much less specific than that obtained from CVC, only providing general characteristics of watercourses, rather than detailed measurements. Additionally, meander belt widths were provided for several watercourses, and were assessed and viewed in analyses, but were not used in the calculation of the empirical models to maintain consistency in meander belt delineations.

3.2.4 Contours

A 2003 5-metre interval contour map for southern Ontario was obtained from the Ontario Ministry of Natural Resources. Although the resolution or interval of the contours is low, the contours were used only to identify whether a watercourse was confined or unconfined within a well-defined valley, for which the data are reliable.

3.2.5 Provincial Digital Elevation Model

The Provincial Digital Elevation Model (DEM) v.2 (OMNR, 2006) for southern Ontario is composed of 10 metre by 10 metre cells with elevation values with a 2.5 metre vertical accuracy representing the ground surface. The data are available as a series of tiles covering parcels of terrain. The watershed for the Credit River requires 3 tiles: 086, 087, and 090. The DEM tiles were imported to ArcGIS 10.4, and were merged together using the mosaic data management tool to create one file (Figure 3.13).

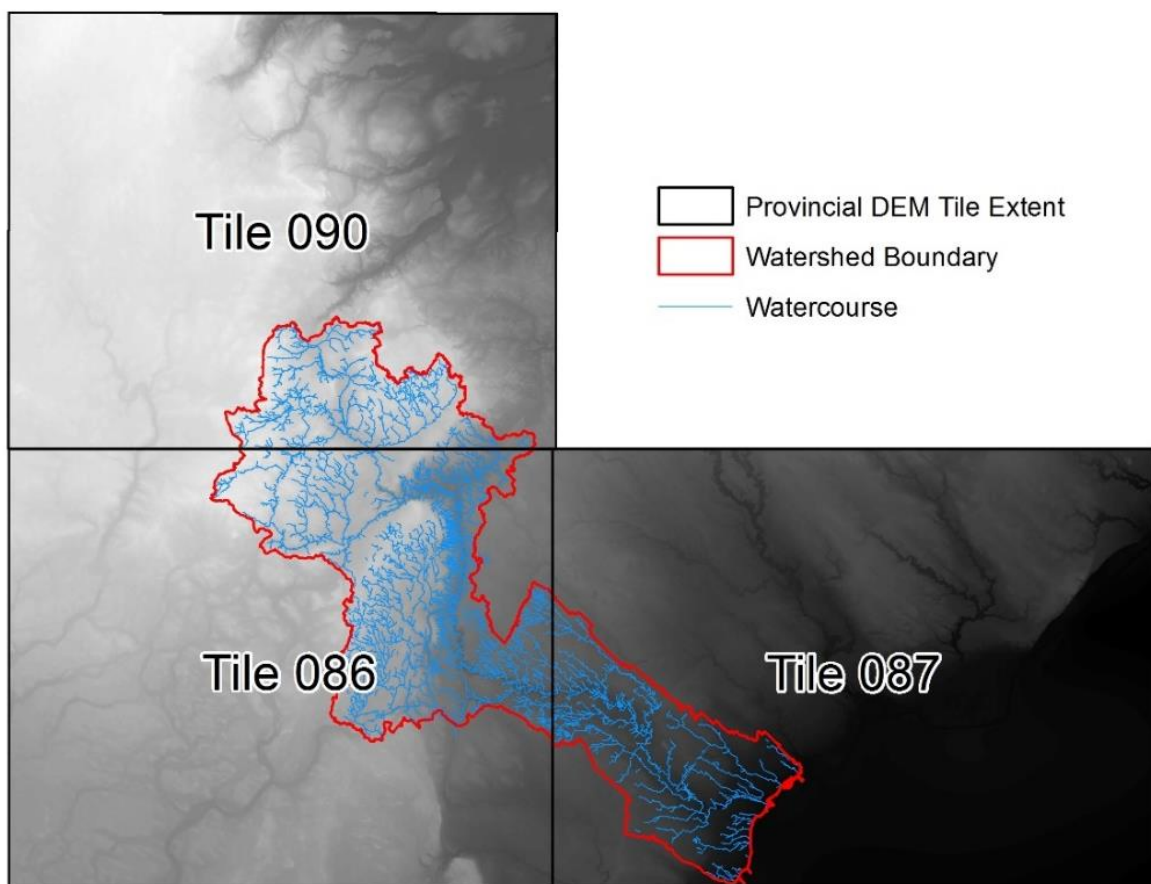


Figure 3.13 – Provincial digital elevation model tiles (OMNR, 2006).

3.3 Summary

The Credit River watershed is comprised of representative geomorphic and geological settings, and a range of river types and sizes, which may allow for the results of this study to be transferrable to similar landscapes in southern Ontario. The data available for the Credit River watershed, primarily based on existing CVC monitoring sites, provide the primary data for analysis in the thesis.

Chapter 4

4 Site Selection and Measurement of Parameters

4.1 Site Selection

Sites were selected from the CVC geomorphic database based on the following conditions:

- The drainage area of the site is greater than 1km²
- There are little to no channel alterations or modifications apparent
- The channel is largely unconfined or partially confined
- The channel is visible using the orthoimagery
- The site was accessible for field investigations

These conditions were selected to ensure the delineation of a meander belt was appropriate and feasible. Headwater watercourses with less than 1km² tend to show characteristics of wetlands, where meander belt delineation is not applicable because there is no defined channel. Watercourses that have been previously altered or straightened would not demonstrate natural meandering tendencies, and therefore would influence the predictive model for meander belt width. Channels that are confined in a valley setting (see Chapter 2) are said to not be subject to meander belt delineation based on the Ministry of Natural Resources Technical Guideline policy document (MNR, 2002) and the belt width delineation guidelines from Parish Geomorphic (2004), and therefore were avoided in the dataset of selected sites.

Using these criteria, 38 sites were selected from the CVC database. In order to supplement the number of sites used in this analysis, additional sites were selected using information regarding channel confinement from the watershed study conducted by Aquafor Beech Ltd. As stated, the Credit River watershed is a large system within southern Ontario. In order to quickly eliminate confined systems from the analysis, the Aquafor Beech study was used to discretize the

watercourses present within the watershed, and select only those that were unconfined systems. In addition to the previous conditions, site access was also considered in order to conduct field investigations to verify the previously collected data. The total sample size for the presented research 46 river reaches (Figure 4.1).

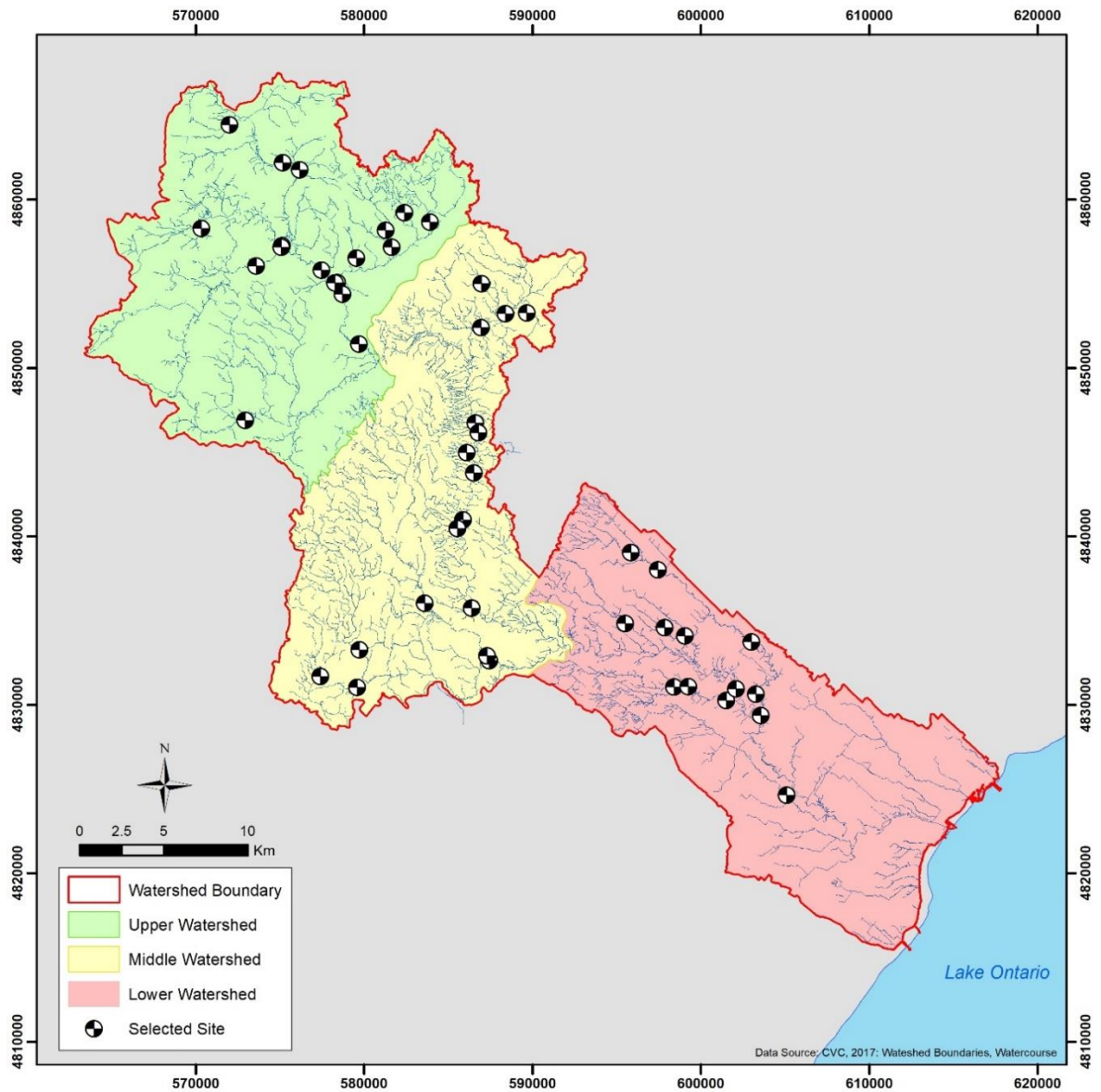


Figure 4.1 – Selected sites within the Credit River watershed.

4.1.1 Characteristics of Selected Sites

Sites selected for analysis range in size (drainage area, bankfull channel dimensions), channel setting, sinuosity, geology, and other physiographic conditions. Appendix A lists the locational, hydrological, geomorphological and geologic characteristics for each of the selected sites, with descriptive statistics for each parameter summarized in Appendix B. Figure 4.2 to Figure 4.4 display three examples of the varied channel size, sinuosity, confinement, and degree of regularity in meandering tendencies.

Figure 4.2 displays a small or low-order watercourse used in this analysis, which exhibits a high sinuosity and a fairly regular and simple meandering form. The watercourse is also unconfined within a valley, and is vegetated in the surrounding local area. The conditions and characteristics of this particular watercourse was similar to several others selected within this thesis. For the current database, 2nd and 3rd order streams ranged in sinuosity from 0.11 – 5.36, with an average of 2.16.

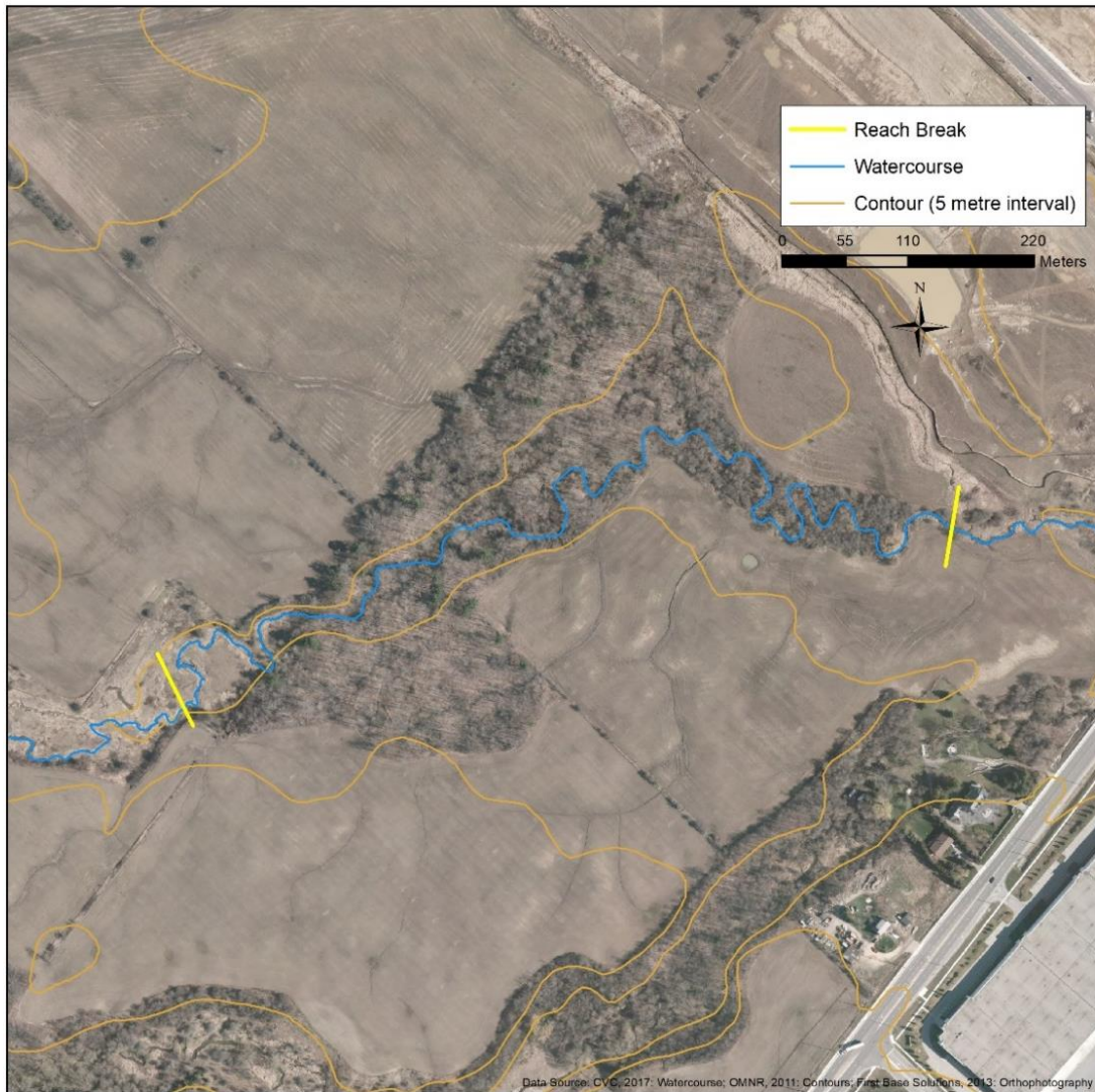


Figure 4.2 – Sinuous low-order channel with some degree of regular meandering (Reach LC3).

Figure 4.3 displays a slightly larger, or medium-sized watercourse that was selected. In contrast to the previous watercourse, this system demonstrates a more irregular meandering form, with inconsistent channel orientation, particularly in the downstream end of the reach before the confluence with the main branch of the Credit River. The meandering nature of this reach causes issue when measuring meander amplitude, as it is difficult to distinguish which particular meander

bend is the governing amplitude of the reach. Again, this channel demonstrates an unconfined setting, common amongst the selected sites as it was a selected characteristic.



Figure 4.3 – Irregular meandering apparent in a medium-sized watercourse (Reach FC1).

Figure 4.4 displays a larger watercourse which displays a more regular meandering planform, a characteristic of many of the larger systems included within this analysis. Of the selected reaches, the larger order systems (4th to 6th order) ranged from 0.07 – 2.89 in sinuosity, with an average of

1.16. When compared to the sinuosity characteristics of low-order reaches, it appears there is a tendency for low-order or headwater streams to exhibit higher sinuosity values.



Figure 4.4 – Larger fluvial system with regular meandering tendencies (Reach CR11).

The mobility or the change in meander planform over time of the selected watercourses was also assessed visually using digital aerial photographs from 1954, with a 2.5 metre resolution, produced by Hunting Survey Corporation Limited (2016). Unfortunately, the images which cover the aerial extent of the Credit River watershed are not georeferenced, and display varying degrees of

distortion; therefore, were not used in detailed migration analyses, but were only visually assessed. Upon analysis, many of the selected channels appeared to remain relatively stable since 1954. Figure 4.5 and Figure 4.6 display two examples of watercourses which were selected for analysis that exhibit very little movement from 1954 to 2013. Although a detailed comparison is difficult due to the differences in scale, both systems depicted appear relatively stable with only slight increases in channel sinuosity in local portions of the reach. This is a common feature of several selected sites, with 27 of the 46 sites demonstrating relative stability since 1954. The majority of the relatively stable reaches were found in the middle watershed zone, with a range in total stream power from 19 to 5340 W/m².



Figure 4.5 – Watercourse which exhibits relative stability from 1954-2013 (Reach HC1).

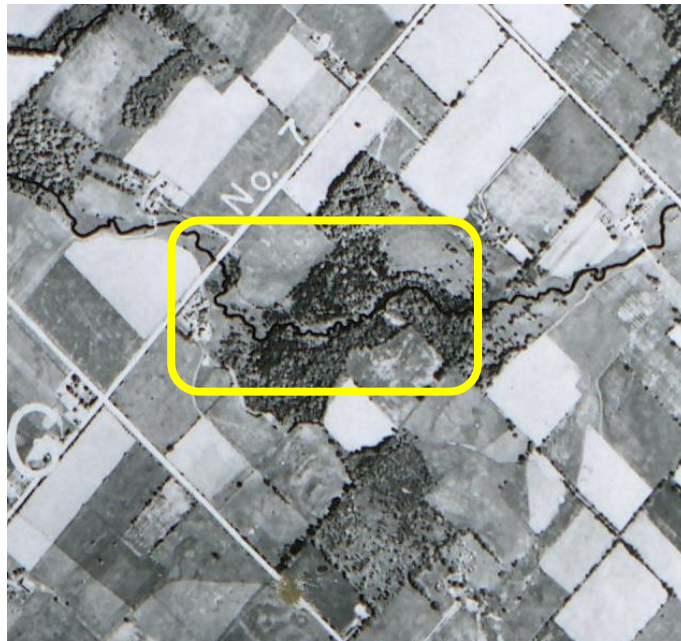


Figure 4.6 – Watercourse which exhibits relative stability from 1954-2013 (Reach BC2).

Although this stability in planform was apparent in the majority of selected reaches, there were some that exhibit channel mobility based on previous channel configurations. From the 46 selected sites, 16 appeared to be relatively active since 1954. The most active channels were found in the upper watershed zone, and ranged in total stream power from 4 to 1484 W/m². Three selected reaches were not visible on the 1954 imagery. Figure 4.7 and Figure 4.8 show two examples of selected sites which have changed in planform since their 1954 configuration. Both watercourses appear to have increased in sinuosity and natural meandering tendencies since 1954. This could be explained, in part, by land use changes, where previously much of the watershed was used for agriculture, much has been restored to more natural areas. These types of channels demonstrate the necessity for meander belt width models to be established on watercourses that display natural meandering planforms. Using channels which have been recently altered or previously straightened could result in underestimation of the meander belt width.

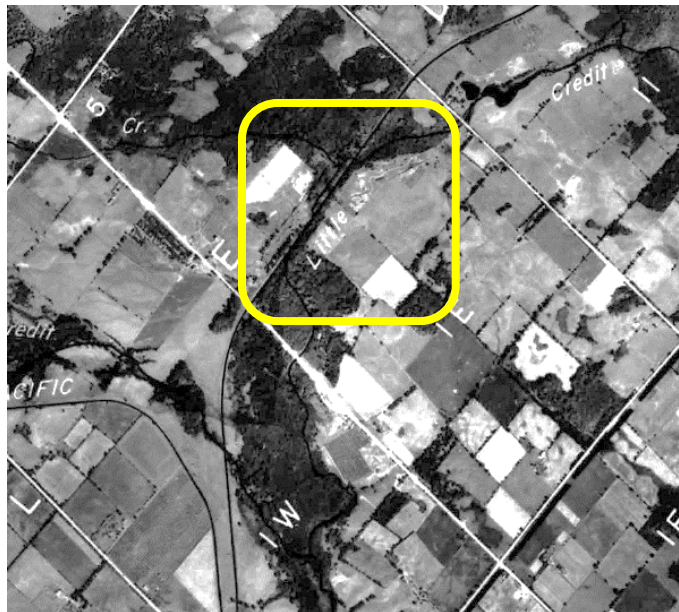


Figure 4.7 – Watercourse which exhibits relative instability from 1954-2013 (Reach LCR1).

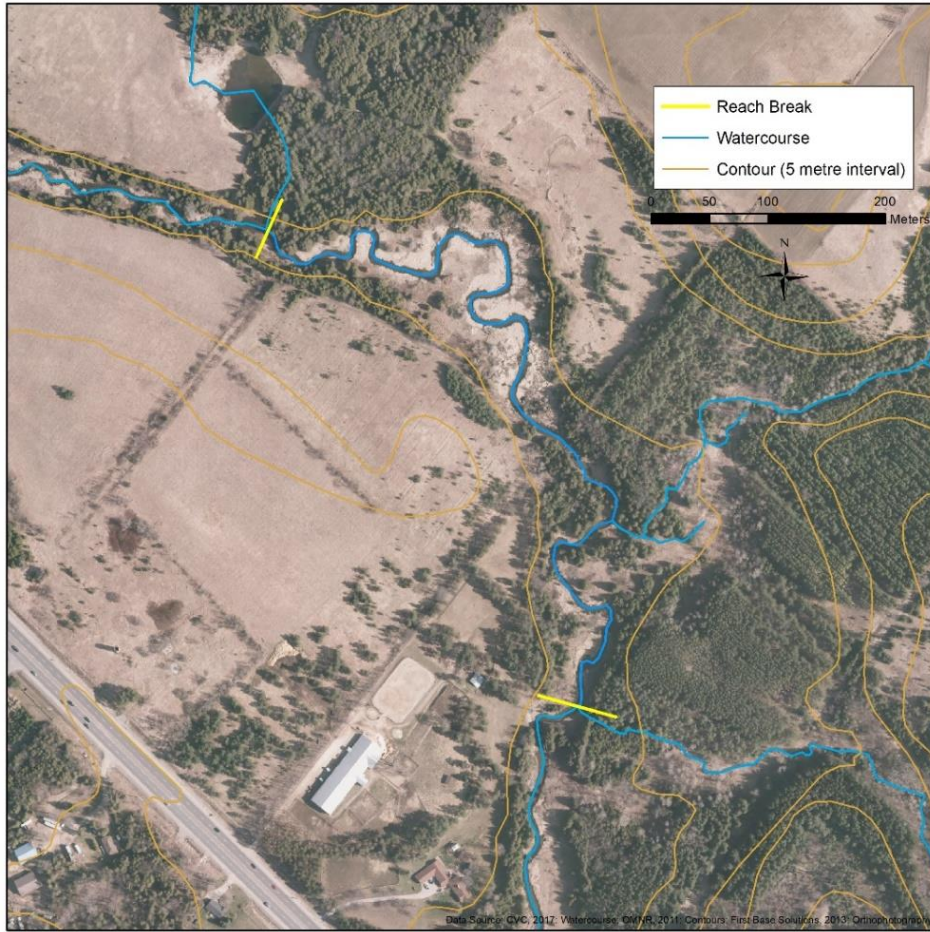


Figure 4.8 – Watercourse which exhibits relative instability from 1954-2013 (CR9).

4.2 Field Investigations

All sites were visited in the field in order to confirm channel conditions and bankfull dimensions. Priority was given to additional sites, which were selected with assistance from the Aquafor Beech Ltd. watershed study, as well as sites that were either discontinued by CVC's monitoring program or sites which were assessed during subwatershed studies by consulting companies. Bankfull widths and depths were measured several times throughout a reach in order to determine a mean bankfull value. Additionally, bank materials and riparian vegetation type were generally characterized and confirmed. The form used for field investigation recordings is in Appendix C.

4.3 Desktop Analysis

4.3.1 Drainage Area

Drainage areas for each site were delineated in the GIS software ArcGIS 10.4 using the Provincial DEM. Points for each site were created at the most downstream end of the reach in order to capture complete drainage areas for each watercourse. The process by which drainage areas were delineated, as well as the inputs required for delineation for each site are outlined in Figure 4.9.

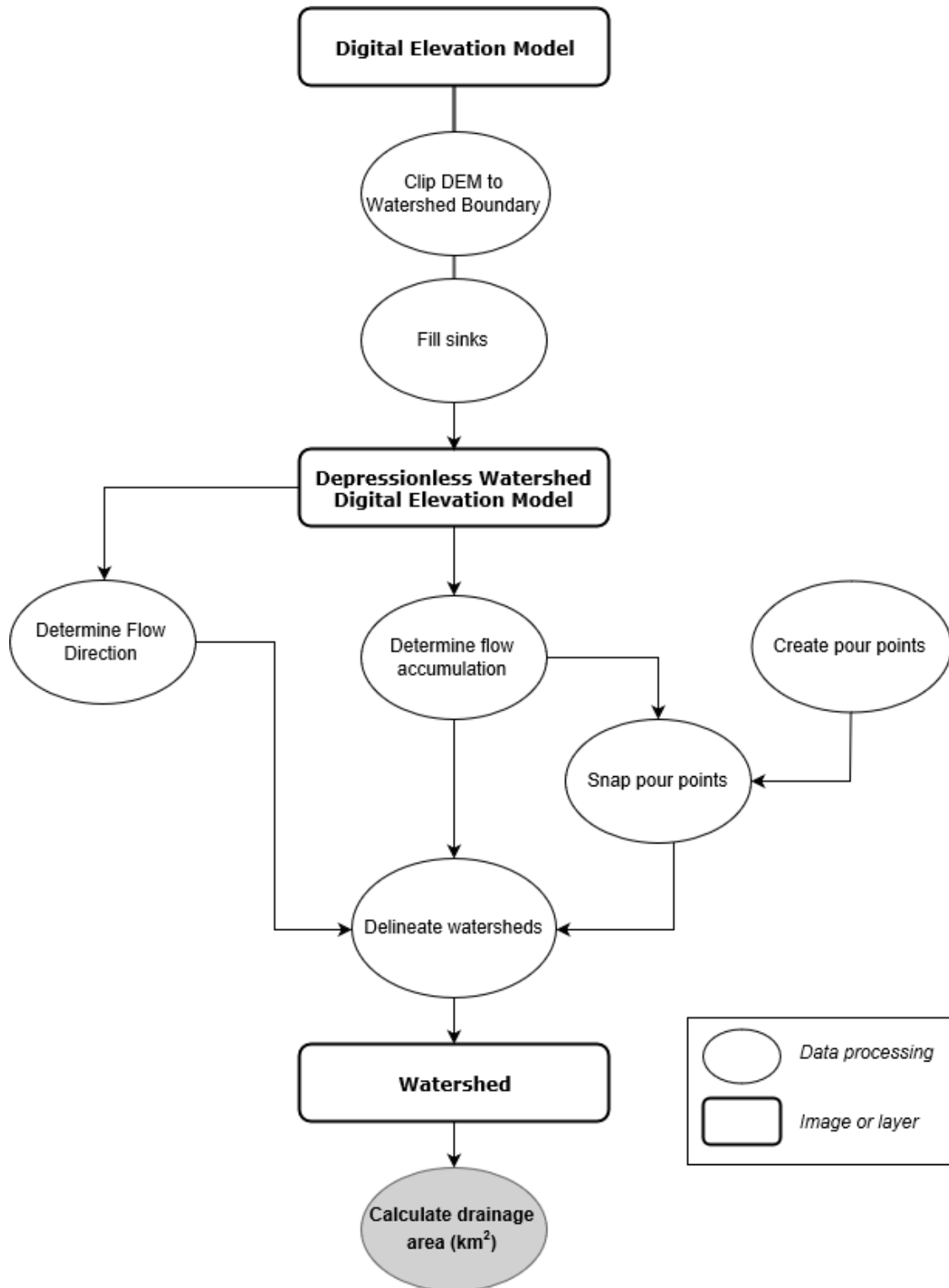


Figure 4.9 – GIS-based drainage area measurement flow chart.

4.3.2 Discharge

The Ontario Flow Assessment Tool (OFAT III), developed by the Ontario Ministry of Natural Resources and Forestry, was used to estimate two-year mean daily discharge for each of the selected sites. OFAT III is an online application, which automates extraction of several measurements of hydrology and stream flow statistics. Where gauged data are available, OFAT uses those data to provide hydrologic information for watercourses. Within the Credit River watershed, there are nine gauges present, operated by Water Survey Canada. Only two of the selected 46 sites are located directly upstream from a gauge station; therefore, discharge values were estimated using OFAT III for all of the selected sites. Additionally, the use of only estimated discharge values will assist with consistency of measurement across the entire data sample. Discharge was estimated using the Moin & Shaw (1985) multiple regression method employed by OFAT III. Regression equations were developed for three distinct regions across Ontario, with southern Ontario characterized as Region C. Parameters used to estimate discharge include drainage area, base flow index, slope of the main channel, areas controlled by lakes and swamps, mean annual runoff, and mean annual precipitation, listed in order of importance. The influence of additional parameters on the estimated discharge values other than drainage area can be seen in regression plots to follow.

4.3.3 Other Hydrogeomorphic Parameters Measured or Calculated

Although some sites from the geomorphological database obtained from CVC had channel gradients that were measured, the spatial extent of the gradient, as well as the procedure of measurement were unknown. Therefore, for consistency, valley gradients were calculated using the GIS software ArcGIS 10.4 with the Provincial DEM. Elevations were obtained for the

upstream and downstream extents of each selected reach. The change in elevation over the reach was then divided by the valley length to determine the valley gradient.

Total stream power (ω) and specific stream power (Ω) were calculated using the following equations (Leopold, Wolman, & Miller, 1964):

$$\omega = yQS \quad 4.1$$

$$\Omega = \frac{\omega}{w} \quad 4.2$$

where y is the specific weight of water ($9806 \text{ kg/m}^2\text{s}^2$), Q is the two-year recurrence interval mean daily discharge, S is the channel gradient, and w is mean bankfull channel width. Sinuosity and amplitude were both measured using methods described in Chapter 2.

4.4 Meander Belt Delineation Procedure

The method of delineating a meander belt, which was employed by the presented research, was that of the *Belt Width Delineation Procedures* guideline document written by Parish Geomorphic (2004) for Toronto and Region Conservation Authority (TRCA). The guideline document outlines five procedures which can be used to delineate a meander belt under different circumstances. Only *Procedure 1*, which focuses on delimiting a preliminary meander belt, or the general location of a meander belt, was used. As highlighted in Chapter 2, *Procedures 2-4* include future channel adjustments based on anticipated changes within the fluvial system. The goal of this thesis is to develop a model for preliminary meander belt width prediction without the additional erosion belt calculation or hydrologic changes. The following sections highlight the methods associated with meander belt width delineation.

4.4.1 Reach Delineation

A reach may be defined as a length of channel, which displays similarity with respect to channel form, valley and floodplain setting, and hydrologic and sediment functions. Therefore, a meander belt is delineated at a reach scale as all processes are expected to occur at similar rates and the channel is anticipated to respond in a similar manner throughout the river segment (Parish Geomorphic, 2004).

In order to delineate reach breaks for the selected sites, orthophotography, contours, and a watercourse layer were used in ArcGIS 10.4. Particular differences within the landscape which were used to identify a break in a river reach included:

- Valley setting (channel confinement)
- Vegetation
- Sinuosity
- Confluence of a tributary

Figure 4.10 demonstrates an example of reach delineation, where reach breaks were placed due to the culvert located under the road crossing at the upstream end, and the addition of a pond inlet at the downstream end.

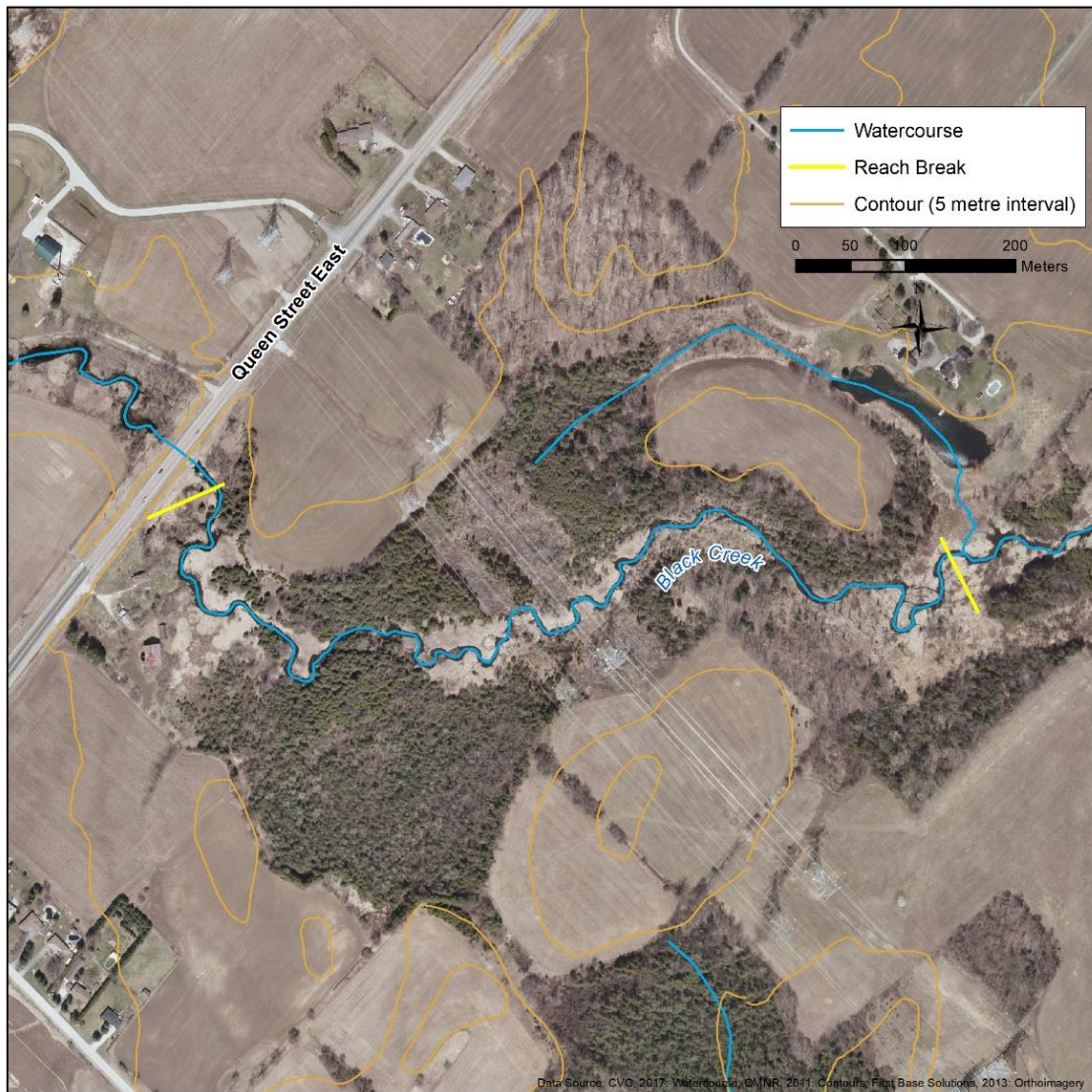


Figure 4.10 - Reach delineation (Reach BC2).

4.4.2 Digitizing Meander Axis

A meander axis is a term used to identify the down-valley orientation of a meandering channel reach (Parish Geomorphic, 2004) from which meander belt width is measured in order to remove large-scale valley sinuosity. Identifying a meander belt axis can be relatively straightforward for simple meander patterns but can be more difficult for compound meander patterns. Figure 4.11 demonstrates an example of meander axis identification for a compound meander pattern, where

the meander axis follows secondary meandering trend. Although the Parish Geomorphic guideline states that the identification of a meander axis is not necessary for preliminary meander belt width delineations, meander axes were documented in order to supplement meander belt width measurement. Meander axes were identified for each of the selected sites in ArcGIS 10.4 using orthophotography, contours, and a watercourse layer.

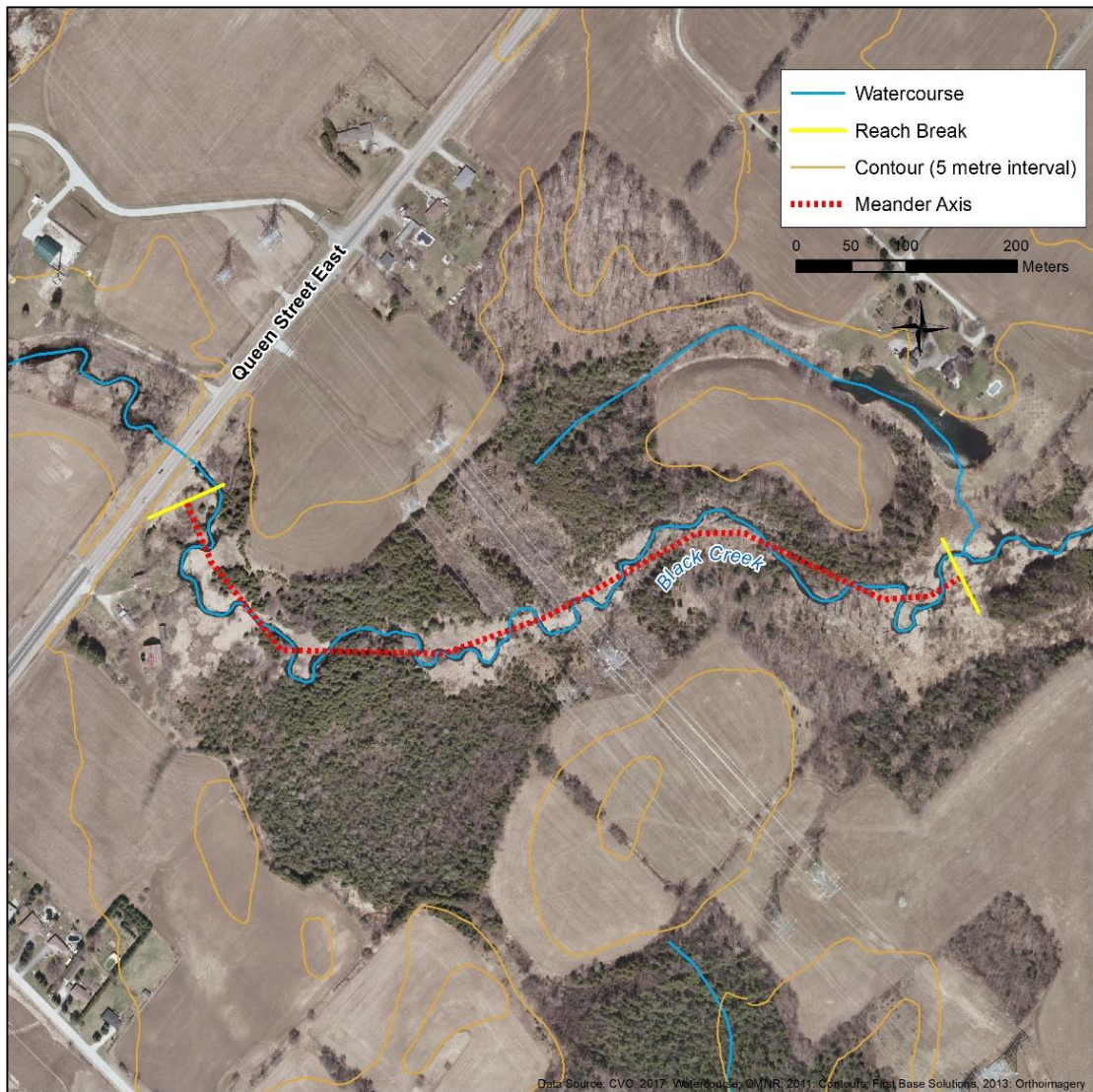


Figure 4.11 – Meander axis identification (Reach BC2).

4.4.3 Digitizing Meander Belt

Using the meander axis as a centreline, a meander belt can be delineated as, “parallel lines drawn tangential to the outside meanders,” (Parish Geomorphics, 2004). Meander belts were delineated following *Procedure 1* from the *Belt Width Delineation Guideline* (Parish Geomorphics, 2004), using orthophotography, contours, a watercourse layer, and the previously identified meander axis. It is necessary to consider the valley setting in that partially confined watercourses will be limited by valley walls. Contours were used to identify any restrictions of channel planform, and therefore played a role in the meander belt placement.

There are various assumptions and limitations associated with meander belt delineation analysis, as outlined in the Parish Geomorphics (2004) guideline, as follows:

Assumptions:

- Existing meander configuration represents equilibrium condition between meander pattern and the driving forces of meander form;
- Meander belt is not actively shifting across the floodplain.

Limitations:

- Accuracy of meander belt width position is dependent on scale of mapping;
- Meander belt does not take into account future changes in meander configuration;
- Meander belt does not take into account future geotechnical slope stability adjustments.

The scale of mapping was consistent for all selected sites; therefore, smaller watercourses may be less accurate. As only preliminary meander belt widths were delineated, the limitations of future channel configurations and geotechnical slope stability adjustments were not relevant. With these assumptions and limitations recognized, meander belts were delineated for each of the selected sites. Figure 4.12 demonstrates an example of a meander belt delineation, where parallel lines were drawn to encompass the meandering tendencies of the reach, centred around the meander axis. Meander belt width was then measured as the distance between the parallel lines for each site,

resulting in a measurement of the maximum belt width for the particular reach, as demonstrated in the Parish Geomorphic (2004) *Procedure 1* methods.

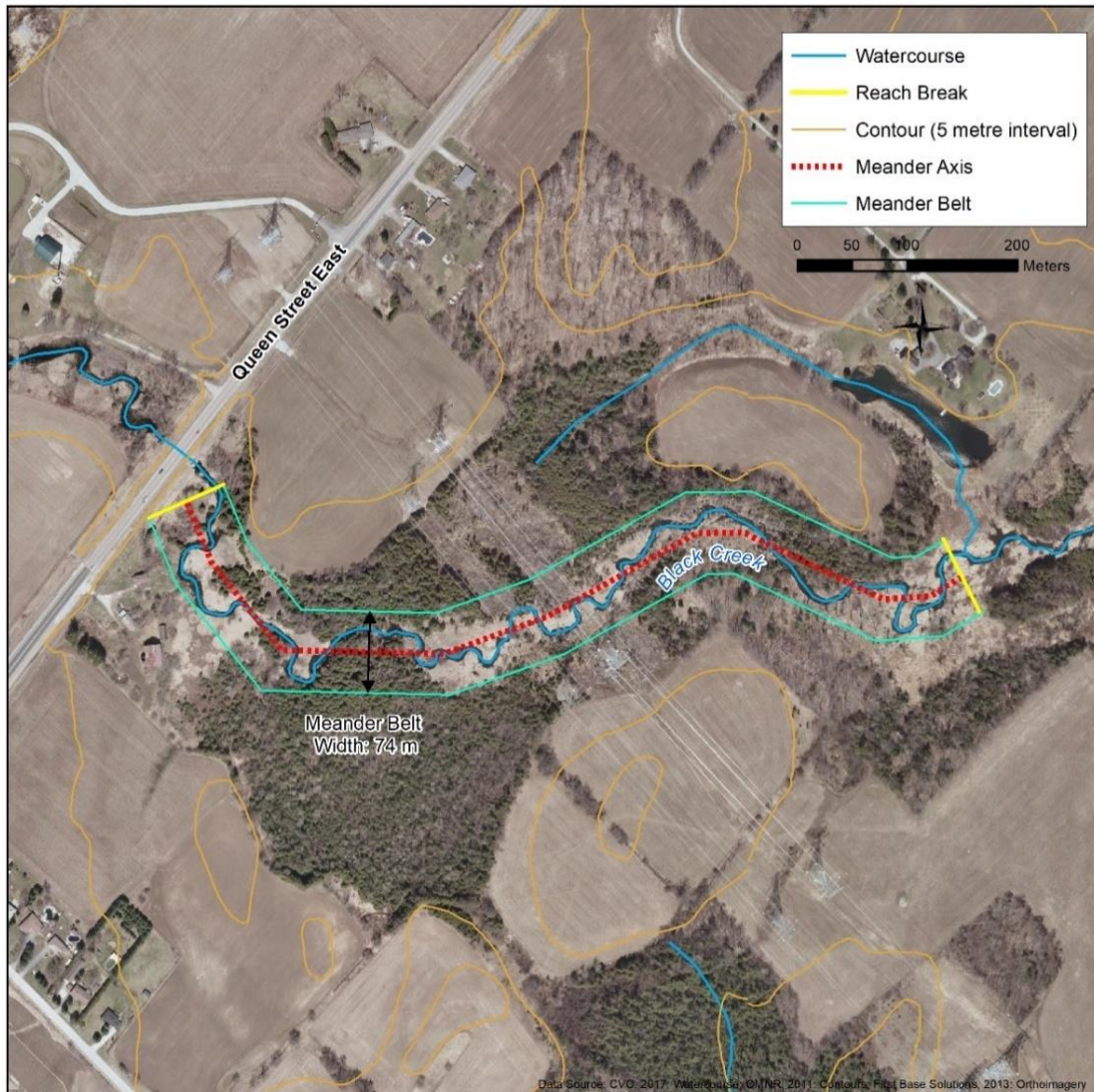


Figure 4.12 – Meander belt delineation (Reach BC2).

4.5 Summary

Using the geomorphological database obtained from CVC, as well as the sources described above, meander belt widths were determined for 46 channel reaches through the Credit River watershed.

By adopting the procedures that were previously established by Parish Geomorphic (2004),

meander belts were delineated using standard protocol which is used throughout southern Ontario. The corresponding widths of meander belts were used in statistical analyses, along with hydrogeomorphic parameters associated with each reach, to develop a method of meander belt width prediction.

Chapter 5

5 Statistical Analysis of Meander Belt Width and Hydrogeomorphic Parameters

In order to develop an empirical model for meander belt width prediction, it was necessary to analyze the association of hydrogeomorphic parameters with meander belt width. Associations were first assessed using a product-moment correlation coefficient, also known as Pearson's correlation coefficient, which is a parametric measure of the relationship between two variables. Once the correlation structure of the data was assessed, specific relationships among variables were tested using regression analyses to establish predictive relationships for meander belt width and also to examine other morphological interrelationships. A least squares regression analysis was selected; however, based on the reduced major axis regression being adopted by Williams (1986) in his investigation of meander geometry relations, significant relations were also assessed using the reduced major axis form. The following sections outline the process and results of these analyses.

5.1 Correlations Analysis

Pearson's correlation coefficients for selected hydrogeomorphic parameters and meander belt width were derived using the XLSTAT statistical software for Microsoft Excel. A Pearson's correlation coefficient, which measures the degree of association between variables, and the corresponding significance level (p-value) were obtained for each relation. The correlation coefficient can range from -1.0 and 1.0, with 0.0 indicating no correlation between the selected parameters. The null hypothesis of the correlation analysis is that there is no relation between the parameters, or that the parameters are independent of one another (Neter, Kutner, Nachtsheim, &

Wasserman, 1996), which may be rejected with a p-value less than the selected alpha ($\alpha = 0.05$). Appendix D summarizes all correlations between twelve hydrogeomorphic variables and meander belt width in a correlation matrix.

5.1.1 Correlations with Meander Belt Width

Table 5.1 displays a summary of the correlation coefficients between meander belt width and twelve selected variables. The hydrogeomorphic parameters were selected based on the idea that they represent the independent driving variables (e.g., stream power or discharge) and boundary conditions (e.g., valley gradient) which influence channel form, are direct or surrogate for controls of channel dimension (e.g., discharge or drainage area), and are (inter)dependent variables which describe meander morphology (e.g., sinuosity and amplitude).

Meander belt width exhibits a significant correlation with ten of the twelve variables, excluding specific stream power and channel sinuosity. Both insignificant relationships were unexpected on the basis of known principles of fluvial morphological adjustment (Leopold, Wolman, & Miller, *Fluvial Processes in Geomorphology*, 1964; Charlton, 2008). As discussed (Chapter 2), stream power is a measure of the potential of flowing water in a river channel to perform geomorphic work, and specific stream power is a measure of stream power per unit channel width. In theory, the greater the specific stream power within a channel, the greater probability of channel migration within the floodplain, and therefore, the possibility of larger meanders forming, resulting in larger meander belt widths. This notion has also been recognized in the case of sinuosity, where specific stream power has been used to denote the transition between single-thread and multi-thread channels associating energy potential and sinuosity (Ferguson, 1987; van den Berg, 1995). This may suggest that specific stream power affects the rate of channel migration, but not the size of meanders. Not only does specific stream power have poor association with meander belt width, it

also shows little correlation with the other hydrogeomorphic variables with which it might be expected to correlate, such as channel width (Cao & Knight, 1996). Sinuosity also displays a very poor association with meander belt width, and even more unexpectedly, demonstrates a negative relation. It was anticipated that the greater the sinuosity, the greater the meander belt width; however, this does not appear to be the case. Sinuosity also shows a negative correlation with mean bankfull width, drainage area, discharge, and stream power, with significant correlation coefficients of -0.34, -0.31, -0.32, and -0.37, respectively. One possible explanation is a sampling effect in which the most sinuous channels selected are small or low-order streams (see Chapter 4), which may be a characteristic of headwater tributaries in southern Ontario more generally.

Significant correlations with meander belt width include: mean bankfull width, mean bankfull depth, drainage area, valley gradient, discharge, total stream power, and meander amplitude. All channel dimensions demonstrated a significant positive correlation with meander belt width. Although other channel dimensions were considered, such as mean width-depth ratio and cross-sectional area, mean bankfull width displays the highest significant correlation to meander belt width, and therefore, was considered as the most important channel dimension parameter for predictive model development. The use of bankfull channel width as the channel dimension parameter is also consistent with previous studies of meander belt or meander geometry more generally (Inglis, 1949; Carlston, 1965; Ackers & Charlton, 1970; Lorenz, Heinze, Clark, & Searls, 1985; Williams, 1986). Additionally, meander belt width shows a strong positive correlation with drainage area and discharge, suggesting that meanders are scaled to the amount of water entering the system thus resulting in scaled meander belt widths. Stream order was considered within the correlation analysis, and demonstrates a strong positive correlation with meander belt width, but is fundamentally a surrogate of drainage area and mean bankfull width, as channels with greater

stream orders have larger drainage areas, and thus, larger bankfull widths. This also reflects the scaled relationship along the stream network, which demonstrates the downstream changes in hydraulic geometry as a single river system has been considered. Meander belt width is most strongly correlated with meander amplitude. Meander amplitude is the measure of the most extreme meander bends within a reach and a meander belt must be large enough to contain these meanders. In other words, they are closely comparable variables in describing meander planimetry. Finally, meander belt width is negatively correlated with valley gradient, and although the relation is somewhat weak, this may be expected as slope has a tendency to decrease moving downstream in a system where greater discharge values and drainage areas are present. This is supported by the inverse relationship apparent between slope and drainage area and discharge (Appendix D). The results of this correlation analysis were used to select variables for regression analysis for developing a meander belt width prediction model.

Table 5.1 – Meander belt width and hydrogeomorphic parameter correlation coefficients.

Variable	Pearson's Correlation Coefficient	p-value
Mean Bankfull Width (m)	0.739	0.000
Mean Bankfull Depth (m)	0.312	0.035
Width Depth Ratio	0.544	0.000
Cross-sectional Area (m ³)	0.708	0.000
Drainage Area (km ²)	0.748	0.000
Valley Gradient (%)	-0.320	0.030
Discharge (m ³ /s)	0.756	0.000
Total Stream Power (W/m ²)	0.504	0.000
Specific Stream Power (W/m)	0.234	0.118
Sinuosity	-0.053	0.002
Stream Order	0.762	0.000
Amplitude	0.957	0.000

Values in bold are different from 0 with a significance level $\alpha = 0.05$, therefore the null hypothesis is rejected. (n = 46)

5.1.2 Correlations between Hydrogeomorphic Parameters

Hydrogeomorphic parameters were correlated with one another to assist in the interpretation of controls of meander belt width. Additionally, the relations between the parameters may offer insight as to whether this data set is consistent with established theories of hydraulic geometry and characteristic relations of channel dimensions.

Many statistically significant correlations are present among the hydrogeomorphic variables (Table 5.2). Mean bankfull channel width demonstrates a significant positive correlation with both drainage area and discharge, which follows theories of hydraulic geometry, discussed below. Drainage area and discharge show a strong positive correlation. However, discharge was estimated, in part, by the drainage area; thus, the relationship is somewhat pre-determined. Total stream power exhibits a significant positive correlation with mean bankfull channel width and drainage area, which is consistent with established theory and observation of hydraulic geometry of rivers in that larger total energy produces larger channel dimensions (van den Berg, 1995; Knighton, 1999). A notable outcome from the correlation analysis among hydrogeomorphic parameters is those of meander amplitude, which demonstrates significant positive correlations with all of the hydrogeomorphic variables considered. This result may indicate meander amplitude is scaled to such parameters, which differs from the poor correlations found in the literature. Based on the correlation results it may be suggested that drainage area, discharge and total stream power are surrogate variables of which meander amplitude and bankfull channel width are dependent on.

Table 5.2 – Correlation matrix for significantly related hydrogeomorphic variables.

Variable		Mean Bankfull Width (m)	Drainage Area (km ²)	Discharge (m ³ /s)	Stream Order	Meander Amplitude (m)	Total Stream Power (W/m ²)
		Significance (p-value)					
Mean Bankfull Width (m)	Pearson Correlation Coefficient		<0.0001	<0.0001	<0.0001	<0.0001	<0.0001
Drainage Area (km ²)		0.924		<0.0001	<0.0001	<0.0001	<0.0001
Discharge (m ³ /s)		0.940	0.990		<0.0001	<0.0001	<0.0001
Stream Order		0.814	0.762	0.784		<0.0001	<0.0001
Meander Amplitude (m)		0.647	0.700	0.706	0.679		0.002
Total Stream Power (W/m ²)		0.705	0.691	0.730	0.589	0.443	
<p><i>Values in bold are different from 0 with a significance level alpha = 0.05, therefore the null hypothesis is rejected. (n = 46)</i></p>							

5.2 Regression Analysis Procedures

5.2.1 Least Squares Regression

In order to quantify the relations of meander belt width and hydrogeomorphic variables, statistical regression analysis was pursued using the ordinary least squares method. A linear regression model is a formal means of expressing two components of a statistical relationship: the systematic variation of the independent variable with the dependent variable, and a scattering of the observations which occurs around this systematic element (Burt & Barber, 1996). In the ordinary least squares regression (OLS) method, the model coefficients are estimated by minimizing the sum of the squared deviations of the dependent residuals (Ferguson, 1978). This form of regression

is most common in developing predictive models, and has been used to estimate meander planform parameters by Williams (1986), Carlston (1965), Lorenz et al. (1985), Leopold and Wolman (1960), and Ackers and Charlton (1970). Linear least squares regression analyses were conducted using XLSTAT statistical software for Microsoft Excel. Deterministic models for the selected parameters were written for observation i as follows (Neter, Kutner, Nachtsheim, & Wasserman, 1996):

$$y_i = a + \beta_i x_i \quad 5.1$$

Where y represents the estimated dependent variable, a is the regression constant, and β_i is the regression coefficient for the explanatory variable x_i . The assumptions associated with linear regression include: a linear relationship present between the independent and response variables, the residuals follow a normal distribution, and the data are homoscedastic, or that variance around the regression line is equal across all predictor values (Neter, Kutner, Nachtsheim, & Wasserman, 1996). Many relations were visually shown to be better fit by power or semi-logarithmic functions, and required logarithmic transformations made prior to linear regression analyses. Ferguson (1986) identified the statistical bias that is inherent in logarithmic transformations and back-transformations for linear regression analyses. Once parameters are back-transformed or anti-logged, the resulting predictive model can underestimate due to an unrepresentative intercept coefficient a , with the values of the dependent variable being estimated by 20% in Ferguson's (1986) example. Ferguson developed a method of bias correction, which corrects the intercept coefficient for antilog bias while maintaining the slope coefficient of the predictive model. The following equation was used to correct intercepts of log-log or power relations (Ferguson, 1986):

$$\tilde{a} = 10^a * EXP(2.65 * s^2) \quad 5.2$$

where \tilde{a} is the bias-corrected intercept, a is the intercept retrieved from the logarithmic regression analysis, and s^2 is the variance of the residuals, calculated by (Neter et al., 1996):

$$s^2 = \frac{\sum_{i=1}^n (y_i - \hat{y}_i)^2}{n - 1} \quad 5.3$$

Following the bias-correction, additional analyses were conducted in order to ensure the accuracy or goodness of fit of the model was sustained in antilog corrected form.

5.2.2 Reduced Major Axis Regression

The reduced major axis (RMA) regression line model was developed by Kermack and Haldane (1950) and was originally applied to paleontological data, but is now widely used in many disciplines. Also known as standardized mean axis, RMA regression minimizes the sum of the product of independent and dependent parameter residuals, which is equivalent to the area of triangles formed by the deviation of a point from the line in both X and Y directions (Smith, 2009). This is different from a least squares regression, which minimizes the sum of vertical deviations, or only in the Y variable. There are two significant assumptions associated with RMA analysis: errors are present in both independent and dependent variables, and the relation between the parameters is symmetrical, which is sometimes thought as determining the ‘true’ relationship between variables (Smith, 2009). Errors, defined as any deviations from a perfect fit between independent and dependent variables can be due to the measurement of the parameter, the sampling variation, or the intrinsic natural variation within the parameter (Smith, 2009). The symmetry of the regression line suggests that if the independent and dependent axes were inverted, the slope of the regression line would be an exact reciprocal, resulting in a single RMA regression line, rather than a difference in intercept and slope which is a potential result in least squares regression. Although it is argued that the error consideration is of utmost importance for RMA analysis, Smith (2009) argues that the essential difference between OLS and RMA regression is that of model

symmetry, and should be the factor which provides reasoning for RMA use. Williams (1986) employed RMA analysis when developing empirical relations to estimate meander morphology. As many of Williams (1986) relations are currently considered in applied geomorphology, significant relations of meander belt width prediction were also subjected to RMA analysis. All RMA analyses were conducted using the statistical analysis program R. RMA and OLS models were compared using a two-sample Kolmogorov-Smirnov test to determine whether the models were significantly different from one another.

5.2.3 Goodness of Fit Statistics

In order to assess the accuracy of the models produced, the coefficient of determination (r^2) goodness of fit statistic was considered. This coefficient, whose value ranges from 0 to 1 describes the amount of variation within the data that is explained by the regression line, and is defined by (Neter et al., 1996):

$$r^2 = 1 - \frac{\sum_{i=1}^n x_i (y_i - \hat{y}_i)^2}{\sum_{i=1}^n x_i (y_i - \bar{y})^2} \quad 5.4$$

Unlike the r^2 value, the adjusted coefficient of determination (\hat{r}^2) takes into account the number of variables used in the model, as well as the sample size. The adjusted determination coefficient is defined by (Neter et al., 1996):

$$\hat{r}^2 = 1 - (1 - r^2) \frac{X - 1}{X - n - 1} \quad 5.5$$

Mean squared error (MSE), which is a measure of the how well the regression line fits the set of data, is defined by (Neter et al., 1996):

$$MSE = \frac{1}{n} \sum_{i=1}^n (y_i - \hat{y}_i)^2 \quad 5.6$$

Standard error of the prediction (SEP), which quantifies the deviation of the predicted values from the observed values, is defined by (Neter et al., 1996):

$$SEP = \sqrt{\frac{\sum_{i=1}^n (y_i - \hat{y}_i)^2}{n}} \quad 5.7$$

5.3 Explored relations of meander belt width and hydrogeomorphic variables

Regression analyses were directed based on the correlation results and the inferred predictive model structure for meander belt width. Based on the correlation results, four relations were tested as predictors of meander belt width: meander amplitude, mean bankfull channel width, drainage area, and discharge. Based on these parameters, it appears that meander belt width is scaled to channel dimensions, or factors that control channel dimensions (e.g., discharge or drainage area). Sections below include the detailed results from the OLS and RMA analyses. Appendix E contains all statistical data and goodness of fit statistics for each regression analysis. Samples were also discretized identify possible relational differences for smaller or low-order streams versus larger channel systems, and by channel physiography using the following discretization conditions:

- Median value of the control parameter
- Strahler stream order
- Watershed zone

5.3.1 Mean bankfull channel width

Meander belt width shows a significant positive correlation with mean bankfull channel width (Figure 5.1) however, from the four relations which were considered, this model displays the lowest coefficient of determination value, at a r^2 value of 0.59. Based on the results of this

regression, meander belt width is predicted with mean bankfull channel width with the following equation:

$$M_B = 26.16w^{0.47} \quad 5.8$$

This indicates meander belt width is proportional to approximately the square root of mean bankfull channel width. The RMA regression (Figure 5.2) returns a model for meander belt width that exhibits a lower r^2 value of 0.58, defined by the following equation:

$$M_B = 20.42w^{0.61} \quad 5.9$$

Both OLS and RMA models demonstrate normally distributed residuals, passing a Shapiro-Wilk normality test with p-values of 0.322 and 0.293 respectively, with an alpha value of 0.05. Returning a p-value of 0.95 ($\alpha = 0.05$) for the Kolmogorov-Smirnov two sample test, the two models follow the same distribution and therefore, are not significantly different.

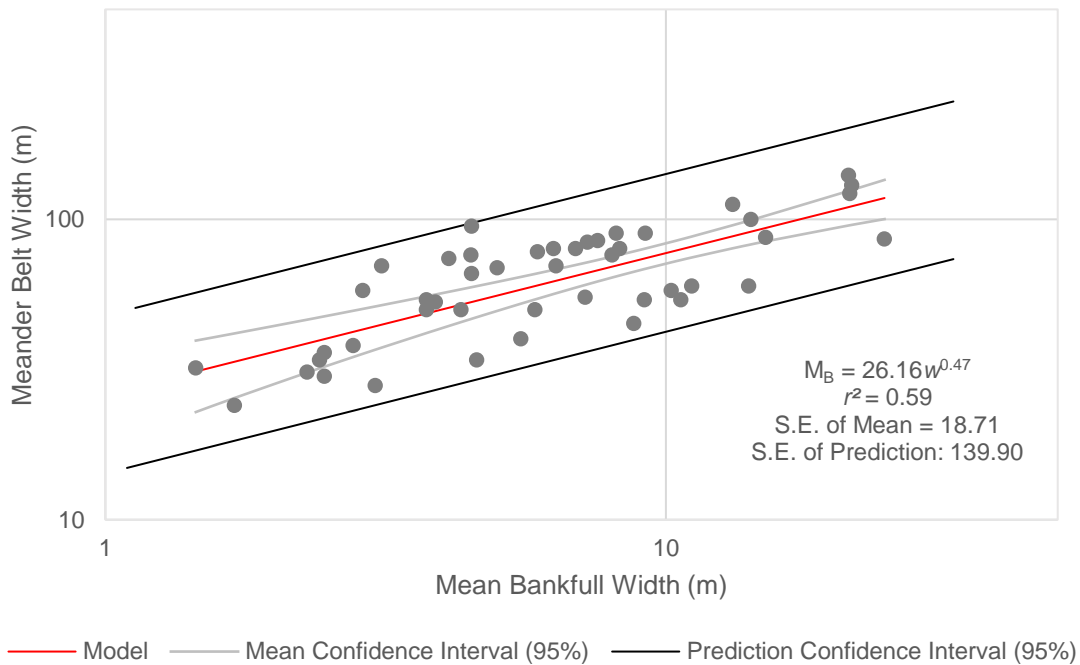


Figure 5.1 – OLS relation of meander belt width and mean bankfull channel width.

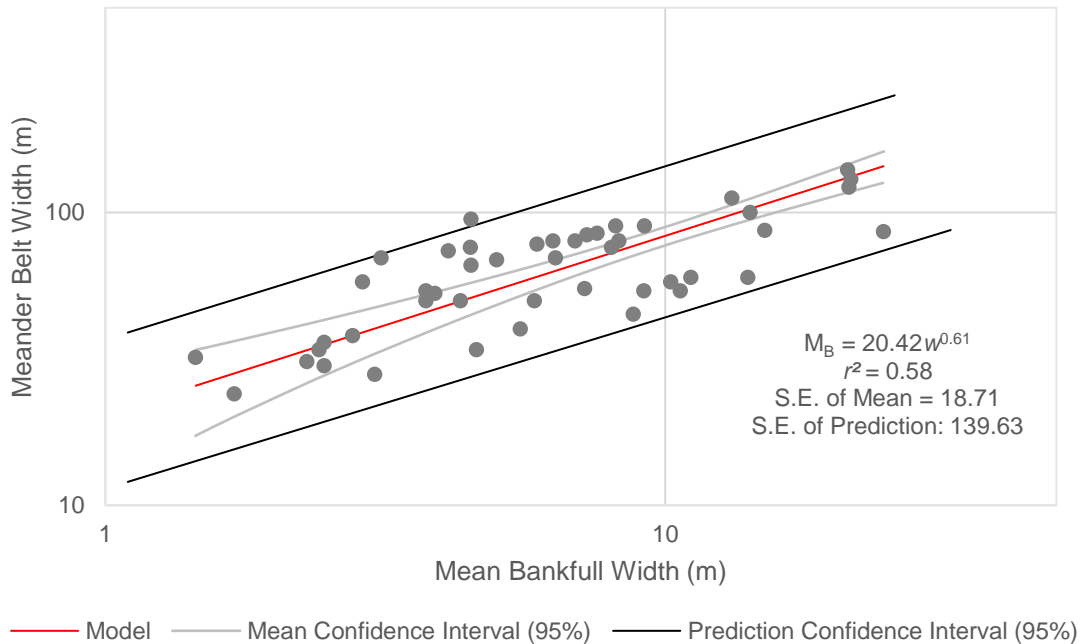


Figure 5.2 – RMA regression model for meander belt width and mean bankfull channel width.

5.3.2 Discharge

Meander belt width shows a significant positive correlation with two-year recurrence interval mean daily discharge (Figure 5.3), with the corresponding model producing a higher explanatory power than mean bankfull channel width (r^2 of 0.65). Based on the results of this OLS regression, meander belt width is predicted with discharge using the following equation:

$$M_B = 34.69Q_2^{0.27} \quad 5.10$$

The RMA regression returns a model for meander belt width (Figure 5.4) that exhibits a r^2 value of 0.65, the same as the OLS model. The standard error of the prediction increased, with some of the data points outside of the confidence intervals for the model prediction. Meander belt width is predicted with discharge using the following RMA equation:

$$M_B = 30.90Q_2^{0.34} \quad 5.11$$

Both OLS and RMA models demonstrate normally distributed residuals, passing a Shapiro-Wilk normality test with p-values of 0.543 and 0.832 respectively, with an alpha value of 0.05. Based on analysis of the Q-Q plots for both regression analyses, the RMA model produces more normally distributed residuals, demonstrating less of a trend in the residuals about the axis (Appendix E). Returning a p-value of 0.66 ($\alpha = 0.05$) for the Kolmogorov-Smirnov two sample test, the two models follow the same distribution and therefore, are not significantly different.

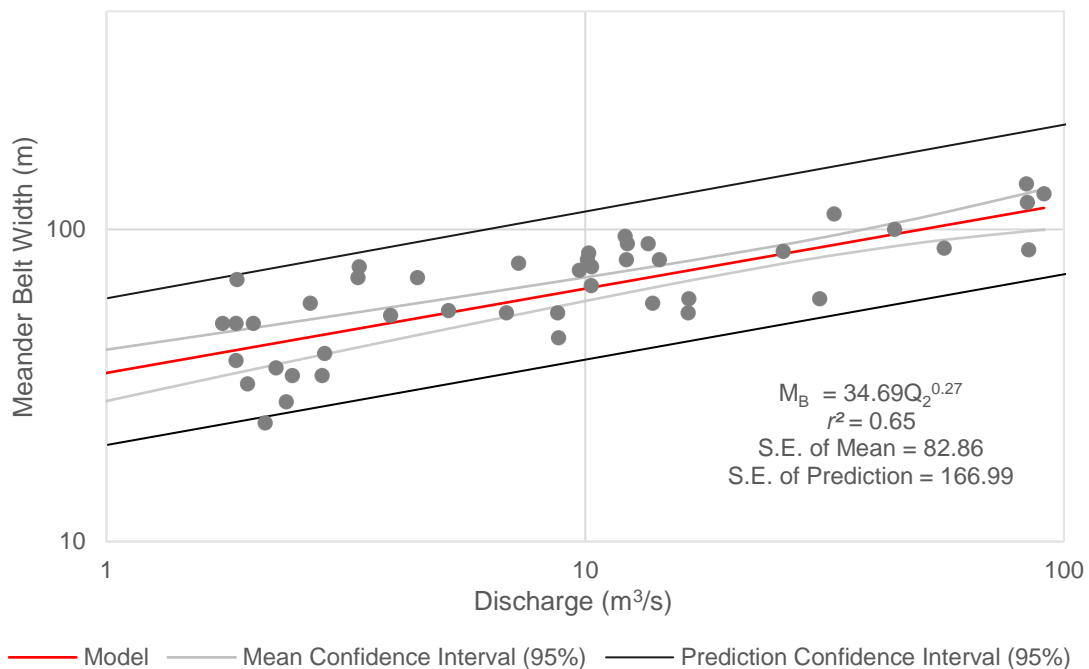


Figure 5.3 – OLS relation of meander belt width and discharge.

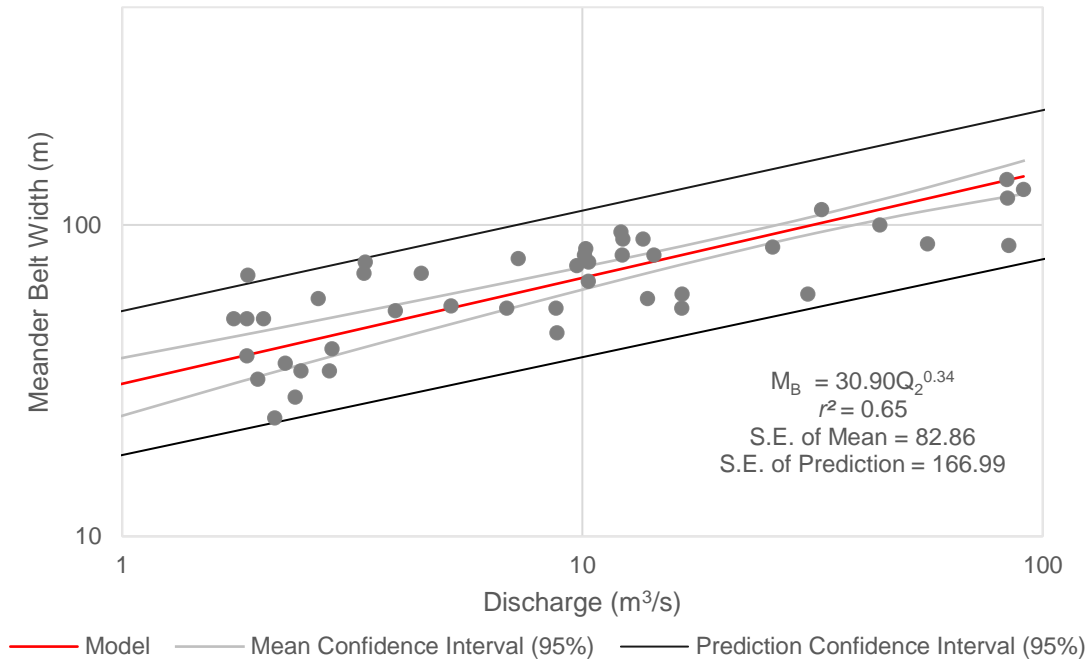


Figure 5.4 – RMA regression model for meander belt width and discharge.

5.3.3 Drainage Area

Meander belt width shows a significant positive correlation with drainage area (Figure 5.5), with the corresponding model producing a higher explanatory power than mean bankfull channel width and discharge, at a r^2 value of 0.67. Based on the results of this OLS regression, meander belt width is predicted with drainage area using the following equation:

$$M_B = 29.57DA^{0.23} \quad 5.12$$

The RMA regression returns a model for meander belt width (Figure 5.6) that exhibits a r^2 value of 0.67, the same explanatory power of the least squares model. The lower intercept in the RMA model (Equation 5.13) appears to result in under prediction occurring for smaller channels, or those with a smaller drainage area.

$$M_B = 25.12DA^{0.25} \quad 5.13$$

Both OLS and RMA models demonstrate normally distributed residuals, passing a Shapiro-Wilk normality test with p-values of 0.267 and 0.416 respectively, with an alpha value of 0.05. Returning a p-value of 0.99 ($\alpha = 0.05$) for the Kolmogorov-Smirnov two sample test, the two models follow the same distribution and therefore, are not significantly different.

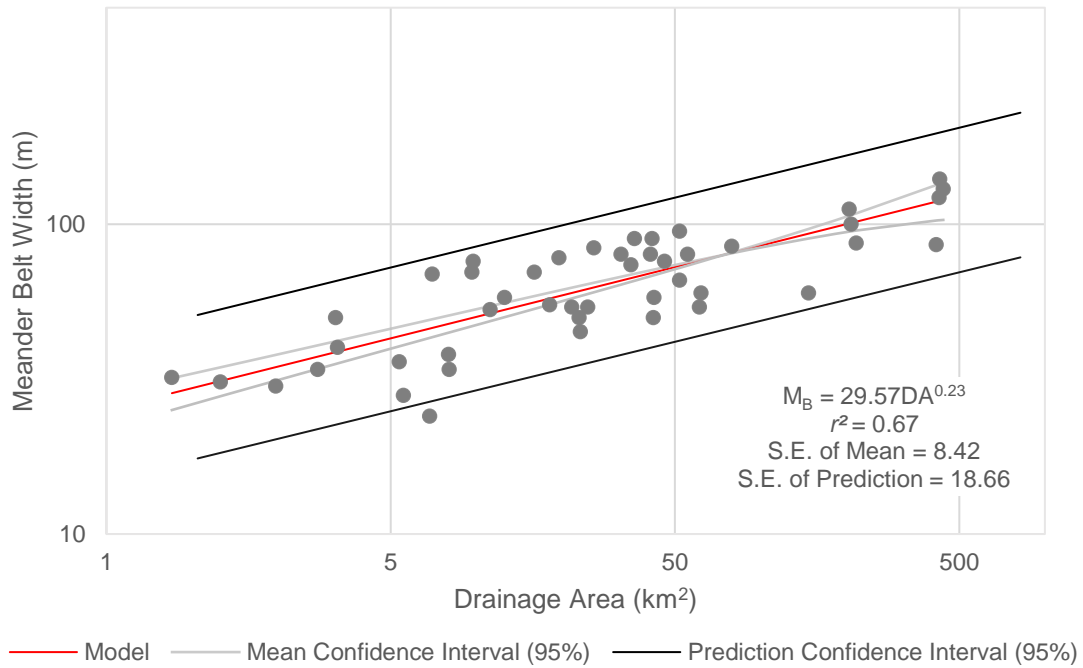


Figure 5.5 – OLS relation of meander belt width and drainage area.

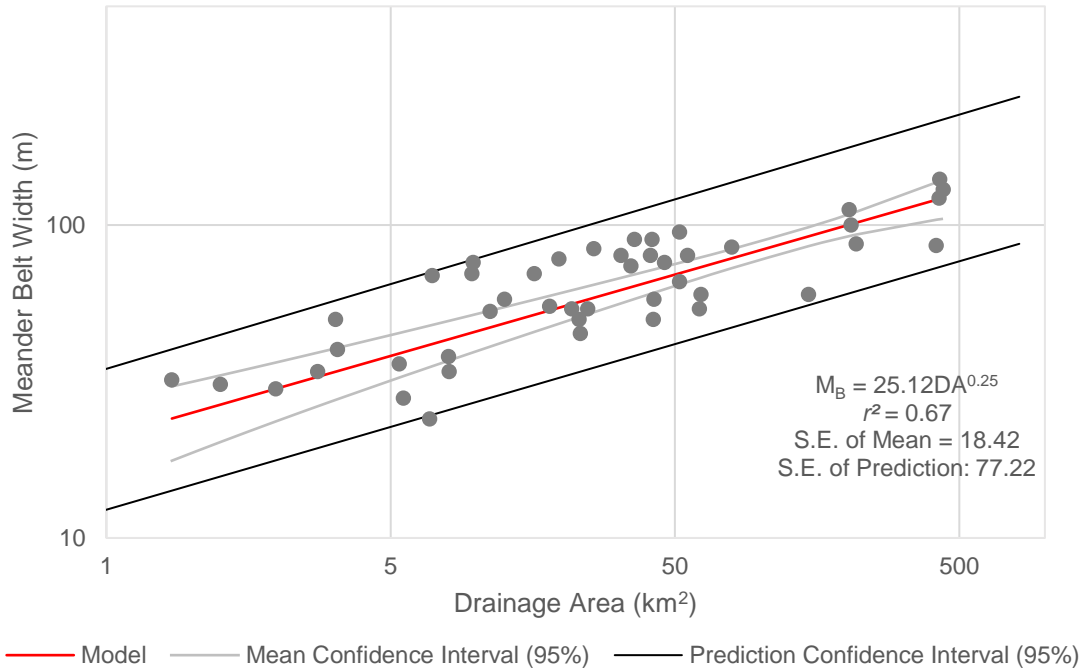


Figure 5.6 – RMA regression model for meander belt width and drainage area.

5.3.4 Meander Amplitude

Meander belt width shows a significant positive correlation with meander amplitude (Figure 5.7), with the corresponding model producing a r^2 value of 0.91. Based on the results of this OLS regression, meander belt width is predicted with meander amplitude using the following equation:

$$M_B = 1.01A_p + 12.97 \quad 5.14$$

This indicates meander belt width is scaled to meander amplitude at a near-linear relationship. The developed RMA model (Figure 5.8) also shows a near-linear relation with a slope of 1.06 (Equation 5.15). The r^2 value has increased slightly from the OLS model, at a value of 0.92.

$$M_B = 1.06A_p + 10.57 \quad 5.15$$

A second regression using meander amplitude versus meander belt width was pursued, with the addition of mean bankfull channel width to meander amplitude. As meander amplitude is measured

from the channel centreline, by adding bankfull channel width to the equation, the areal extent of the new parameter is extended to the outer bank of the channel (Figure 5.9). The model produced a slightly higher r^2 value of 0.94. When assessing the regression plot, it appears that the new model results in a greater over prediction of the channels with smaller meander amplitudes; however, the slope and intercept of the model are very similar to that of the OLS meander amplitude model (Equation 5.16).

$$M_B = 0.89(A_P + w) + 12.67 \quad 5.16$$

Meander amplitude with the addition of bankfull width demonstrates normally distributed residuals, passing a Shapiro-Wilk test with a p-value of 0.058, with an alpha value of 0.05. Conversely, with a p-value of 0.004, the model for meander belt width prediction via meander amplitude does not demonstrate normally distributed residuals, failing the Shapiro-Wilk normality test, and thus, breaching one of the assumptions of the least squares regression analysis.

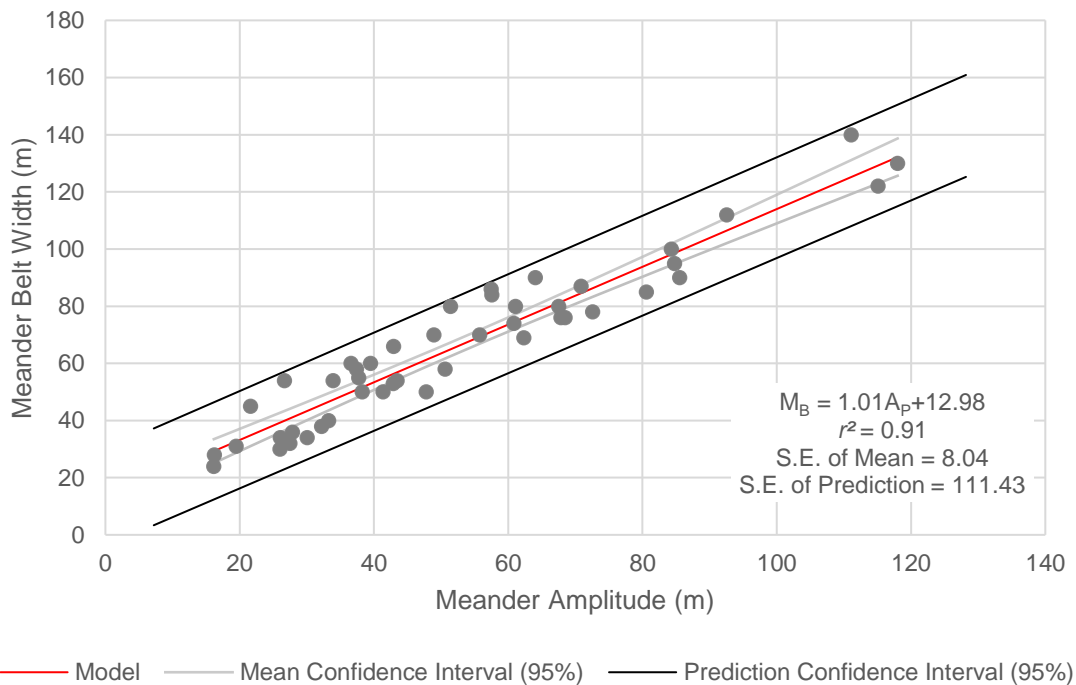


Figure 5.7 – OLS relation of meander belt width and meander amplitude.

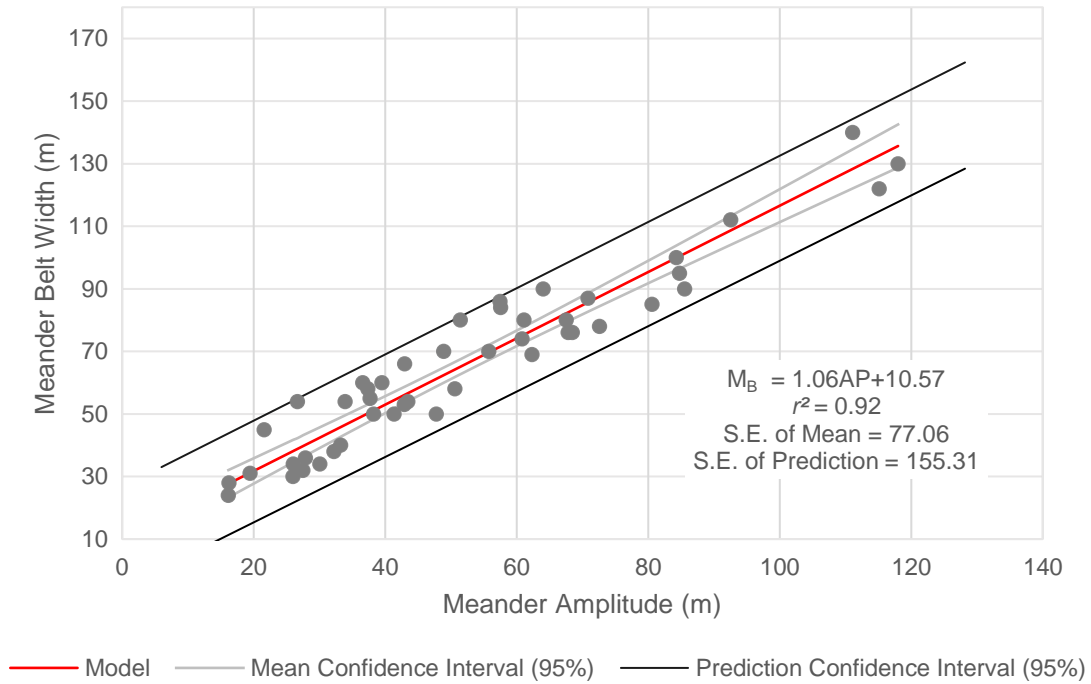


Figure 5.8 – RMA relation of meander belt width and meander amplitude.

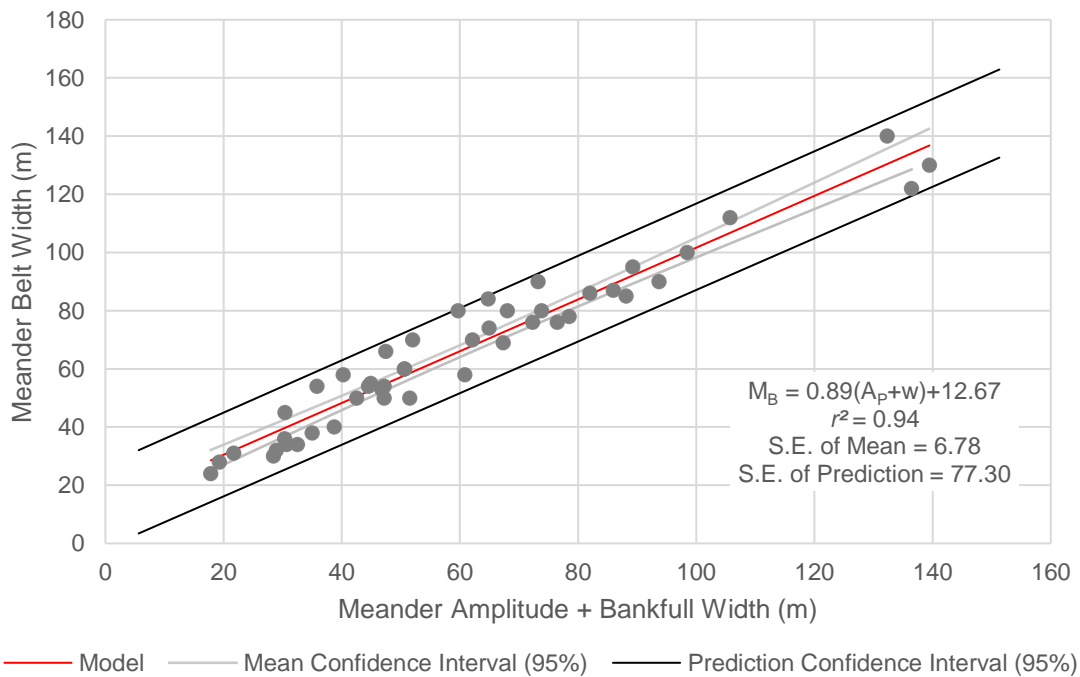


Figure 5.9 – OLS relation of meander belt width and meander amplitude with the addition of mean bankfull channel width.

5.3.5 Discretization of Meander Belt Relations

Three parameters, which demonstrated significant relations with meander belt width, were discretized by the median of the independent variable in order to assess if relational differences are apparent among larger or smaller systems using OLS regression. Relations were visually compared, as seen in Figure 5.10 to Figure 5.12. Additionally, the separate relations were compared using a two-sample Kolmogorov-Smirnov test to indicate whether there was a significant difference between the predicted values of meander belt width. From the three variables, discharge was the only variable to show a significant difference between the two discretized relations for meander belt width prediction; drainage area and mean bankfull channel width both passed the Kolmogorov-Smirnov test with p-values greater than the alpha (0.05). All relations for meander belt width prediction suffer from the reduced samples sizes, thus, the reduced explanatory power of the relations in comparison to the entire data set relation was anticipated. Additional data are necessary to confirm whether there are significant differences in meander belt width relations for varied sizes of channel dimensions.

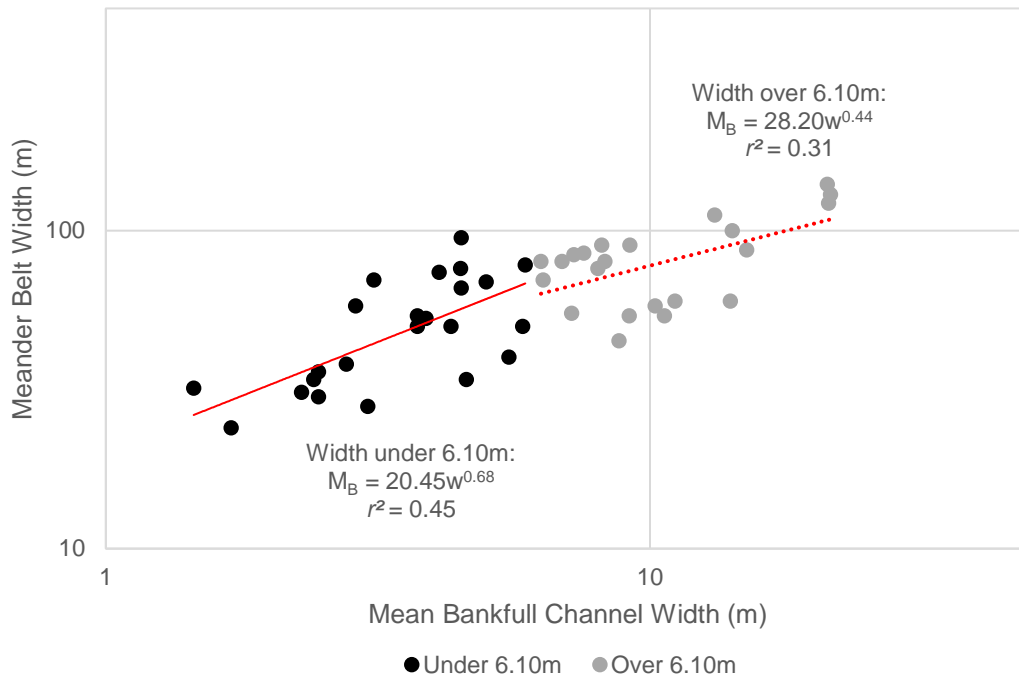


Figure 5.10 – Discretization of the OLS model for meander belt prediction via mean bankfull channel width using the median of bankfull width at 6.10 m.

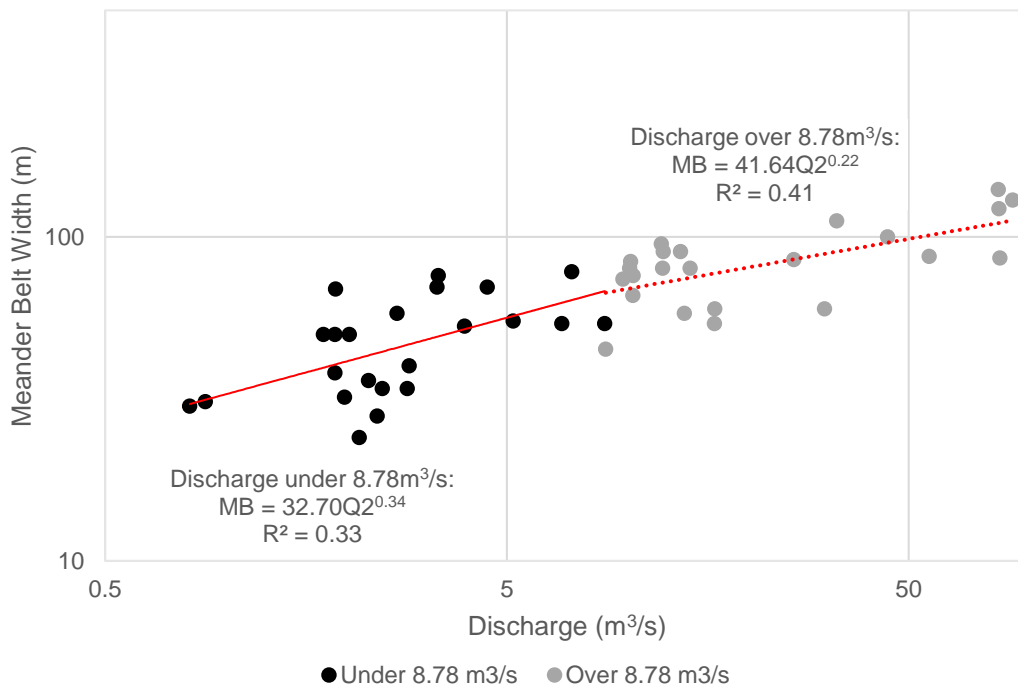


Figure 5.11 – Discretization of the OLS model for meander belt prediction via discharge using the median of discharge at 9.23 m³/s.

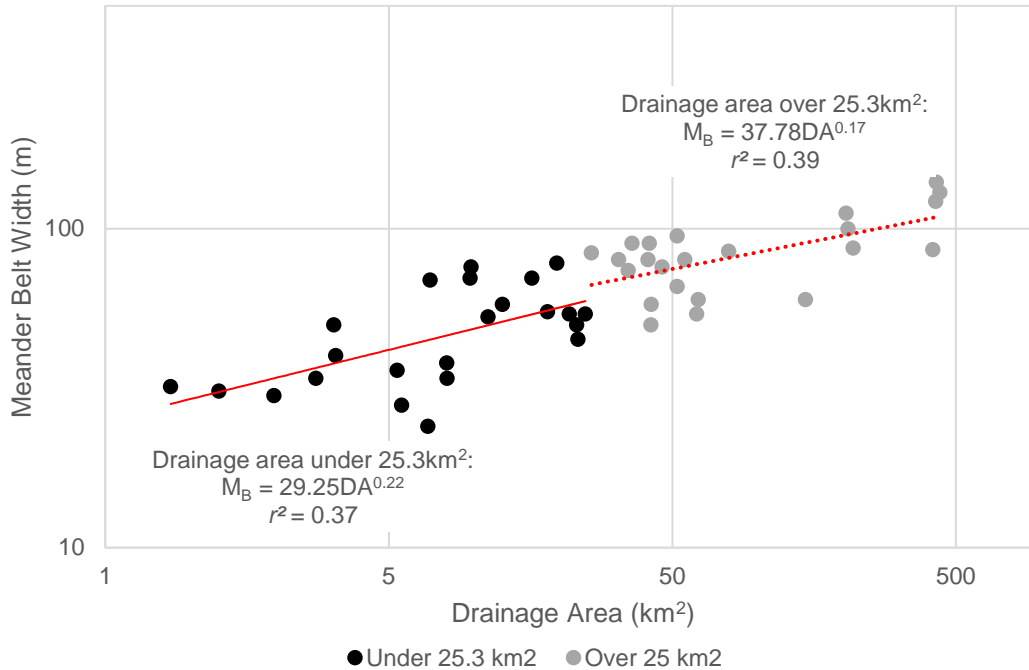


Figure 5.12 – Discretization of the OLS model for meander belt prediction using drainage area, with the median of drainage area at 25.3km².

The relations of meander belt width and mean bankfull channel width, discharge, and drainage area, were also discretized based on the watershed zone of the particular site. As delineated by CVC, each of the three watershed zones are characterized by specific geology and physiography. One drawback of this discretization process is the uneven number of sites located in each watershed zone. However, for all three of the relations described in Figure 5.13 to Figure 5.15, the relations for the upper and middle watershed zones has increased explanatory power from that of the entire data set. This may indicate the sub-regional trends in meander belt width, and the effect of local geology and physiography. However, when models were analysed in a Kolmogorov-Smirnov two sample test, all three hydrogeomorphic variables and each corresponding watershed relation computed p-values greater than the alpha ($\alpha = 0.05$), which indicates that the relations follow the same distribution and are not significantly different.

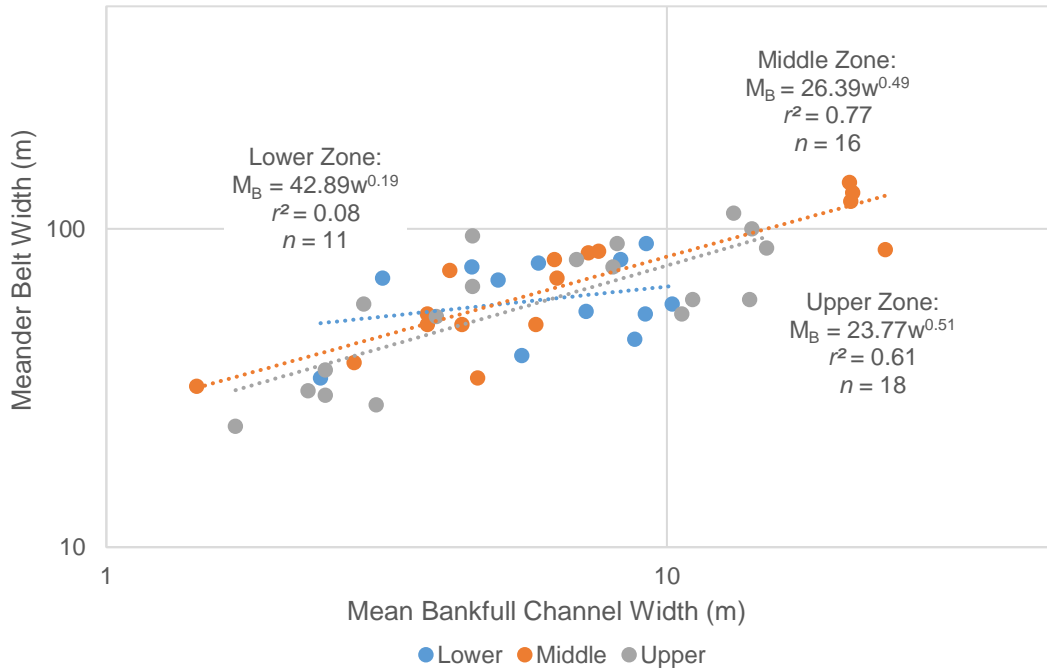


Figure 5.13 – Discretization of meander belt width OLS relation to mean bankfull channel width using watershed zones.

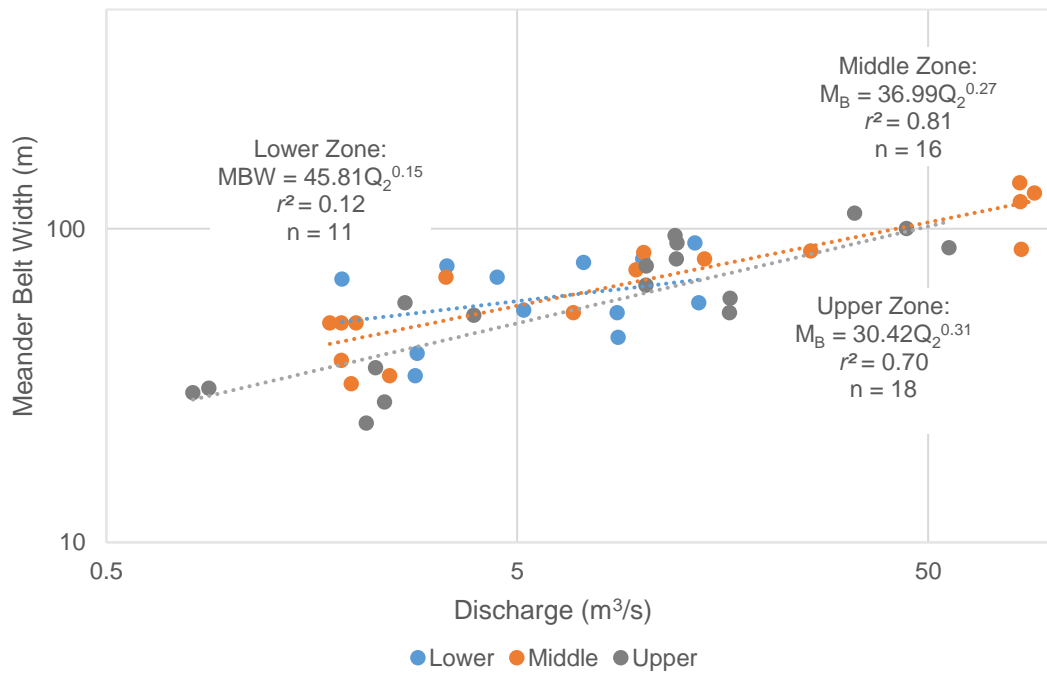


Figure 5.14 – Discretization of meander belt width OLS relation to discharge using watershed zones.

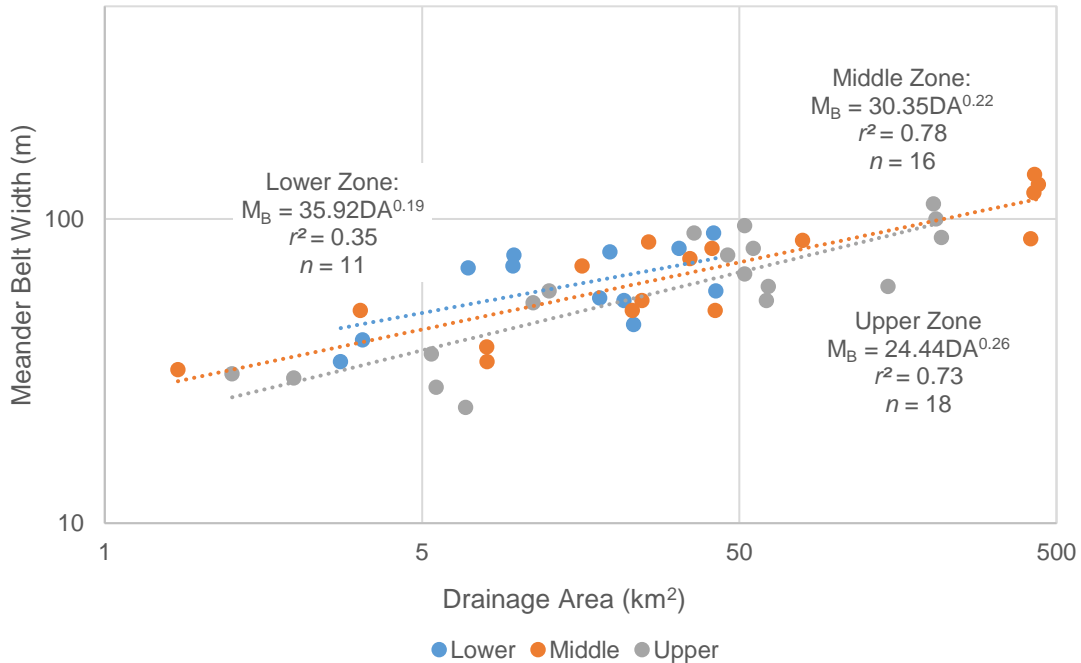


Figure 5.15 – Discretization of meander belt width OLS relation to drainage area using watershed zones.

Meander belt relations were also organized by Strahler stream order to address the previously established positive correlations with stream order. The sample sizes for each stream order are too small to develop significant relations for each stream order however, clustering is apparent based on the stream order of the site, as displayed in Figure 5.16 to Figure 5.18. Low order streams, orders 2 and 3, cluster towards the lower end of the plots, displaying smaller widths, discharge, and drainage areas, while mid-order streams cluster in the centre of the plots. Additional sites would be necessary to confirm the significance of this organization, and the value of discretizing meander belt relations by stream order. A notable outcome of this discretization process was the confirmation that meander belt width appears to scale with drainage area, or increase in a downstream direction within a fluvial system (e.g., larger meander belt widths are apparent for larger ordered watercourses).

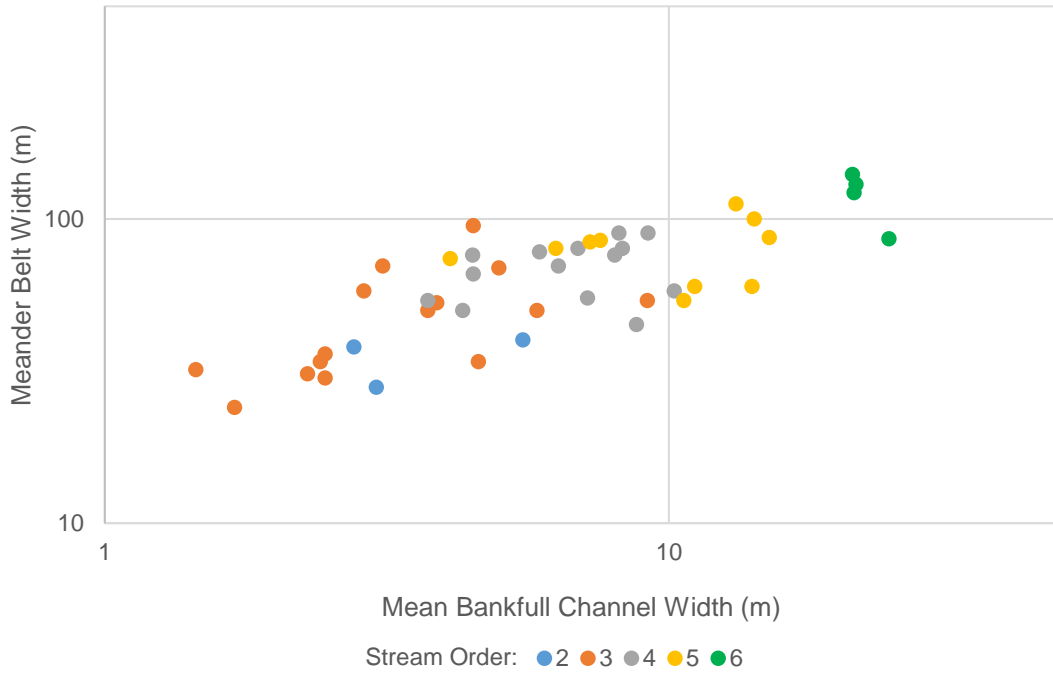


Figure 5.16 – Organization of meander belt width and mean bankfull channel widths by Strahler stream order.

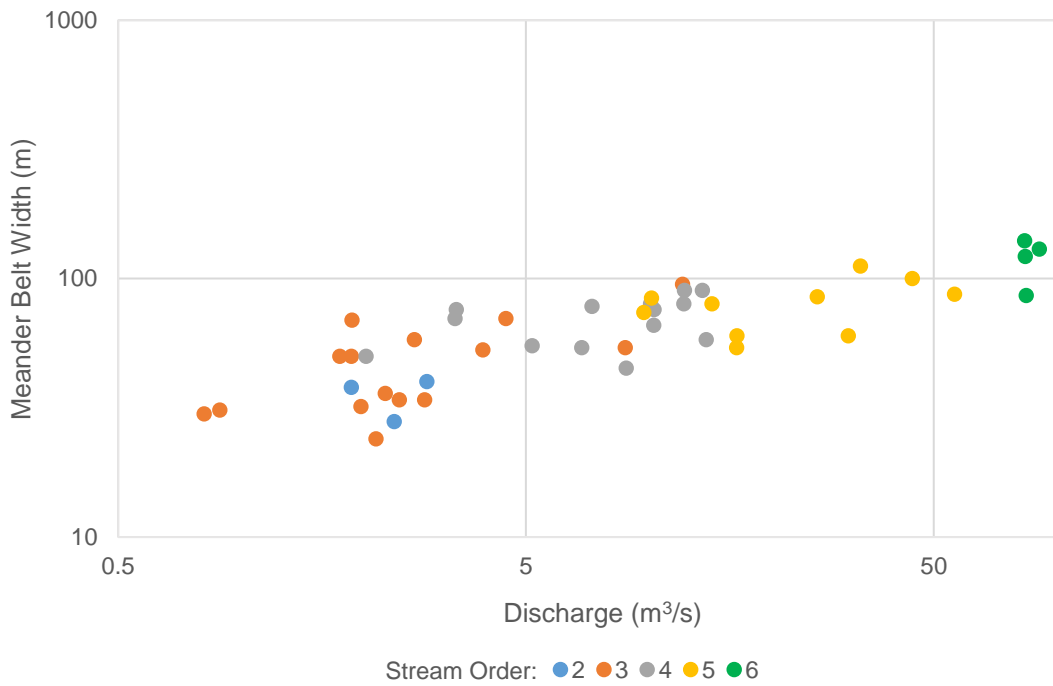


Figure 5.17 – Organization of meander belt width and discharge values by Strahler stream order.

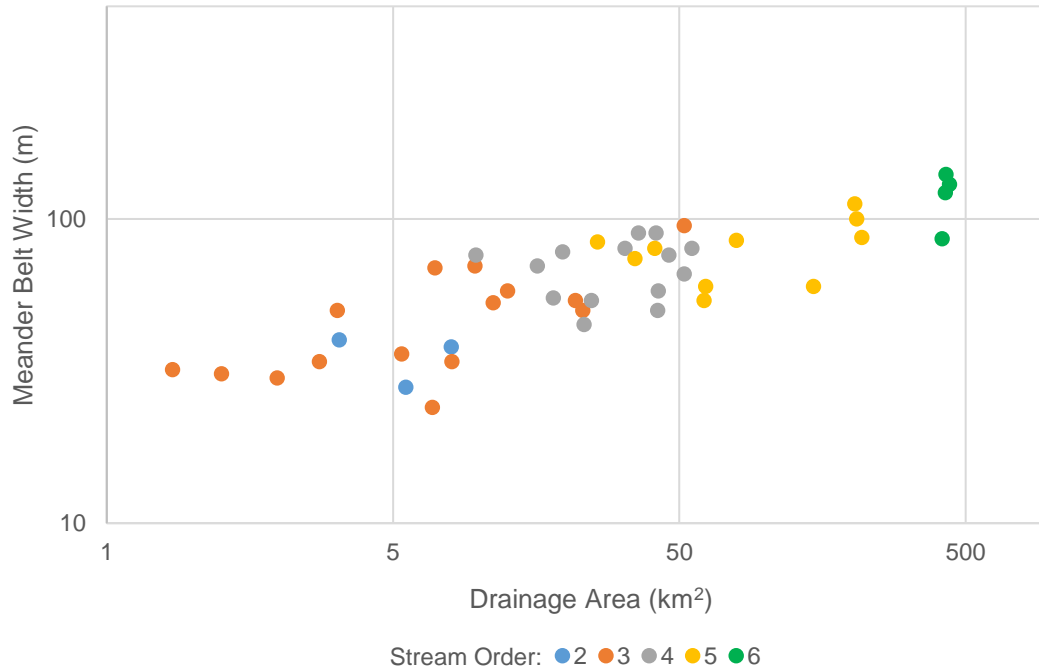


Figure 5.18 – Organization of meander belt width and drainage areas by Strahler stream order.

5.4 Relations between Hydrogeomorphic Parameters

In order to warrant comparability between previously developed models and the models developed within this thesis, as well as ensuring consistency current literature, OLS regression was used rather than RMA for relations between hydrogeomorphic parameters.

5.4.1 Relations between Drainage Area and Discharge

Discharge can be expressed as a power-law function of drainage area as:

$$Q = zDA^y \quad 5.17$$

with the coefficient y commonly ranging from 0.6-1.0 (Leopold, Wolman, & Miller, 1964; Knighton, 1987; Jennings, Thomas, & Riggs, 1993; Mohamoud & Parmar, 2006; Faustini & Kaufmann, 2009). This function describes the rate at which discharge typically increases with drainage area. Two studies conducted within southern Ontario found coefficients of 0.74 (Annable,

1996) and 0.91 (Phillips & Desloges, 2014), both which fall within the stated range. The present data set returned a coefficient of 0.75, which is very close to that of Annable (1996). When analyzed in a Kolmogorov-Smirnov test, the returned p-value of 0.49 states the two models are not statistically different. Figure 5.19 demonstrates the variability about the regression line due to the role of the other parameters within the hydraulic model influencing the discharge values. Furthermore, the differences between the models for the southern Ontario region and the model developed within the present research may be due to the way in which discharge was measured. Annable (1996) and Phillips and Desloges (2014) obtained the majority of their data from gauged stations, with data obtained from Water Survey of Canada’s hydrometric monitoring program and corresponding HYDAT database. Comparing gauged flow data with estimated discharge, largely influenced by drainage area, may be the reason why there are discrepancies apparent between the relations. Nevertheless, both previously established equations appear to underestimate discharge for larger drainage areas.

Table 5.3 – Relations of discharge and drainage area in southern Ontario.

Source	Model	r²
Annable (1996)	$Q_2 = 0.52DA^{0.74}$	-
Phillips & Desloges (2014)	$Q_2 = 0.25DA^{0.91}$	0.86
Thesis	$Q_2 = 0.66DA^{0.75}$	0.87

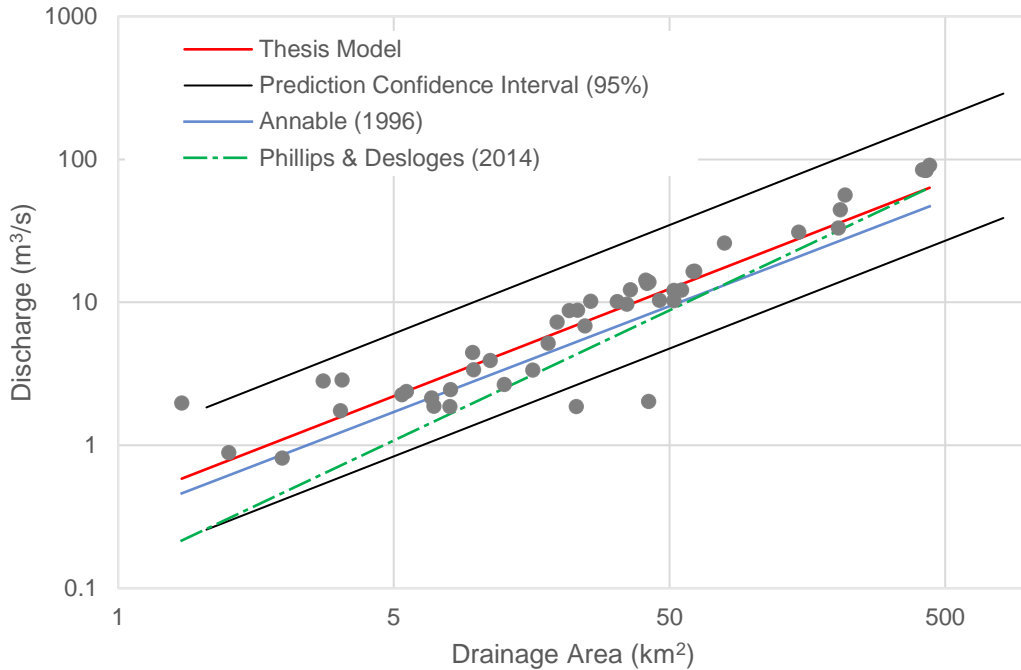


Figure 5.19 – OLS relation of discharge and drainage area.

5.4.2 Relations with Mean Bankfull Channel Width

Mean bankfull width was found to be significantly correlated with both drainage area and discharge, demonstrating strong positive relations. The systematic variation of channel width with discharge was termed “hydraulic geometry” by Leopold and Maddock (1953), and was expressed with the following equation:

$$w = aQ^b \quad 5.18$$

The value of the coefficient b has been found to remain relatively constant across fluvial systems, with a validated average of 0.5 (Leopold & Maddock, 1953; Leopold, Wolman, & Miller, 1964; Langbein & Leopold, 1966; Dury, 1976; Klein, 1981; Yang, 1971; Ferguson, 1986). Additionally, Chong (1970) confirmed that the hydraulic geometry relations were similar for varying environments, permitting their generalized use across regions. For the rural streams in southern Ontario, Annable (1996) found bankfull width to relate to bankfull discharge with an exponent

coefficient of 0.49 and an intercept of 3.71, with an associated standard error of 0.11. The relation found with the current data set (*Equation 5.19*) is close to Annable’s (1996) slope, with a coefficient of 0.49 (r^2 of 0.79) (Figure 5.20). Again, the differences between the relations may be influenced by the measurement of discharge using the OFAT III estimation, or perhaps by the measurement of bankfull channel width.

$$w = 2.24Q^{0.49} \quad 5.19$$

Four other data sets from the Great Lakes region were used for comparison of the width-drainage area relationship: three from southern Ontario (Annable, 1996; Phillips & Desloges, 2014), and one for the Great Lakes region in the United States (Faustini & Kaufmann, 2009) (Table 5.4). For the Credit River watershed data used in this thesis drainage area to associated with mean bankfull channel width using the following OLS relation:

$$w = 1.68DA^{0.40} \quad 5.20$$

The coefficient of 0.40 fits well with the model developed previously for the Credit River region, as found by Phillips and Desloges (2014), and has a high explanatory power of 0.79. Additionally, the intercept seems to fall within the array seen in all four models which range from 1.2 to 2.69 (Figure 5.21).

Table 5.4 – Regional models for bankfull channel width via drainage area.

Source	Region	Equation	r^2	Sample size
Annable (1996)	Southwestern Ontario	$w = 2.69DA^{0.36}$		47
Phillips & Desloges (2014)	Southwestern Ontario	$w = 1.2DA^{0.5}$	0.88	542
	Rouge River, Humber River, <i>Credit River</i> , 16 Mile Creek	$w = 1.85DA^{0.41}$	0.88	47
Faustini & Kaufmann (2009)	Great Lakes Region (U.S.A)	$w = 2.45DA^{0.33}$	0.62	53
Thesis	Credit River	$w = 1.68DA^{0.40}$	0.79	46

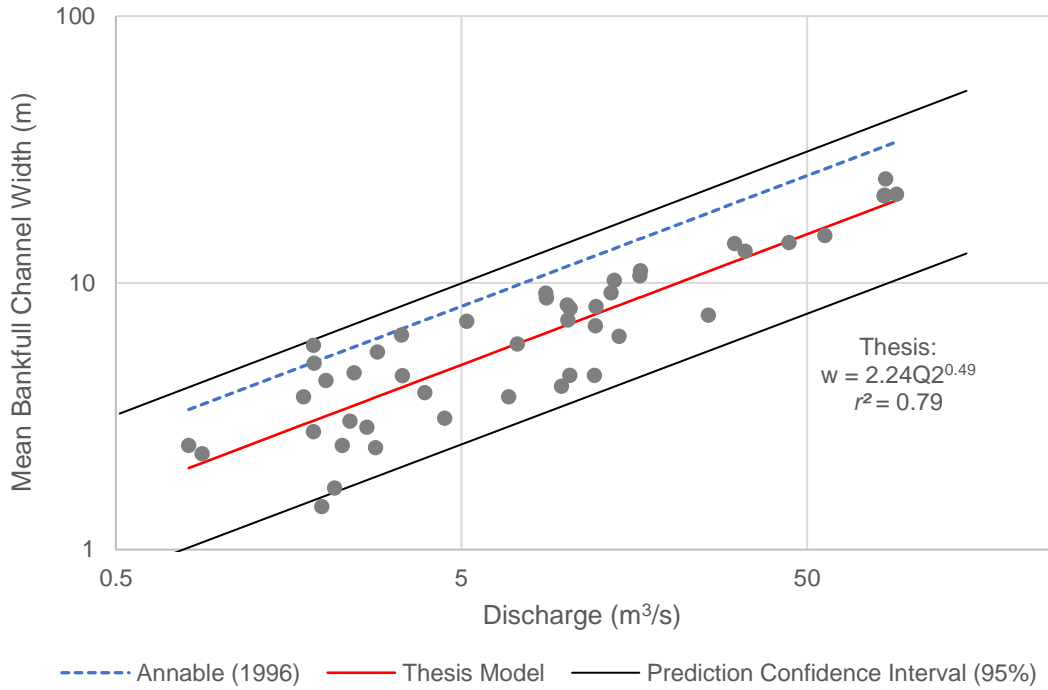


Figure 5.20 – OLS relation of mean bankfull channel width and discharge.

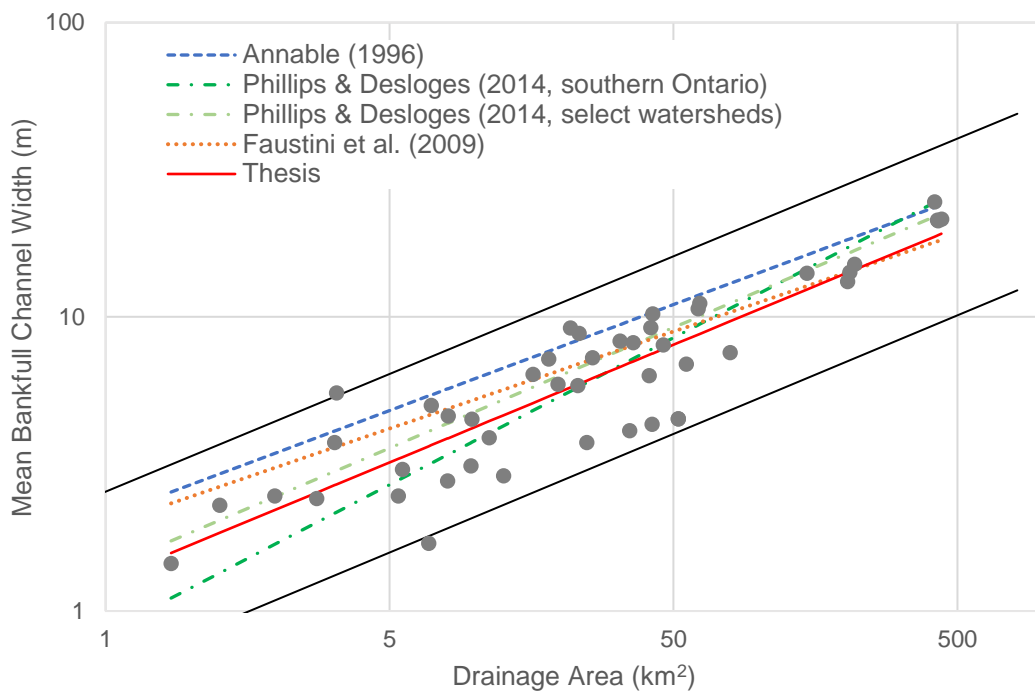


Figure 5.21 – OLS relation of mean bankfull channel width and drainage area.

5.4.3 Relations with Meander Amplitude

Meander amplitude has been previously shown to correlate poorly with hydrogeomorphic parameters and it has been suggested that it is determined more by the erosional characteristics of the channel banks and by other local factors (Leopold, Wolman, & Miller, 1964; Williams, 1986). The poor correlation may not be as apparent for meander amplitude in the current data set; however, the relations developed display relatively low explanatory power. As demonstrated in Figure 5.22 to Figure 5.24, the r^2 of the relations ranges from 0.32 to 0.50. Similar to the predictive relations for meander belt width, drainage area exhibits the strongest relation. The most common parameter associated with meander amplitude in the literature is bankfull channel width. Previously established relations of meander amplitude and bankfull channel width are listed in Table 5.5. The large variation in coefficients may support the idea of meander amplitude being largely controlled by local conditions rather than hydrogeomorphic principles. Additionally, only Annable (1996) found meander amplitude to have a non-linear relation with bankfull width. This is consistent with the relation developed using the current data set, which suggests meander amplitude is approximately proportional to the square root of mean bankfull channel width. Certainly, this large variability in the models associated with meander amplitude and channel width and the lack of strong relation provides evidence for the uncertainty that still remains regarding controls of meander amplitude. The absence of a strong relation for meander amplitude may also have implications for understanding meander belt width relations, as it has been shown that the two measurements are closely related.

Table 5.5 – Relations of meander amplitude and channel width.

Source	Equation
Inglis (1949, Bates data)	$A_P = 10.9w^{1.04}$
Inglis (1949, Fergusson data)	$A_P = 18.6w^{0.99}$
Leopold & Wolman (1960)	$A_P = 2.7w^{1.10}$
Annable (1996)	$A_P = 7.83 w^{0.62}$
Thesis	$A_P = 22.39 w^{0.41}$

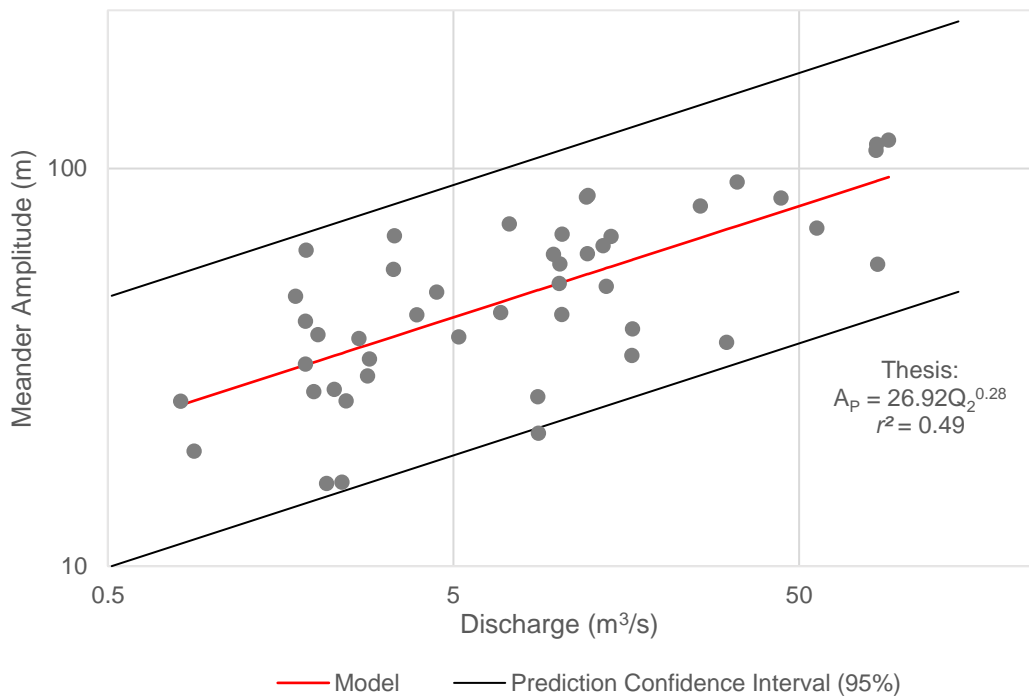


Figure 5.22 – OLS relation of meander amplitude and discharge.

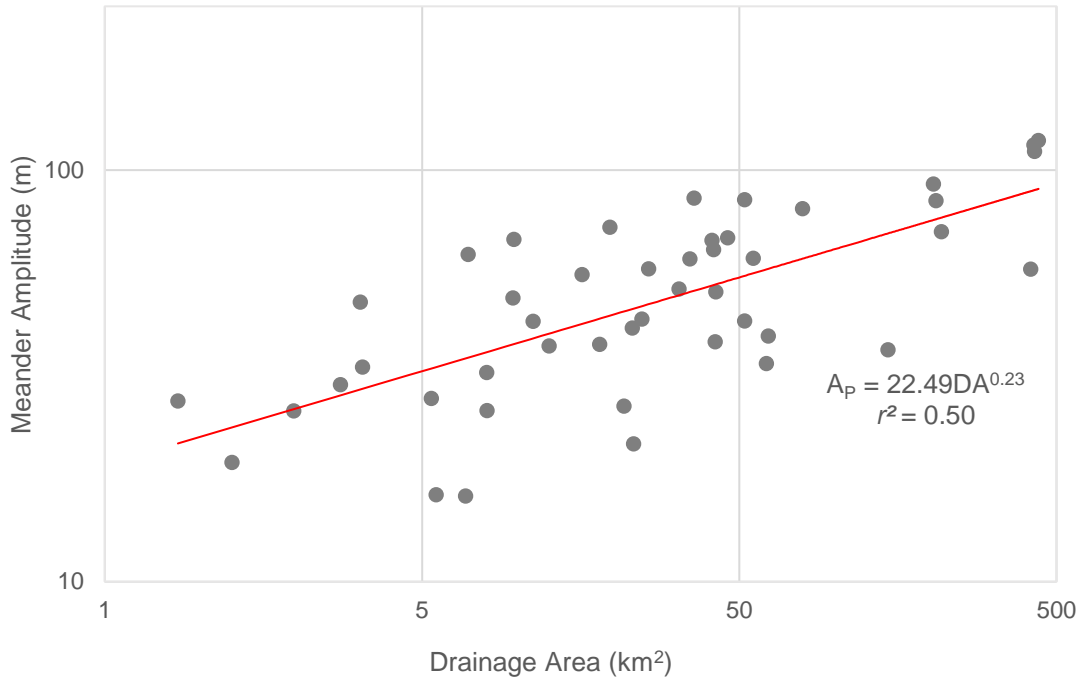


Figure 5.23 – OLS relation of meander amplitude and drainage area.

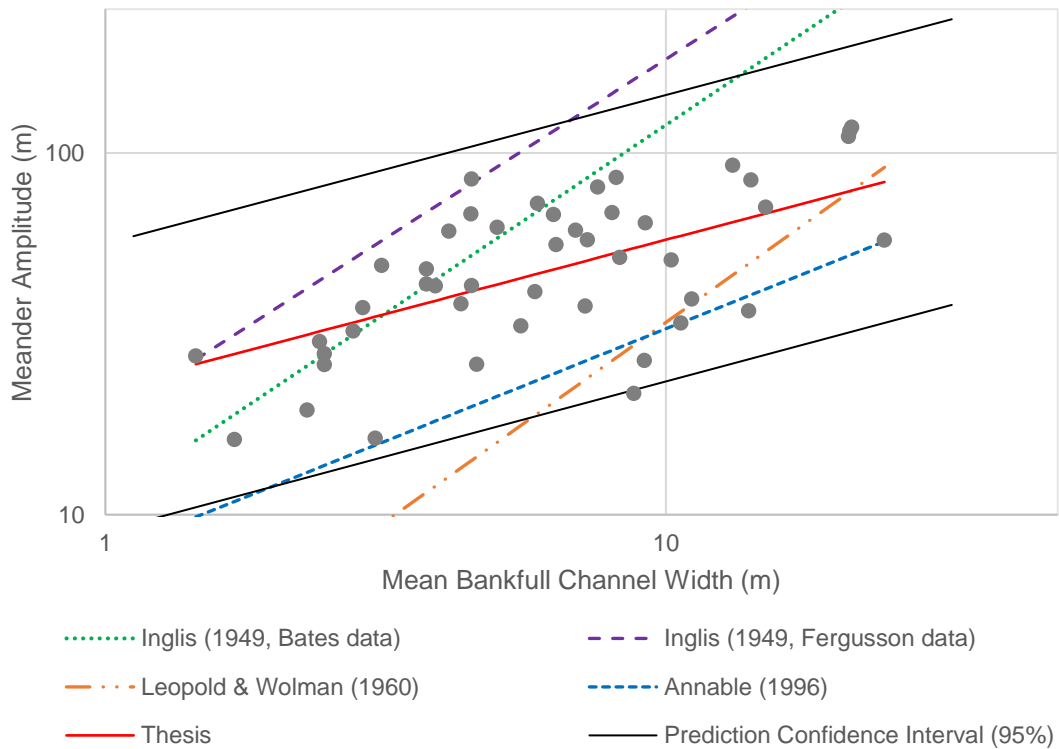


Figure 5.24 – OLS relation of meander amplitude and bankfull channel width.

Chapter 6

6 Discussion

The following sections summarize the characteristics of watercourses selected for analysis and discuss definitions and measurement methods of meander belt width. Additionally, relations of meander belt width prediction developed in this thesis, and those which are commonly in the literature are compared, along with implications for meander belt policies in southern Ontario and future research needs.

6.1 Characteristics of selected watercourses

The watercourses throughout the Credit River watershed selected for the current research offer insight as to the meander morphology and channel characteristics which may be present throughout southern Ontario. The selected reaches had a range of drainage areas, discharge values, channel dimensions, and physiographic conditions. Selected watercourses demonstrated trends related to the three physiographic watershed zones as delimited by CVC. The most sinuous and relatively active channels assessed were located in the upper watershed zone, with lower sinuosity values apparent in the middle and lower watershed zones in the larger channels. Although there were some channels which appeared to be relatively active since 1954, the large majority of the selected watercourses exhibit stable planform. This may indicate the presence of glacial relic meanders or meander planform which was previously configured by large channel forming events, which is a common characteristic in southern Ontario (Phillips, 2014). If such stability is apparent in these watercourses, it is questionable whether meander migration analyses are necessary for many planimetric meander belt delineations.

6.2 Definition and Measurement of Meander Belt Width

There are issues apparent for meander belt width measurement due to inconsistent definitions and delineation procedures. This is partly related to whether it is defined on individual bends or on more extensive reaches. Current protocol states that a meander belt is drawn as tangential to the apex of the extreme lateral extent of meander bends (MNR, 2002; Parish Geomorphic, 2004). For regular symmetrical channels, this task may be straightforward; however, for irregular or compound meandering channels, the identification of such extreme meanders may be much more difficult. This difficulty in meander belt width delineation consistency is demonstrated in Figure 6.1, where for sites with data available, meander belts from the CVC geomorphological database and from the Aquafor Beech Ltd. watershed study were plotted against the meander belt widths measured in this thesis. Although a trend is demonstrated in the data, the majority of meander belt widths measured by other sources are lower than that of this research, with two major outliers having much higher values than that of this research. Furthermore, there are differences apparent between the CVC and Aquafor Beech Ltd. measurements of meander belt widths. This discrepancy could be the result of differences in reach delineation, or the orientation of the meander belt delineated about the meander axis. Even with the guidelines provided, there are systematic differences in the definition and measurement of the meander belt width for the same sites by different practitioners.

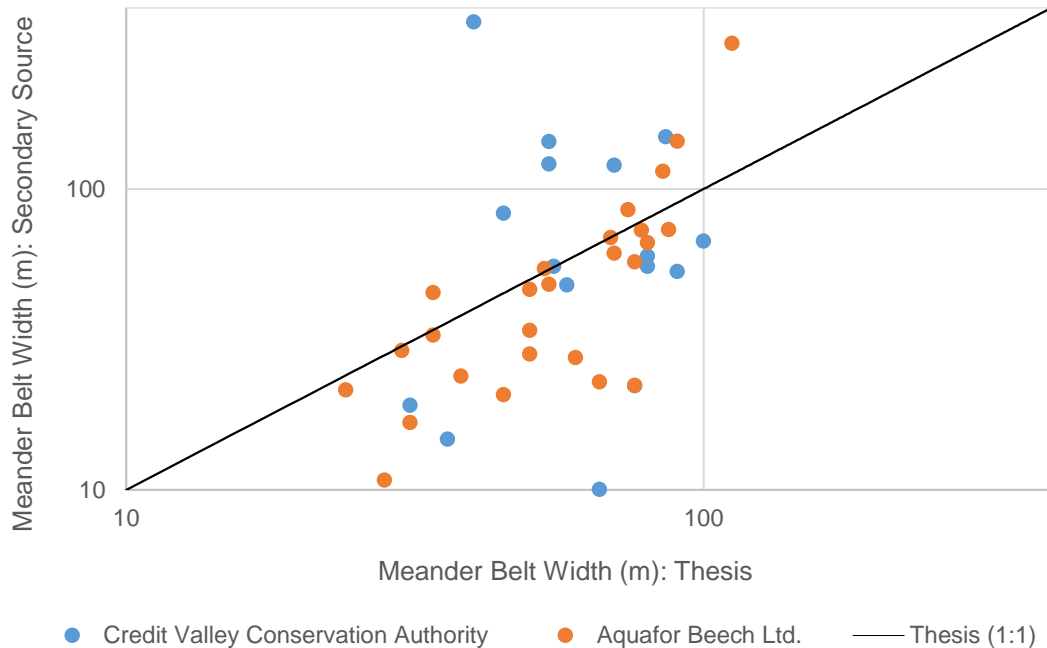


Figure 6.1 – Meander belt width measurement discrepancies.

6.3 Comparability of Models to Predict Meander Belt Width

Although the errors associated in the dependent variable is the most common consideration for using RMA regression, it has been suggested that the symmetry between the variables is the most significant consideration (Smith, 2009). As the “true” relation or the nature of symmetry between meander belt width with hydrogeomorphic parameters is still uncertain and based on the insignificant differences between the models developed, OLS relations were adopted for meander belt width empirical models, rather than RMA. This may also provide greater consistency with the literature regarding general meander morphology.

6.3.1 Mean Bankfull Width Relation to Meander Belt Width

One of the most common predictors of meander belt width used in empirical models is bankfull channel width. Table 6.1 exhibits previously established models which use bankfull channel width (also listed in Chapter 2), as well as the model developed using the current data set. The exponents

for the previously established models are very similar, ranging from 1.01 to 1.12. The model developed by the current data set is much lower, with meander belt width showing an approximately square root relation to bankfull channel width, rather than a near-linear relation. The differences in this coefficient and the implications of meander belt width prediction is seen in Figure 6.2. All three models developed by other authors greatly under predict meander belt widths for channels with a bankfull width less than five metres. The under prediction may be due to the channel sizes sampled within the previous research, perhaps lacking smaller channels. This sampling effect is demonstrated by the relation developed by Williams (1986), which were based on much larger and mobile rivers. This is also, in part, due to the low intercepts associated with the models, all which are below 10 metres, while the current model has an intercept of 26.16 metres. This discrepancy could be due to inconsistencies with reach delineation procedures, or methods of orienting a meander belt about a watercourse. Many applications of meander belt width models include an addition of an error parameter, accounting for some of the prediction error. Nevertheless, the amount of under prediction apparent with the previously developed models, especially that of Williams (1986), which is used widely across the southern Ontario region in applied geomorphology, is of great concern. The discrepancies between the collected data and the previously established models indicates that careful consideration of regional differences, measurement, and statistical error are needed applying empirical models.

Because the previously established models listed in Table 6.1 have near-linear relations, a linear model was developed for the current data set to assess similarities. The recommended MNR meander belt dimension of twenty times bankfull width appears to greatly overestimate meander belt widths for larger channel systems. The linear model developed from the current data set falls between the models developed by Lorenz *et al* (1985) and Williams (1986) (Figure 6.2). With a

p-value of 0.001 returned in a Kolmogorov-Smirnov test, the linear relation and power relation developed from the current data set are significantly different. Although the r^2 value for the developed linear model is lower than that of the power model, this outcome in linear model similarities suggests that meander belt width may demonstrate a linear relation with bankfull width. However, the linear model greatly underestimates meander belt widths for channels with smaller widths. The current dataset is not sufficient to determine whether the relation is a linear or square-root function; therefore, additional sites are necessary to confirm this finding.

Table 6.1 – Bankfull width models for meander belt width prediction.

Source	Model	r^2
Lorenz <i>et al.</i> (1985)	$M_B = 7.53 w^{1.01}$	-
Williams (1986)	$M_B = 4.30 w^{1.12}$	0.90
MNR (2002)	$M_B = 20 w$	-
Thesis (Linear Model)	$M_B = 6.89 w$	0.55
Thesis (Power Model)	$M_B = 26.16 w^{0.47}$	0.59

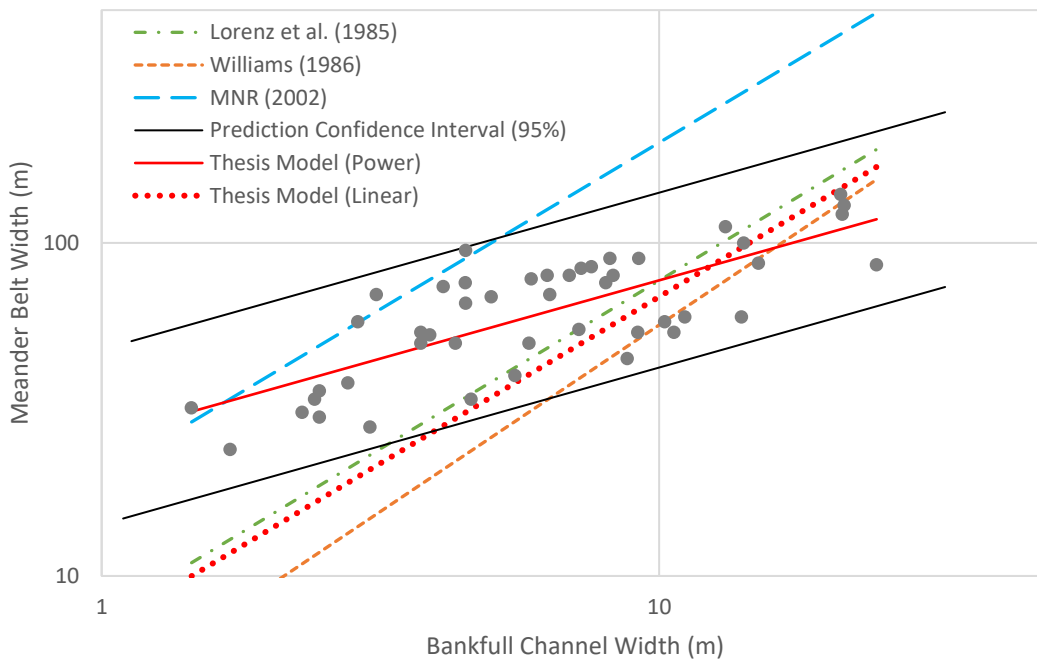


Figure 6.2 - Comparison of OLS meander belt width prediction models using bankfull width.

6.3.2 Discharge Relation to Meander Belt Width

Another method within the literature of estimating meander belt width uses discharge as a predictive parameter. Table 6.2 lists two previously established models, which use discharge for meander belt prediction, as well as the current model developed for the thesis data set. The model developed by Carlston (1970), which defines meander belt width as average meander width taken along the outside of bank lines, demonstrates greater intercept and slope coefficients, resulting in a large over prediction of all meander belt dimensions collected within the current data set (Figure 6.3). Although the relation developed by Ackers & Charlton (1970) demonstrates a greater slope coefficient of 0.51, due to the lower intercept, the model is able to capture some of the meander belt widths measured. The relations developed by Ackers & Charlton (1970) were based on experimental data which may also account for the existing discrepancies. Nevertheless, smaller channels with discharges from 0.05-7.00 m³/s are still largely under predicted by this model, and with the steeper slope coefficient, would also result in over prediction in larger channels. Meander belt width was also related to discharge by dividing the meander belt width by bankfull width by Ackers and Charlton (1970). The same model was developed for the current data set, and is significantly different from the Ackers and Charlton (1970) model in having a negative relation with discharge (Figure 6.4). The low r^2 value suggests that this model is not a good fit for predicting meander belt width.

Table 6.2 – Discharge relations for meander belt width prediction.

Source	Model	Goodness of fit Statistic
Carlston (1965)	$M_B = 65.8 Q^{0.47}$	$r^2 = 0.96$
Ackers & Charlton (1970)	$M_B = 18.5Q^{0.51}$	S.E. = 0.21
	$M_B/w = 2.71Q^{0.19}$	
Thesis	$M_B = 34.69Q^{0.27}$	$r^2 = 0.65$
	$M_B/w = 15.49Q^{-0.22}$	$r^2 = 0.35$

Standard Error (S.E.); Coefficient of determination (r^2)

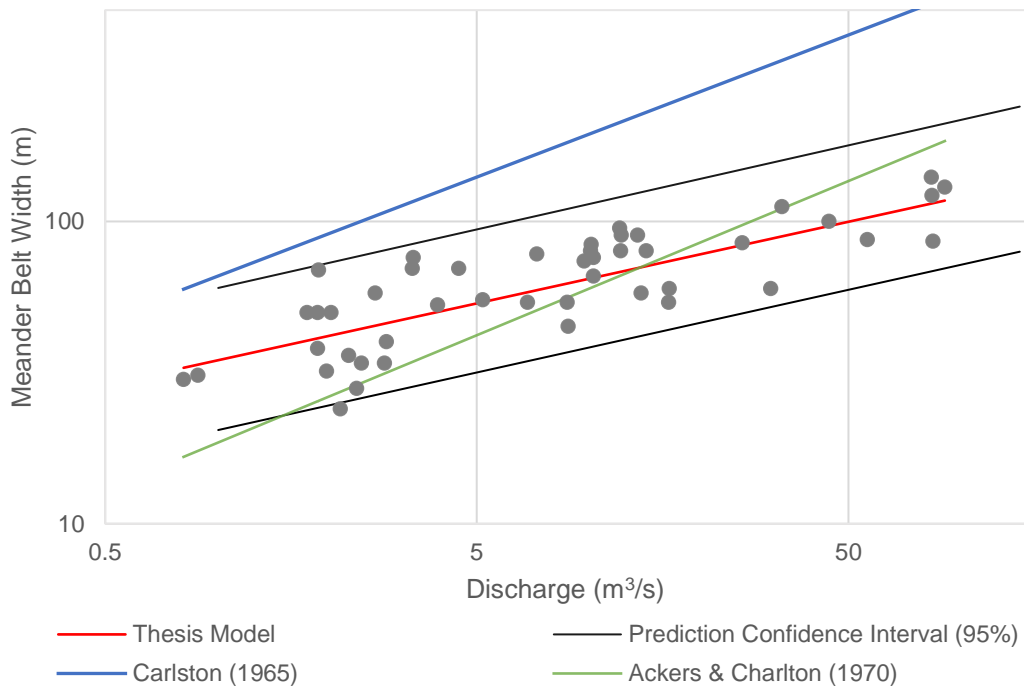


Figure 6.3 – Comparison of OLS meander belt width prediction models using discharge.

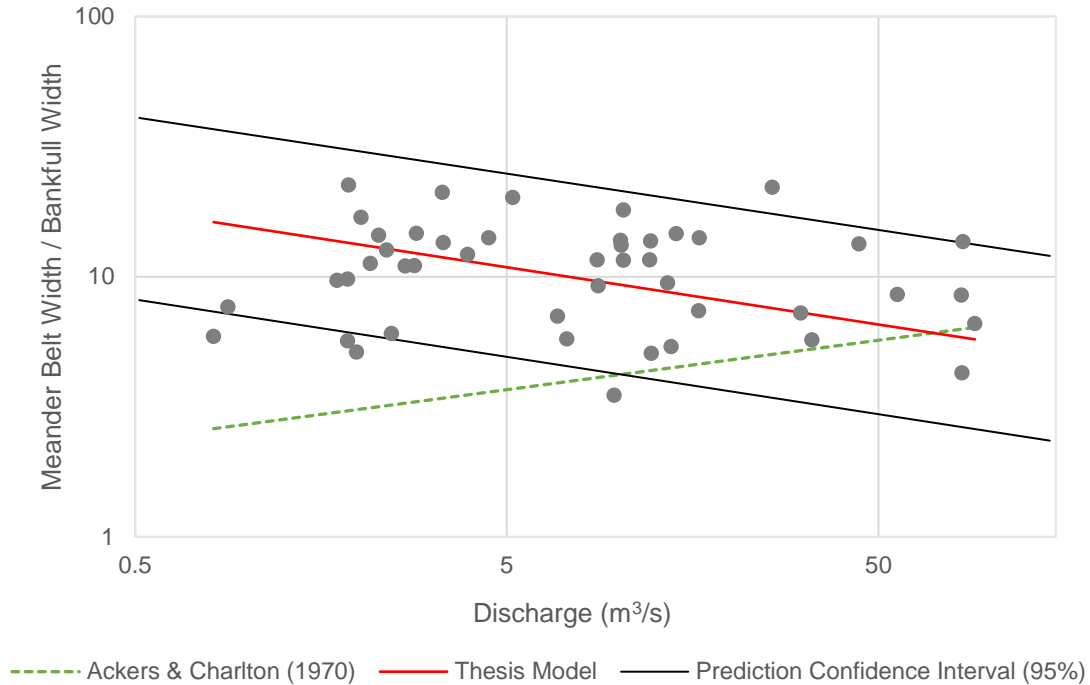


Figure 6.4 – Comparison of OLS meander belt width prediction models using discharge and bankfull width.

6.3.3 Drainage Area Relation to Meander Belt Width

Parish Geomorphic Ltd. developed a model for meander belt width prediction that uses both drainage area and total stream power as the predictive parameters. Although the particular data set from which the model was developed is unknown, the relation is commonly applied throughout southern Ontario, and is believed to be based on watercourses within the area. Although the relation of drainage area and stream power was not pursued within this research, as the correlation coefficient and the explanatory power of the relation appeared low, Table 6.3 exhibits the model which was developed in a linear regression using these parameters, as well as the Parish Geomorphic (2004) relation. Figure 6.5 displays the under prediction apparent with the Parish Geomorphic (2004) model, with all current sites are greatly under predicted. One condition of the previously established model is that it is to only be applied on systems which exhibit drainage areas less than 25km². Selected sites which adhere to this condition are highlighted in Figure 6.5.

Although the under prediction of the Parish Geomorphic (2004) model is less for these sites when compared to the rest of the data, they are still greatly under predicted. As the Parish Geomorphic (2004) model is used widely in applied geomorphology within southern Ontario, it could be said that many of the meander belt widths being predicted are greatly under estimated. Even with the addition of the standard error of the model, at 8.63, the meander belt widths estimated are below the measured dimensions for this data set. Certainly, if policies and regulations wish to continue using this guideline, the predictive model requires re-assessment.

Table 6.3 – Relations of drainage area and stream power for meander belt width.

Source	Model	r^2
Parish Geomorphic (2004)	$M_B = -14.827 + 8.319 \ln(\omega * DA)$	$r^2 = 0.74$
Thesis	$M_B = 1.98 + 16.66 \ln(\omega * DA)$	$r^2 = 0.54$

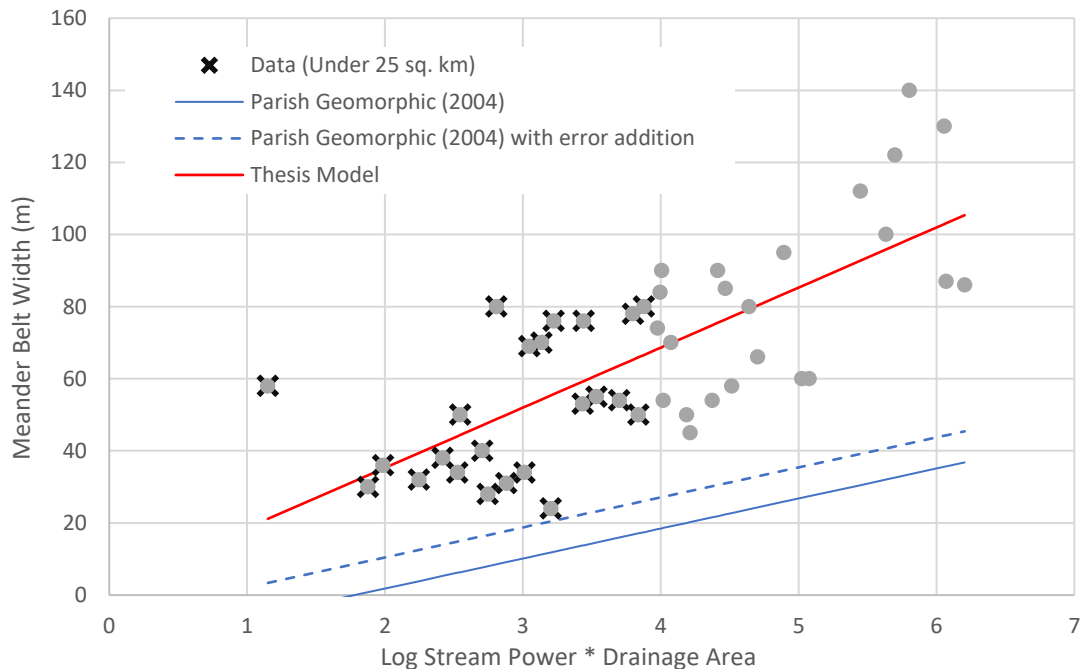


Figure 6.5 – Parish Geomorphic (2004) model for meander belt width prediction via drainage area and stream power.

6.4 Interpretations

The differences between the predictive models developed could be due to several factors, including but not limited to, the region in which the models were developed and the types of watercourses, how meander belt width is defined and measured, as well as the measurement of hydrogeomorphic parameters. Causes of the discrepancies between meander belt measurement and meander belt width prediction models are difficult to identify, however acknowledging such discrepancies will assist in determining proper meander belt measurement and the applicability of models to particular watercourses. The results of this research are influenced by the small sample size, and resulting models are not adequate substitutes for current empirical models; however, the results illustrate that applying meander belt prediction models without careful consideration of the types of channels and regions from which they were based is potentially problematic.

Although the circumstances under which meander belt delineation are required in Ontario are still somewhat ambiguous in regulatory literature, the practice of meander belt delineation is used widely across the province in development practices and species-at-risk legislation. Planimetric and historical assessment methods for meander belt delineation incorporate hydrogeomorphic parameters specific to a given reach, as well as a historical context of channel migration, which allows for a reasonable river corridor to be delineated. The issue of delineating a river corridor or meander belt for watercourses which lack this information becomes a great concern for environmental practitioners. The use of an empirical model to predict the width of a meander belt for such watercourses is a viable approach; however, based on the reliability of previously established models for the current data set, a greater understanding of the controls of meander belt width is necessary to fully validate this method.

The current research suggests meander belt is scaled to drainage area, discharge, and bankfull channel width. The relation that demonstrates the greatest explanatory power for predicting meander belt width is that of drainage area. Although additional data is required to confirm this relation, the use of drainage area to predict meander belt width may benefit practitioners. There is less uncertainty and subjectivity associated with calculating drainage area in comparison with other hydrogeomorphic parameters as drainage area can be measured remotely through a variety of standardized methods (i.e., GIS-based analysis, OFAT III). One disadvantage of using drainage area as the predictive variable for meander belt width is that changes in future hydrologic regime are not accounted for. The current dataset suggests discharge is also a strong predictor of meander belt width. This relation could potentially be used in cases where a change in hydrologic regime is anticipated, as discussed in the scenarios for *Procedures 3-4* in the Parish Geomorphic (2004) meander belt delineation document.

6.5 Future Research Perspectives

The results of this research offer insight as to the issues associated with applying empirical models for meander belt width prediction to rivers in southern Ontario. Although relations have been developed, additional data is necessary to confirm the predictive models as the current data set suffers from a limited sample size. Additionally, the sites selected are only located within the Credit River watershed. In order to develop a greater understanding of the controls of meander belt dimensions, watercourses outside of the current study area should be assessed. Pooling data from multiple studies is an option but careful cross-checking of meander belt widths is necessary because of difficulties in consistently delineating belt widths. This inconsistency in meander belt width measurement also indicates the need to assess the variability in meander belt delineation procedures.

The presented research has also demonstrated the difficulty of using empirical data for model conception in the case of meander belt width. Although the current data suggests meander belt width is scaled to drainage area, discharge, and bankfull width, there are still various unknowns present in meander belt development, and the specific controls of those dimensions. Perhaps a theoretical approach to meander belt width would be beneficial to develop knowledge regarding relations between hydrogeomorphic variables in a more controlled environment.

As stated, the large majority of selected watercourses appear to be relatively stable when compared to previous channel configurations. Further comparison of active alluvial meanders versus the inactive or possibly relic meanders in glaciated terrain in southern Ontario and different physiographic regions is needed to assess whether meander belt width predictions are transferrable between hydrogeomorphic regions.

A further assessment of policy and procedures regarding river corridor management in Ontario is necessary. An integrative or watershed approach may be more beneficial to fluvial management in southern Ontario. Rather than adopting a piecemeal approach, incorporating erosion, flooding, and slope instability hazards into the delineation of a river corridor may offer a more desirable and feasible future. Such concepts have been developed as forms of river corridor management, as discussed in Chapter 2, and would require investigation as to the applicability in southern Ontario. Nevertheless, there may be an alternative to meander belt corridor management for the region. Policies require a more definitive strategy that clearly indicates the goals and criteria for river corridor management. Moreover, the communication and involvement of both policy-makers and practitioners may result in more consistent methods and results of river corridor management throughout southern Ontario.

Chapter 7

7 Conclusion

The concept of river corridor management allows practitioners to address fluvial systems as assets, rather than liabilities, by permitting space surrounding a watercourse for natural processes to occur. One of the most common forms of river corridor management is meander belt delineation. Although it is commonly defined as the space a watercourse occupies or can occupy within the floodplain within the literature relevant to southern Ontario, an absolute definition of a meander belt which applies throughout geomorphic literature is absent. The lack of a common definition has consequences for the measurement of meander belt, and therefore, influences empirical models which are intended to provide reliable estimates of the meander belt width.

In conclusion, the research presented found that:

1. The geomorphic and hydrologic variables which appear to primarily influence meander belt width are drainage area, discharge, and mean bankfull channel width, with drainage area demonstrating the most significant predictive power.
2. The range of meander morphology for the current data set demonstrate trends in sinuosity and relative channel immobility: the most sinuous watercourses are low-order or headwater channels, and the majority of channels have stable meanders. This observation may have implications for both empirical and planimetric procedures for meander belt delineation in applied geomorphology.
3. Direct application of the equations derived from this study is premature because of the limited geographical coverage and relatively small sample size, but they add to the literature and range of relations for meander belt width. The relations in this research are different from those which are currently applied to low-order or previously altered

watercourses and consequently a re-assessment of the validity of these equations with a larger data set and consistent delineation of meander belts is needed to give a comprehensive basis for river corridor management in southern Ontario.

References

- Ackers, P., & Charlton, F. (1970). The geometry of small meandering streams. In *Proceedings of the Institution of Civil Engineers* (Vol. 47, pp. 1753-7789).
- Andrle, R. (1996). Measuring channel planform of meandering rivers. *Physical Geography*, 17(3), 270-281.
- Annable, W. (1996). *Morphologic relationships of rural watercourses in southern Ontario and selected field methods in fluvial geomorphology*. Toronto: Ontario Ministry of Natural Resources.
- Ashmore, P., & Church, M. (2001). *The impact of climate change on rivers and river processes in Canada*. Natural Resources Canada. Geological Survey of Canada, Bulletin 555.
- Biron, P., Buffin-Belanger, T., Larocque, M., Chone, G., Cloutier, C., Ouellet, M., . . . Eyquem, J. (2014). Freedom space for rivers: a sustainable management approach to enhance river resilience. *Environmental Management*, 54, 1056-1073.
- Brice, J. (1974). Evolution of meander loops. *Geological Society of America Bulletin*, 85, 581-586.
- Brice, J. (1975). *Air photo interpretation of the form and behaviour of alluvial rivers*. Durham, Washington University, St. Louis: Final Report to the U.S. Army Research Office.
- Brice, J. (1982). *Stream channel stability assessment*. Federal Highway Administration, Offices of Research and Development, Report No. FHWA/RD-82/021.
- Bridge, J., & Mackey, S. (1993). A theoretical study of fluvial sandstone body dimensions. In S. Flint, & I. Bryant, *Special publication No. 15 of the international association of sedimentologists*. Blackwell scientific publications.
- Bull, W. (1979). Threshold of critical power in streams. *Geological Society of America Bulletin*, 90, 453-464.
- Burt, J., & Barber, G. (1996). *Elementary Statistics for Geographers* (2nd ed.). NY, New York: The Guilford Press.
- Cao, S., & Knight, D. (1996). Regime theory of alluvial channels based upon the concepts of stream power and probability. *ICE Proceedings Water Maritime and Energy*, 118 (3), pp. 160-167.
- Carlston, C. (1965). The relation of free meander geometry to stream discharge and its geomorphic implications. *American Journal of Science*, 263, 864-885.
- Carson, M., & Lapointe, M. (1983). The inherent asymmetry of river meander planform. *The Journal of Geology*, 91(1), 41-55.
- Chang, H. (1984). Analysis of river meanders. *Journal of Hydraulic Engineering*, 110(1), 37-50.
- Chang, T., & Toebes, G. (1970). A statistical comparison of meander planforms in the Wabash Basin. *Water Resources Research*, 557-587.

- Chapman, L., & Putnam, D. (1984). *The physiography of southern Ontario*. Ontario Ministry of Natural Resources.
- Charlton, R. (2008). *Fundamentals of fluvial geomorphology*. Oxon, UK: Routledge.
- Collinson, J. (1978). Vertical sequence and body shape in alluvial sequences. In A. Miall, *Fluvial Sedimentology* (pp. 577-588). Canadian Society of Petroleum Geologists, Memoir 5.
- CVC. (2009). *Rising to the challenge: A handbook for understanding and protecting the Credit River watershed*. Credit Valley Conservation Authority.
- Department of Water Resources (state of California). (1998). *Sacramento River Conservation Area Handbook*. The Resources Agency State of California by the Sacramento River Advisory Council (SB1086 Program).
- Dury, G. (1976). Discharge prediction, present and former, from channel dimensions. *Journal of Hydrology*, 30, 219-245.
- Faustini, J., & Kaufmann, P. (2009). Downstream variation in bankfull width of wadeable streams across conterminous United States. *Geomorphology*, 108, 292-311.
- Ferguson, R. (1975). Meander irregularity and wavelength estimation. *Journal of Hydrology*, 26, 315-333.
- Ferguson, R. (1978). *Linear Regression in Geography. Concepts and Techniques in Modern Geography*. Norwich: Geo Abstracts Ltd.
- Ferguson, R. (1986). Hydraulics and hydraulic geometry. *Progress in Physical Geography*, 10, 1-31.
- Ferguson, R. (1986). River loads underestimated by rating curves. *Water Resources Research*, 22, 74-76.
- FISRWG. (1998). *Stream corridor restoration: principles, processes, and practices*. Federal Interagency Stream Restoration Working Group. Retrieved from http://www.usda.gov/stream_restoration/
- Friedkin, J. (1945). *A laboratory study of the meandering of alluvial rivers*. Vicksburg, Mississippi: U.S. Waterways Experiment Station.
- Geist, D. (2005). *Grays River Watershed Geomorphic Analysis*. Richland, WA: PNNL-16494, Pacific Northwest National Laboratory.
- Government of Ontario. (1990). *Conservation Authorities Act, R.O.S.: Ontario Regulation 97/04: Content of Conservation Authority Regulations Under Subsection 28 (1) of the Act: Development, Interference with Wetlands and Alterations to Shorelines and Watercourses*. Retrieved from <https://www.ontario.ca/laws/regulation/040097>
- Government of Ontario. (2007). *Ontario Regulation 293/11 made under the Endangered Species Act*. Retrieved from <https://www.ontario.ca/laws/regulation/r11293>
- Hey, R. (1976). Geometry of river meanders. *Nature*, 262, 482-484.

- Hickin, E., & Nanson, G. (1984). Lateral migration rates of river bends. *Journal of Hydraulic Engineering*, 110(11), 1557-1567.
- Hooke, J. (1984). Changes in river meanders: a review of techniques and results of analyses. *Progress in Physical Geography*, 8(4), 473-508.
- Hooke, J. (2013). River meandering. In J. Shroder, *Treatise of Geomorphology* (Vol. 9, pp. 260-287). Elsevier Inc.
- Hooke, J., & Yorke, L. (2010). Rates, distributions and mechanisms of change in meander morphology over decadal timescales, River Dan, UK. *Earth Surface Processes and Landforms*, 35, 1601-1614.
- Inglis, C. (1949). The behaviour and control of rivers and canals. *Central Waterpower Irrigation and Navigation Research Station, Poona, Research Publication*, 13(1), 486.
- Jefferson, M. (1902). Limiting width of meander belts. *The National Geographic Magazine*, 13, 373-384.
- Jennings, M., Thomas, J., & Riggs, H. (1993). *Nationwide Summary of U.S. Geological Survey Regional Regression Equations for Estimating Magnitude and Frequency of Floods for Ungaged Sites*.
- Kennedy, M., & Wilson, J. (2009). *Natural credit: Estimating the value of natural capital in the Credit River watershed*. Credit Valley Conservation & The Pembina Institute.
- Kermack, & Haldane. (1950). Organic correlation and allometry. *Bimetrika*, 37, 30-41.
- Klein, M. (1981). Drainage area and the variation of channel geometry downstream. *Earth Surface Processes and Landforms*, 6, 599-593.
- Kline, M., & Dolan, K. (2008). *River Corridor Protection Guide: Fluvial Geomorphic-Based Methodology to Reduce Flood Hazards and Protect Water Quality*. Vermont Agency of Natural Resources.
- Knighton, D. (1987). River channel adjustment - the downstream direction. In K. Richards, *River Channels: Environment and Process* (pp. 95-128). New York, NY: Oxford University Press.
- Knighton, D. (1999). Downstream variation in stream power. *Geomorphology*, 29, 293-306.
- Knighton, D. (1999). Downstream variation in stream power. *Geomorphology*, 29, 293-306.
- Lagasse, P., Spitz, W., Zevenbergen, L., & Zachmann, D. (2004). *Handbook for predicting stream meander migration*. Washington, D.C.: Transportation Research Board.
- Lagasse, P., Zevenbergen, L., Spitz, W., & Thorne, C. (2004). *Methodology for predicting channel migration*. NCHRP Web-Only Document 67 (Project 24-16). Report prepared for TRB (Transportation Research Board of the National Academies of the US). http://onlinepubs.trb.org/onlinepubs/nchrp/nchrp_w67.pdf.
- Langbein, W., & Leopold, L. (1966). River meanders - theory of minimum variance. *US Geological Survey Professional Paper*, 422-H.

- Lawler, D. (1993). The measurement of river bank erosion and lateral channel change: a review. *Earth Surface Processes and Landforms*, 18, 777-821.
- Leopold, L., & Maddock, T. (1953). *The hydraulic geometry of stream channels and some physiographic implications*. Washington, D.C.: U.S. Government Printing Office.
- Leopold, L., & Wolman, M. (1960). River meanders. *Bulletin of the Geological Society of America*, 71, 769-794.
- Leopold, L., Wolman, W., & Miller, J. (1964). *Fluvial Processes in Geomorphology*. New York: Dover Publications Inc.
- Lorenz, J., Heinze, D., Clark, J., & Searls, C. (1985). Determination of widths of meander-belt sandstone reservoirs from vertical downhole data, Mesaverde Group, Piceance Creek Basin, Colorado. *American Association of Petroleum Geologists Bulletin*, 69(5), 710-721.
- Magilligan, F. (1992). Thresholds and the spatial variability of flood power during extreme floods. *Geomorphology*, 5, 373-390.
- MNR. (2002). *River & Stream Systems: Erosion Hazard Limit - Technical Guide*. Peterborough, Ontario: Ontario Ministry of Natural Resources Water Resources Section.
- Mohamoud, Y., & Parmar, R. (2006). Estimating streamflow and associated hydraulic geometry, the Mid-Atlantic Region, USA. *Journal of the American Water Resources Association*, 42(3), 755-768.
- Moin, S., & Shaw, M. (1985). *Regional Flood Frequency Analysis for Ontario Streams (3 Volumes)*. Burlington, ON: Canada/Ontario Flood Damage Reduction Program, Environment Canada.
- Mueller, J. (1968). An introduction to the hydraulic and topographic sinuosity indexes. *Annals of the Association of American Geographers*, 58(2), 371-385.
- Neter, J., Kutner, M., Nachtsheim, C., & Wasserman, W. (1996). *Applied Linear Statistical Models* (4 ed.). New York, NY: WCB McGraw-Hill.
- Ollero, A. (2010). Channel changes and floodplain management in the meandering middle Ebro River, Spain. *Geomorphology*, 117, 247-260.
- OMNR. (2006). Provincial Digital Elevation Model - Tiled Dataset, version 2.0.0 [computer file]. Peterborough, Ontario : Ontario Ministry of Natural Resources.
- Ontario Ministry of Municipal Affairs. (1996). *Provincial Policy Statement*. Toronto, Ontario: Queens Printer for Ontario.
- Palmer, L. (1976). River management criteria for Oregon and Washington. In *Geomorphology and Engineering*, Coates DR (ed.) (pp. 329-346). Stroudsburg, PA: Dowden, Hutchinson, and Ross.
- Parish Geomorph. (2004). *Belt Width Delineation Procedures*. Toronto and Region Conservation Authority.

- Phillips, R. (2014). Alluvial floodplain classification and organization in low-relief glacially conditioned river catchments. *Ph.D. dissertation*. University of Toronto (Canada).
- Piegay, H., Darby, S., Mosselman, E., & Surian, N. (2005). A review of techniques available for delimiting the erodible river corridor: a sustainable approach to managing river bank erosion. *River Research and Applications*, 21, 773-789.
- Piegay, H., Darby, S., Mosselman, E., & Surian, N. (2005). A review of techniques available for delimiting the erodible corridor concept: a sustainable approach to managing bank erosion. *River Research and Applications*, 21, 773-789.
- Rapp, C., & Abbe, T. (2003). *A Framework for Delineating Channel Migration Zones*. Washington State Department of Transportation.
- Shahjahan, M. (1970). Factors controlling the geometry of fluvial meanders. *Bulletin of the International Association of Scientific Hydrology*, 15(3), 13-24.
- Smith, R. (2009). Use and misuse of the reduced major axis for line-fitting. *American Journal of Physical Anthropology*, 140, 476-486.
- Speight, J. (1965). Meander spectra of the Angabunga River. *Journal of Hydrology*, 1-15.
- Thorne, C., Hey, R., & Newson, M. (1997). *Applied Fluvial Geomorphology for River Engineering and Management*. Chichester, England: John Wiley & Sons Ltd.
- Thorne, C., Masterman, R., & Darby, S. (1992). Riverbank geomorphology, conservation and management. *Proceedings of the English Nature Landscape Conservation Conference* (pp. 133-144). Peterborough, UK: English Nature.
- van den Berg, J. (1995). Prediction of alluvial channel pattern of perennial rivers. *Geomorphology*, 12, 259-279.
- Ward, A., Mecklenburg, D., Mathews, J., & Farver, D. (2002). *Sizing stream setbacks to help maintain stream stability*. Paper presented at the 2002 ASAE Annual International Meeting/CIGR XVth World Congress.
- Weihaupt, J. (1989). *Disparities in the forms of river meanders and oxbow lakes*. Littleton, CO: Water Resources Publications.
- Williams, G. (1986). River meanders and channel size. *Journal of Hydrology*, 88, 47-164.
- Yang, C. (1971). On river meanders. *Journal of Hydrology*, 13, 231-253.

Appendix A – Site Characteristics

Reach	M _b	Zone	W	D	w:D	A	DA	S	Q ₂	ω	Ω	L _c	L _v	P	A _p	Stream Order	Relative Stability	Bank Materials
BC1	85	M	7.56	0.48	16.75	3.63	79.15	0.0014	25.92	344.15	45.82	540.00	551.27	0.98	80.60	5	S	cl, si, fs
BC1A	54	M	3.74	0.43	9.10	1.61	24.70	0.0068	6.85	456.02	121.93	788.00	887.20	1.15	43.46	4	S	cl, si, fs
BC2	74	M	4.10	0.98	4.21	4.00	35.00	0.0030	9.73	286.97	69.89	653.00	823.32	0.79	60.85	5	A	vfs, si
BCT1	34	M	4.90	0.27	17.00	1.24	8.03	0.0040	2.45	113.86	24.75	1334.00	249.05	5.38	28.06	3	S	si-sn
CC1	66	U	4.50	0.39	13.12	1.76	51.98	0.0105	10.30	1059.75	235.50	38.00	566.39	0.07	42.97	4	A	cl, si, fs
CC1A	31	U	2.29	0.26	9.27	0.59	1.28	0.0475	0.89	458.44	200.19	783.00	251.80	3.11	19.48	3	S	cl, vfs
CC1B	95	U	4.50	0.39	13.12	1.76	51.98	0.0125	12.12	1484.08	329.79	809.00	758.25	1.07	84.80	3	A	cl, si, fs
CC1C	24	U	1.70	0.32	5.60	0.54	6.87	0.0105	2.15	221.81	130.48	1107.00	512.49	2.16	16.15	3	NV	cl, si
CC2	53	U	3.88	0.20	19.83	0.79	11.20	0.0041	3.92	186.47	40.33	1378.00	607.50	2.27	42.90	3	A	si, fs
CC2B	30	U	2.48	0.18	14.19	0.45	1.97	0.0069	0.81	38.44	15.63	237.00	235.82	1.01	28.00	3	NV	si, ms
CR1	130	M	21.47	0.76	29.55	16.41	438.00	0.0029	90.86	2574.70	119.92	139.00	1057.31	0.13	118.00	6	S	cl, si, fs
CR2	140	M	21.18	0.87	25.20	18.43	426.90	0.0018	83.55	1487.22	70.22	1126.00	1723.97	0.65	111.13	6	S	cl, si, vfs
CR3	122	M	21.30	0.76	30.56	16.19	424.70	0.0014	83.95	1188.98	55.82	1638.00	1614.57	1.01	115.12	6	S	si, vfs
CR4	86	M	24.55	0.73	36.73	18.00	414.67	0.0046	84.42	3932.90	158.13	1199.00	578.86	2.08	57.50	6	S	si, vfs
CR5	100	U	14.18	0.71	20.12	10.07	208.50	0.0047	44.32	2054.83	144.91	1378.00	609.39	2.28	84.31	5	S	si
CR8	112	U	13.16	0.56	23.46	7.38	205.00	0.0055	33.11	1802.39	136.96	797.00	530.73	1.50	92.57	5	S	vfs, si
CR7	60	U	14.05	0.77	18.88	10.83	147.40	0.0023	30.89	707.33	50.34	254.00	607.12	0.42	36.60	5	S	si, fs
CR8	87	U	15.07	0.69	21.92	10.40	217.12	0.0097	56.25	6340.09	354.35	1200.00	1427.27	0.84	70.88	5	S	si, fs
CR9	80	U	6.90	0.73	9.51	5.05	55.38	0.0012	12.20	138.01	20.00	880.00	571.88	1.54	61.12	4	A	cl, si, ms
CR10	76	U	8.02	0.66	12.15	5.29	48.00	0.0006	10.31	62.68	7.82	793.00	1341.04	0.59	68.49	4	A	cl, si, ms
CRT1	32	M	1.45	0.16	9.57	0.23	0.85	0.0170	1.97	158.36	109.22	2362.00	594.26	3.97	27.50	3	S	cl, si
FC1	58	L	10.23	0.81	17.68	6.20	42.20	0.0058	13.85	794.16	77.83	300.00	589.39	0.51	50.63	4	S	cl, si, ms
FC2	90	L	9.18	0.71	13.52	6.52	41.51	0.0048	13.54	640.14	69.66	918.00	893.79	1.03	64.07	4	A	cl, ms
FC3	80	L	8.27	0.64	13.71	5.25	32.35	0.0002	10.11	19.89	2.42	1020.00	764.21	1.33	51.45	4	S	cl, si, ms
FC4	55	L	7.18	0.80	9.31	5.74	18.15	0.0036	5.19	182.25	25.38	855.00	938.55	0.91	37.73	4	S	cl, si, ms
FC5	69	L	5.00	2.10	2.38	10.50	7.00	0.0087	1.87	159.73	31.95	1505.00	722.83	2.08	62.34	3	S	cl, si, vfs
HC1	76	L	4.49	0.38	12.56	1.72	9.75	0.0062	3.37	149.91	33.39	359.00	743.48	0.48	67.85	4	S	si, fs
LC1	45	L	8.77	0.54	16.28	4.74	23.23	0.0081	8.81	699.27	79.73	1488.00	560.48	2.65	21.63	4	S	cl, si, ms
LC2	78	L	5.90	1.37	4.32	8.07	19.57	0.0044	7.28	315.09	53.41	162.00	468.15	0.35	72.61	4	S	si, ms
LC3	70	L	3.11	0.27	11.60	0.85	9.67	0.0037	4.47	133.37	42.88	964.00	1104.19	0.87	48.93	3	S	cl, ms
LCR1	50	M	4.31	1.30	3.32	5.60	42.00	0.0014	2.03	180.18	41.81	601.00	314.94	1.91	38.26	4	A	cl, si, ms

Variables: meander belt width (M_b), mean bankfull channel width (w), mean bankfull channel depth (D), mean width depth ratio (w:D), channel cross-sectional area (A), drainage area (DA), valley gradient (S), discharge (Q₂), total stream power (Ω), channel length (L_c), valley length (L_v), sinuosity (P), meander amplitude (A_p)
Watershed zone: Lower (L), Middle (M), Upper (U)
Relative stability: active (A), stable (S) channel planform from 1954 imagery (source) to 2013. Some channels were not visible (NV) in 1954 imagery.

Reach	M _b	Zone	W	D	w:D	A	DA	S	Q ₂	ω	Ω	L _c	L _v	P	A _p	Stream Order	Relative Stability	Bank Materials
LCR1A	50	M	3.74	0.39	10.05	1.46	3.20	0.0041	1.75	83.02	22.20	71.00	647.56	0.11	47.79	3	S	cl, si
LCR1B	38	M	2.77	0.63	4.39	1.74	8.00	0.0105	1.87	78.02	28.20	951.00	221.04	4.30	32.23	2	S	cl, si, vfs
LCR2	50	M	5.84	0.39	15.22	2.28	23.00	0.0076	1.87	832.76	108.35	111.00	116.34	0.95	41.37	3	A	si
MC1	28	U	3.03	0.55	5.77	1.67	5.55	0.0031	2.38	96.73	31.92	610.00	149.35	4.08	16.27	2	S	cl, si
MUC1	54	L	9.16	0.41	23.02	3.79	21.67	0.0022	8.77	191.65	20.92	383.00	1058.43	0.36	26.89	3	A	cl, si, fs
RC1	70	M	6.37	0.35	18.17	2.23	15.99	0.0136	3.35	827.37	129.89	1124.00	696.30	1.61	55.77	4	S	cl, si, fs
SBC1	40	L	5.51	0.27	22.12	1.49	3.25	0.0142	2.86	166.53	30.22	1240.00	806.97	1.54	33.25	2	A	si
SBC2	34	L	2.41	0.29	8.97	0.70	2.77	0.0073	2.82	99.06	41.10	971.00	226.53	4.29	30.10	3	A	cl, si
SHC1	54	U	10.84	0.93	11.44	9.90	61.00	0.0023	16.43	370.21	34.79	447.00	519.95	0.86	33.92	5	A	si, vfs
SHC1A	36	U	2.46	0.33	7.56	0.81	5.36	0.0008	2.26	17.56	7.14	161.00	212.37	0.76	27.88	3	N/V	cl, si
SHC2	60	U	11.12	0.43	27.08	4.78	61.80	0.0116	18.48	1875.27	168.84	568.00	509.30	1.10	39.51	5	S	si, vfs
SHC2A	58	U	2.88	0.49	5.93	1.42	12.58	0.0004	2.67	4.16	1.44	422.00	620.51	0.68	37.40	3	A	si
SVC1	80	M	6.30	0.30	22.10	1.89	41.05	0.0082	14.30	1146.59	181.91	1101.00	776.67	1.42	67.55	5	A	cl, si, fs
SVC2	84	M	7.25	0.26	28.32	1.86	25.93	0.0038	10.17	382.39	52.74	864.00	562.33	1.54	57.57	5	A	cl, si, fs
WC2	90	U	8.16	0.53	16.11	4.32	36.07	0.0023	12.25	282.16	34.58	1545.00	536.80	2.88	85.69	4	S	cl, si

Variables: meander belt width (M_b), mean bankfull channel width (w), mean bankfull channel depth (D), mean width depth ratio (w:D), channel cross-sectional area (A), drainage area (DA), valley gradient (S), discharge (Q₂), total stream power (ω), specific stream power (Ω), channel length (L_c), valley length (L_v), sinuosity (P), meander amplitude (A_p)

Watershed zone: Lower (L), Middle (M), Upper (U)

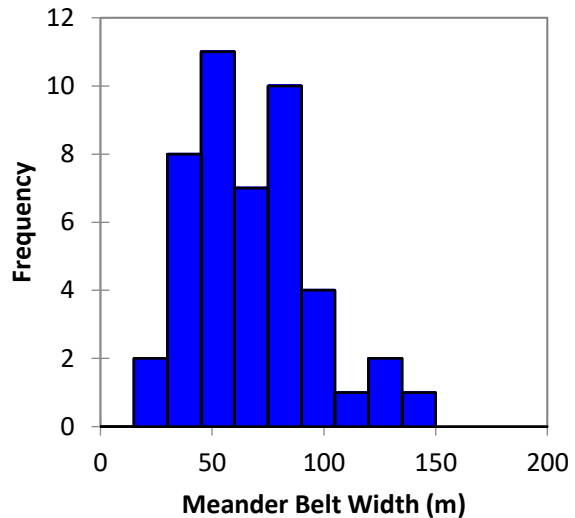
Relative stability: active (A), stable (S) channel planform from 1954 imagery (source) to 2013. Some channels were not visible (N/V) in 1954 imagery.

Appendix B – Descriptive Statistics for Model Development

Descriptive statistics for the considered parameters for meander belt width model development.

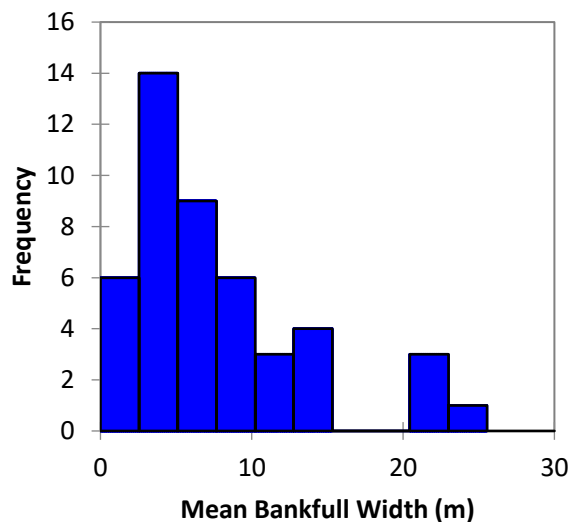
Meander Belt Width

Statistic	M_B
Number of observations	46
Minimum	24.000
Maximum	140.000
1st Quartile	50.000
Median	63.000
3rd Quartile	83.000
Mean	66.696
Variance (n-1)	754.172
Standard deviation (n-1)	27.462
Geometric mean	61.191
Geometric standard deviation	1.536



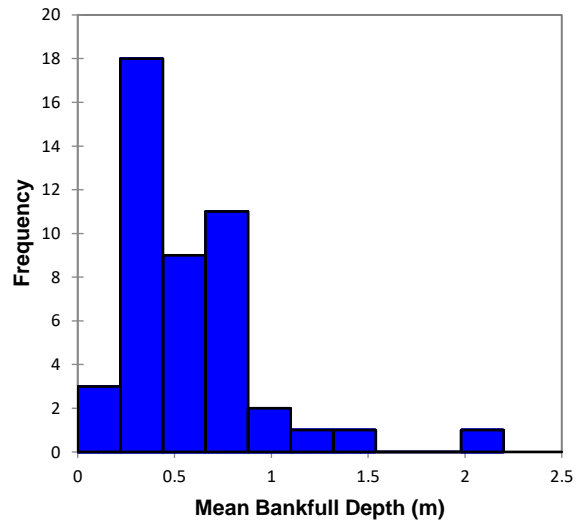
Mean Bankfull Width

Statistic	w
Number of observations	46
Minimum	1.450
Maximum	24.550
1st Quartile	3.775
Median	6.102
3rd Quartile	9.183
Mean	7.712
Variance (n-1)	32.258
Standard deviation (n-1)	5.680
Geometric mean	6.082
Geometric standard deviation	2.009



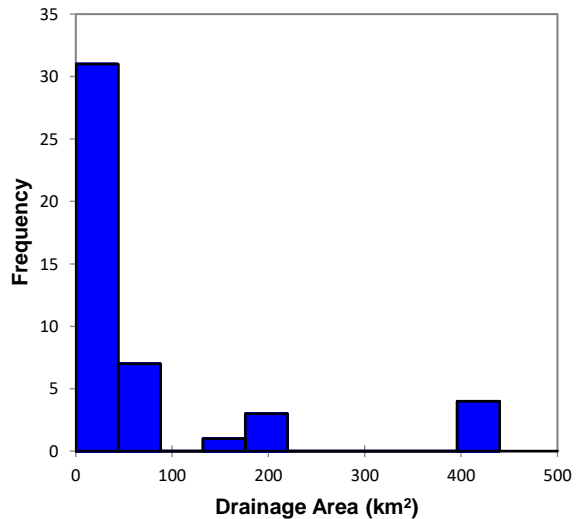
Mean Bankfull Depth

Statistic	<i>D</i>
Number of observations	46
Minimum	0.160
Maximum	2.100
1st Quartile	0.335
Median	0.511
3rd Quartile	0.727
Mean	0.578
Variance (n-1)	0.126
Standard deviation (n-1)	0.355
Geometric mean	0.497
Geometric standard deviation	1.725



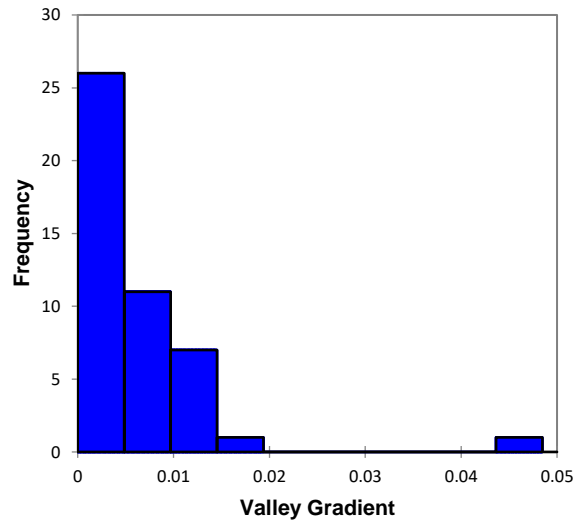
Drainage Area

Statistic	<i>DA</i>
Number of observations	46
Minimum	0.850
Maximum	439.000
1st Quartile	8.440
Median	25.315
3rd Quartile	54.530
Mean	74.572
Variance (n-1)	14785.449
Standard deviation (n-1)	121.595
Geometric mean	25.312
Geometric standard deviation	4.747



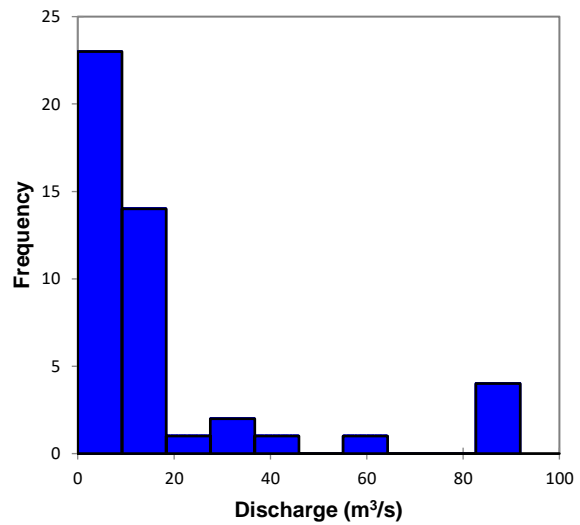
Valley Gradient

Statistic	S
Number of observations	46
Minimum	0.000
Maximum	0.047
1st Quartile	0.002
Median	0.005
3rd Quartile	0.008
Mean	0.006
Variance (n-1)	0.000
Standard deviation (n-1)	0.007
Geometric mean	0.004
Geometric standard deviation	2.805



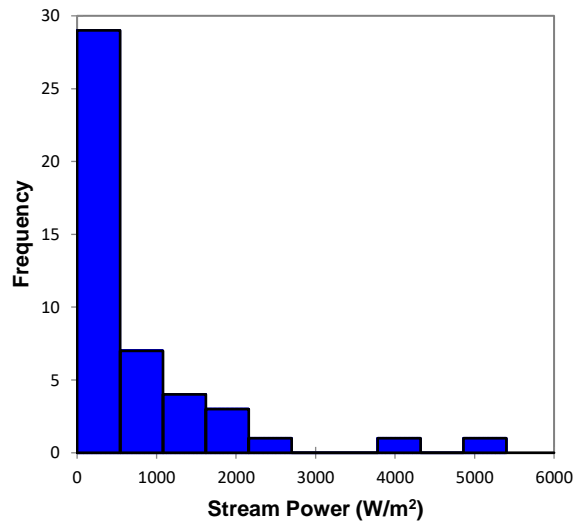
Discharge

Statistic	Q_2
Number of observations	46
Minimum	0.813
Maximum	90.864
1st Quartile	2.502
Median	8.783
3rd Quartile	14.183
Mean	16.907
Variance (n-1)	591.114
Standard deviation (n-1)	24.313
Geometric mean	7.360
Geometric standard deviation	3.537



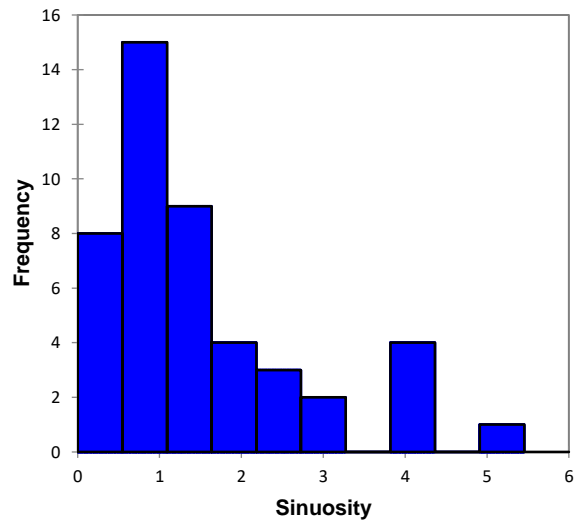
Total Stream Power

Statistic	Ω
Number of observations	46
Minimum	4.157
Maximum	5340.094
1st Quartile	140.985
Median	301.034
3rd Quartile	819.065
Mean	728.154
Variance (n-1)	1094696.138
Standard deviation (n-1)	1046.277
Geometric mean	306.890
Geometric standard deviation	4.325



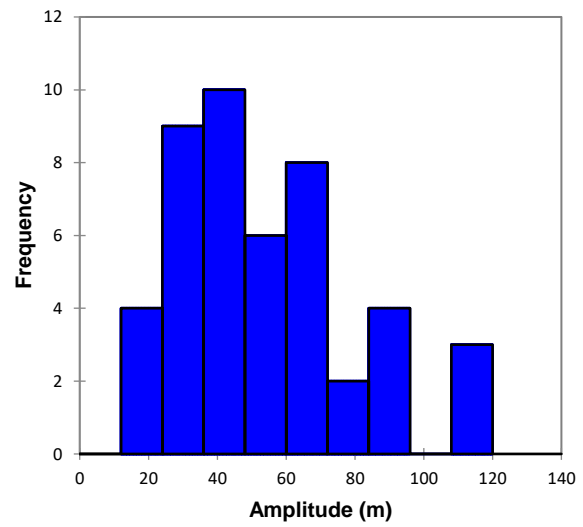
Sinuosity

Statistic	P
Number of observations	46
Minimum	0.070
Maximum	5.356
1st Quartile	0.767
Median	1.081
3rd Quartile	2.081
Mean	1.556
Variance (n-1)	1.549
Standard deviation (n-1)	1.245
Geometric mean	1.103
Geometric standard deviation	2.545



Meander Amplitude

Statistic	A_P
Nbr. of observations	46
Minimum	16.153
Maximum	117.998
1st Quartile	33.416
Median	48.359
3rd Quartile	67.776
Mean	52.931
Variance (n-1)	670.729
Standard deviation (n-1)	25.898
Geometric mean	46.978
Geometric standard deviation	1.656



Appendix C – Field Investigation Form

Date: _____ Watercourse: _____

Location: _____ Reach: _____

Land Use	<input type="checkbox"/> Forest	<input type="checkbox"/> Agriculture	<input type="checkbox"/> Residential
	<input type="checkbox"/> Pasture/Meadow	<input type="checkbox"/> Industrial/Commercial	<input type="checkbox"/> Other

Valley Type	<input type="checkbox"/> Unconfined	<input type="checkbox"/> Confined	<input type="checkbox"/> Partially Confined
--------------------	-------------------------------------	-----------------------------------	---

Channel Characteristics	Platform	Sinuosity	<input type="checkbox"/> Low	<input type="checkbox"/> Medium	<input type="checkbox"/> High				
		Gradient	<input type="checkbox"/> Low	<input type="checkbox"/> Medium	<input type="checkbox"/> High				
		Meandering	<input type="checkbox"/> Low	<input type="checkbox"/> Medium	<input type="checkbox"/> High				
	Bank	Erosion	<input type="checkbox"/> < 5%	<input type="checkbox"/> 5 - 30%	<input type="checkbox"/> 30 - 60%	<input type="checkbox"/> 60 - 100%			
		Failure	<input type="checkbox"/> None	<input type="checkbox"/> Slump	<input type="checkbox"/> Undercut	<input type="checkbox"/> Mass			
		Material	<input type="checkbox"/> Clay/silt	<input type="checkbox"/> Sand	<input type="checkbox"/> Gravel	<input type="checkbox"/> Cobble			
	Channel	Riffle Substrate	<input type="checkbox"/> Clay/silt	<input type="checkbox"/> Sand	<input type="checkbox"/> Gravel	<input type="checkbox"/> Cobble			
			<input type="checkbox"/> Boulder	<input type="checkbox"/> Other:					
		Pool Substrate	<input type="checkbox"/> Clay/silt	<input type="checkbox"/> Sand	<input type="checkbox"/> Gravel	<input type="checkbox"/> Cobble			
			<input type="checkbox"/> Boulder	<input type="checkbox"/> Other:					
Bankfull Width (m)		Riffle	_____	_____	_____	Pool	_____	_____	_____
Bankfull Depth (m)		_____	_____	_____		_____	_____	_____	_____

Appendix D – Correlation Matrix

Variables	Significance (p-value)												
	Meander Belt Width (m)	Mean Bankfull Width (m)	Mean Bankfull Depth (m)	Width Depth Ratio	Cross-sectional Area	Drainage Area (km ²)	Valley Gradient	Q _s (m ³ /s)	Total Stream Power	Specific Stream Power	Sinuosity	Stream Order	Amplitude (m)
Meander Belt Width (m)	0.000	0.035	0.000	0.000	0.000	0.030	0.000	0.000	0.000	0.118	0.002	0.000	0.000
Mean Bankfull Width (m)	0.739	0.062	0.006	0.0001	0.079	0.0001	0.150	0.0001	0.165	0.052	0.0001	0.066	0.035
Mean Bankfull Depth (m)	0.312	0.278	0.115	0.0001	0.088	0.122	0.150	0.547	0.372	0.260	0.066	0.035	0.035
Width Depth Ratio	0.544	0.778	0.235	0.0001	0.544	0.0001	0.065	0.065	0.065	0.221	0.0001	0.001	0.001
Cross-sectional Area (m ²)	0.708	0.924	0.587	0.0001	0.056	0.0001	0.475	0.475	0.475	0.59	0.0001	0.0001	0.0001
Drainage Area (km ²)	0.748	0.928	0.231	0.886	0.180	0.0001	0.081	0.081	0.081	0.136	0.0001	0.0001	0.0001
Valley Gradient	-0.320	-0.261	-0.255	-0.284	-0.201	0.171	0.681	0.681	0.001	0.045	0.064	0.052	0.052
Q _s (m ³ /s)	0.756	0.940	0.216	0.710	0.885	-0.205	0.053	0.053	0.053	0.110	0.0001	0.0001	0.0001
Total Stream Power (w/m ²)	0.504	0.705	0.091	0.613	0.691	0.062	0.730	0.730	0.730	0.255	0.0001	0.0001	0.002
Specific Stream Power (w/m)	0.234	0.208	-0.135	0.274	0.108	0.475	0.288	0.288	0.288	0.597	0.090	0.156	0.156
Sinuosity	-0.053	-0.339	0.041	-0.303	-0.267	-0.223	-0.239	-0.239	-0.248	0.005	0.009	0.009	0.009
Stream Order	0.762	0.814	0.273	0.622	0.757	-0.275	0.784	0.589	0.253	-0.227	0.0001	0.0001	0.0001
Amplitude (m)	0.957	0.647	0.312	0.456	0.640	-0.288	0.706	0.443	0.212	-0.025	0.679	0.679	0.679

Values in bold are different from 0 with a significance level alpha = 0.05

Appendix E – Descriptive Statistics of Regression Analysis

Descriptive statistics of regression analyses with selected parameters.

Meander Belt Width vs. Amplitude

Goodness of fit statistics (Meander Belt Width (m)):

Observations	46.000
Sum of weights	46.000
DF	44.000
R ²	0.916
Adjusted R ²	0.914
MSE	64.714
RMSE	8.044
DW	1.649
AIC	193.774

Analysis of variance:

Source	DF	Sum of squares	Mean squares	F	Pr > F
Model	1	31090.337	31090.337	480.429	< 0.0001
Error	44	2847.402	64.714		
Corrected Total	45	33937.739			

Type I Sum of Squares analysis (Meander Belt Width (m)):

Source	DF	Sum of squares	Mean squares	F	Pr > F
Amplitude (m)	1	31090.337	31090.337	480.429	< 0.0001

Type III Sum of Squares analysis (Meander Belt Width (m)):

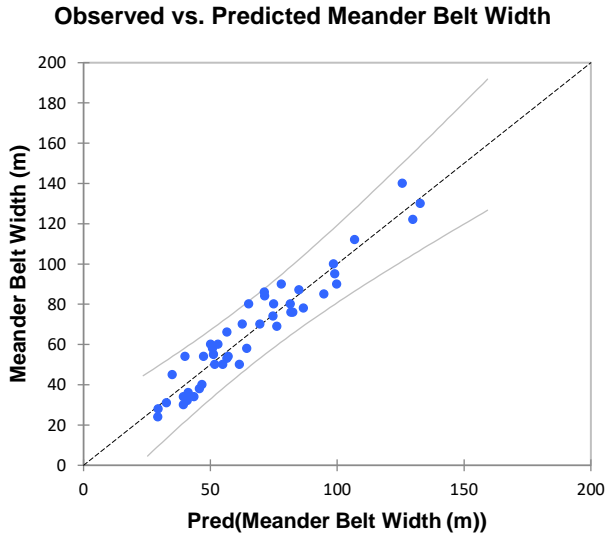
Source	DF	Sum of squares	Mean squares	F	Pr > F
Amplitude (m)	1	31090.337	31090.337	480.429	< 0.0001

Model parameters (Meander Belt Width (m)):

Source	Value	Standard error	t	Pr > t	Lower bound (95%)	Upper bound (95%)
Intercept	12.975	2.723	4.765	< 0.0001	7.488	18.463
Amplitude (m)	1.015	0.046	21.919	< 0.0001	0.922	1.108

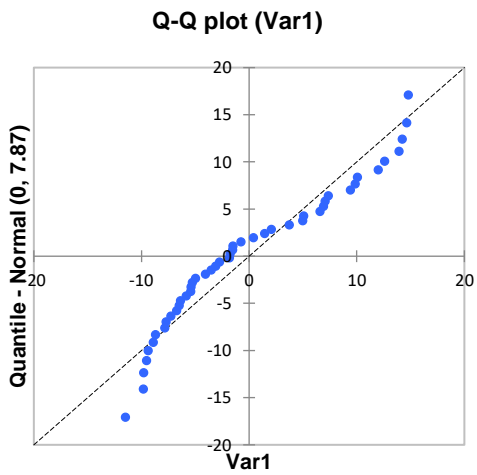
Standardized coefficients (Meander Belt Width (m)):

Source	Value	Standard error	t	Pr > t	Lower bound (95%)	Upper bound (95%)
Amplitude (m)	0.957	0.044	21.919	< 0.0001	0.869	1.045



Shapiro-Wilk test (Var1):

W	0.920
p-value (Two-tailed)	0.004
alpha	0.05



Meander Belt Width vs. Amplitude and Mean Bankfull Channel Width

Goodness of fit statistics:

Observations	46.000
Sum of weights	46.000
DF	44.000
R ²	0.940
Adjusted R ²	0.939
MSE	45.979
RMSE	6.781
DW	1.566
AIC	178.051

Analysis of variance:

Source	DF	Sum of squares	Mean squares	F	Pr > F
Model	1	31914.678	31914.678	694.119	< 0.0001
Error	44	2023.061	45.979		
Corrected Total	45	33937.739			

Type I Sum of Squares analysis (Meander Belt Width (m)):

Source	DF	Sum of squares	Mean squares	F	Pr > F
Amp + W	1	31914.678	31914.678	694.119	< 0.0001

Type III Sum of Squares analysis (Meander Belt Width (m)):

Source	DF	Sum of squares	Mean squares	F	Pr > F
Amp + W	1	31914.678	31914.678	694.119	< 0.0001

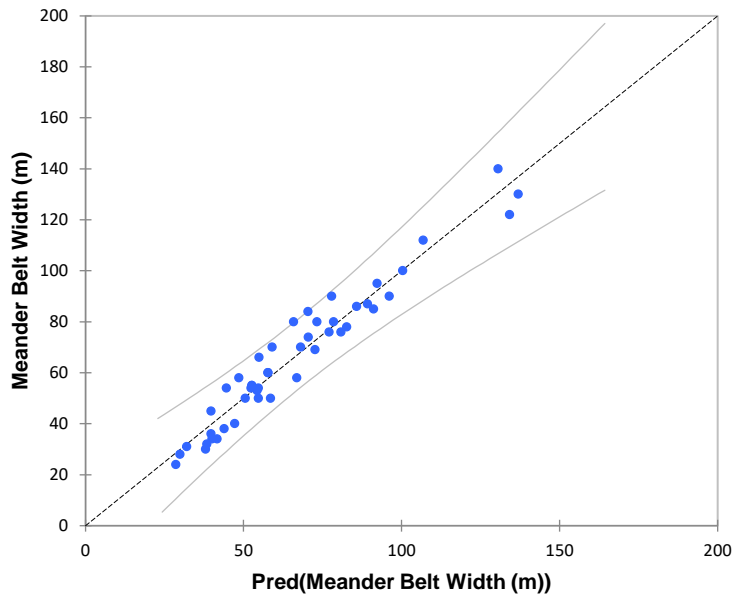
Model parameters (Meander Belt Width (m)):

Source	Value	Standard error	t	Pr > t	Lower bound (95%)	Upper bound (95%)
Intercept	12.667	2.281	5.552	< 0.0001	8.069	17.265
Amp + W	0.891	0.034	26.346	< 0.0001	0.823	0.959

Standardized coefficients (Meander Belt Width (m)):

Source	Value	Standard error	t	Pr > t	Lower bound (95%)	Upper bound (95%)
Amp + W	0.970	0.037	26.346	< 0.0001	0.896	1.044

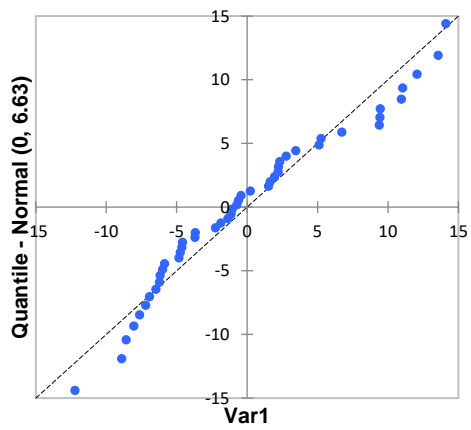
Observed vs. Predicted Meander Belt Width



Shapiro-Wilk test (Var1):

W	0.953
p-value (Two-tailed)	0.060
alpha	0.05

Q-Q plot (Var1)



Meander Belt Width vs. Bankfull Channel Width (Power Relation)

Goodness of fit statistics:

Observations	46.000
Sum of weights	46.000
DF	45.000
R ²	0.589
Adjusted R ²	0.576
MSE	401.780
RMSE	20.044
DW	1.896
Cp	-30.056
AIC	276.801

Analysis of variance (Meander Belt Width (m)):

Source	DF	Sum of squares	Mean squares	F	Pr > F
Model	1	91442.049	91442.049	227.592	< 0.0001
Error	45	18080.089	401.780		
Corrected Total	46	109522.138			

Type I Sum of Squares analysis (Meander Belt Width (m)):

Source	DF	Sum of squares	Mean squares	F	Pr > F
Mean Bankfull Width (m)	1	91442.049	91442.049	227.592	< 0.0001

Type III Sum of Squares analysis (Meander Belt Width (m)):

Source	DF	Sum of squares	Mean squares	F	Pr > F
Mean Bankfull Width (m)	1	91442.049	91442.049	227.592	< 0.0001

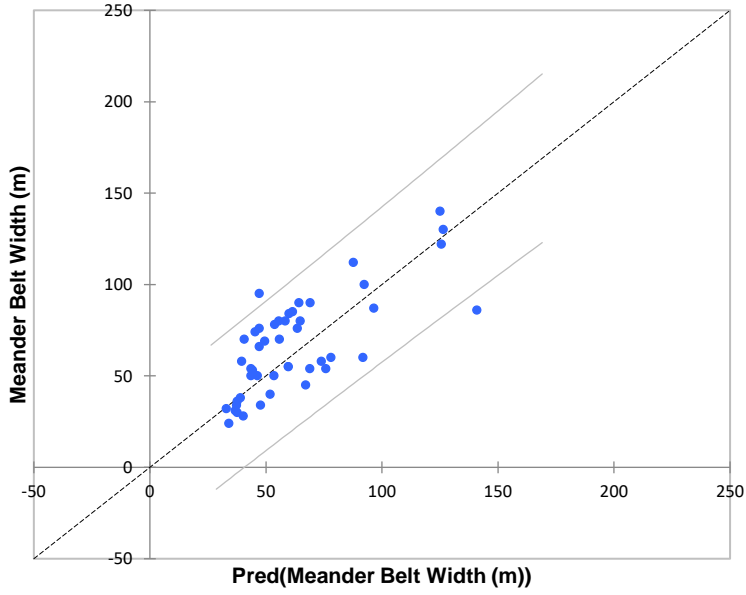
Model parameters (Meander Belt Width (m)):

Source	Value	Standard error	t	Pr > t	Lower bound (95%)	Upper bound (95%)
Intercept	26.160					
Mean Bankfull Width (m)	0.472	0.310	15.086	< 0.0001	4.049	5.297

Standardized coefficients (Meander Belt Width (m)):

Source	Value	Standard error	t	Pr > t	Lower bound (95%)	Upper bound (95%)
Mean Bankfull Width (m)	0.914	0.061	15.086	< 0.0001	0.792	1.036

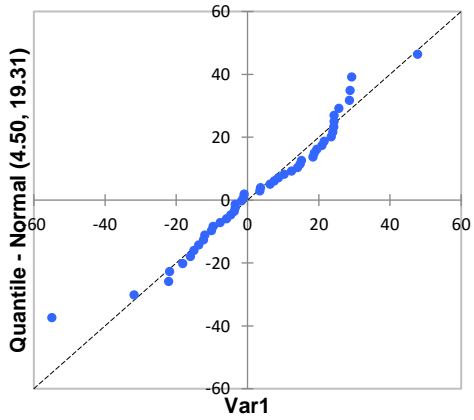
Observed vs. Predicted Meander Belt Width



Shapiro-Wilk test (Var1):

W	0.969
p-value (Two-tailed)	0.252
alpha	0.05

Q-Q plot (Var1)



Meander Belt Width vs. Bankfull Channel Width (Linear Relation)

Goodness of fit statistics (Meander Belt Width (m)):

Observations	46.000
Sum of weights	46.000
DF	45.000
R ²	0.546
Adjusted R ²	
MSE	884.826
RMSE	29.746
DW	1.715
Cp	-37.598
AIC	313.117

Analysis of variance (Meander Belt Width (m)):

Source	DF	Sum of squares	Mean squares	F	Pr > F
Model	1	198742.852	198742.852	224.612	< 0.0001
Error	45	39817.148	884.826		
Corrected Total	46	238560.000			

Computed against model Y=0

Type I Sum of Squares analysis (Meander Belt Width (m)):

Source	DF	Sum of squares	Mean squares	F	Pr > F
Mean Bankfull Width (m)	1	198742.852	198742.852	224.612	< 0.0001

Type III Sum of Squares analysis (Meander Belt Width (m)):

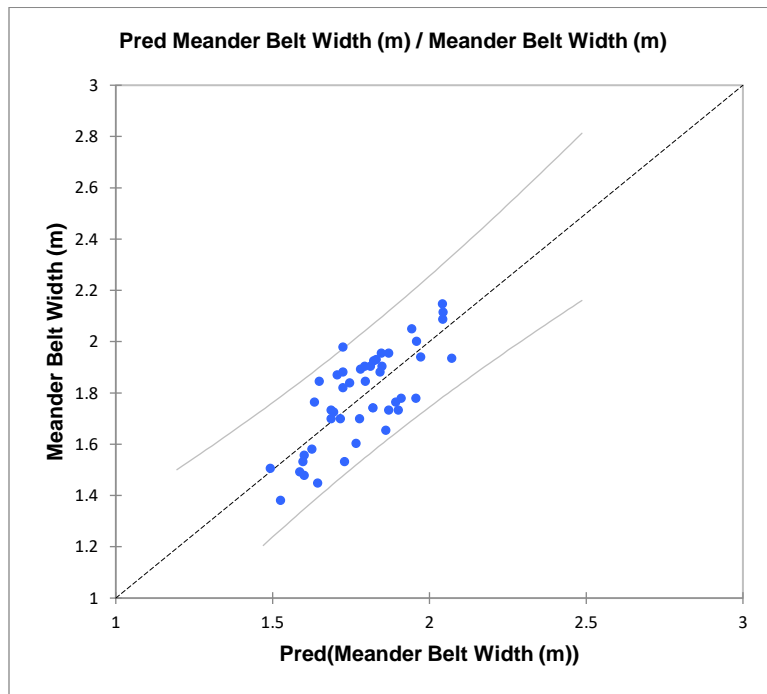
Source	DF	Sum of squares	Mean squares	F	Pr > F
Mean Bankfull Width (m)	1	198742.852	198742.852	224.612	< 0.0001

Model parameters (Meander Belt Width (m)):

Source	Value	Standard error	t	Pr > t	Lower bound (95%)	Upper bound (95%)
Intercept	0.000					
Mean Bankfull Width (m)	6.889	0.460	14.987	< 0.0001	5.963	7.815

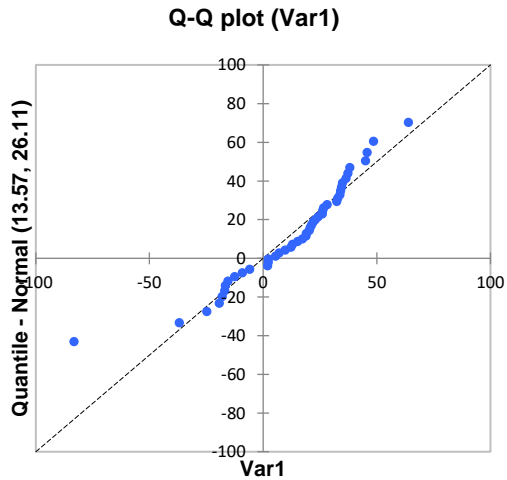
Standardized coefficients (Meander Belt Width (m)):

Source	Value	Standard error	t	Pr > t	Lower bound (95%)	Upper bound (95%)
Mean Bankfull Width (m)	0.913	0.061	14.987	0.0001	0.790	1.035



Shapiro-Wilk test (Var1):

W	0.927
p-value (Two-tailed)	0.006
alpha	0.05



Meander Belt Width vs. Sinuosity

Goodness of fit statistics:

Observations	46.000
Sum of weights	46.000
DF	44.000
R ²	0.190
Adjusted R ²	0.171
MSE	624.852
RMSE	24.997
DW	1.957
AIC	298.081

Analysis of variance:

Source	DF	Sum of squares	Mean squares	F	Pr > F
Model	1	6444.235	6444.235	10.313	0.002
Error	44	27493.504	624.852		
Corrected Total	45	33937.739			

Type I Sum of Squares analysis (Meander Belt Width (m)):

Source	DF	Sum of squares	Mean squares	F	Pr > F
Sinuosity	1	6444.235	6444.235	10.313	0.002

Type III Sum of Squares analysis (Meander Belt Width (m)):

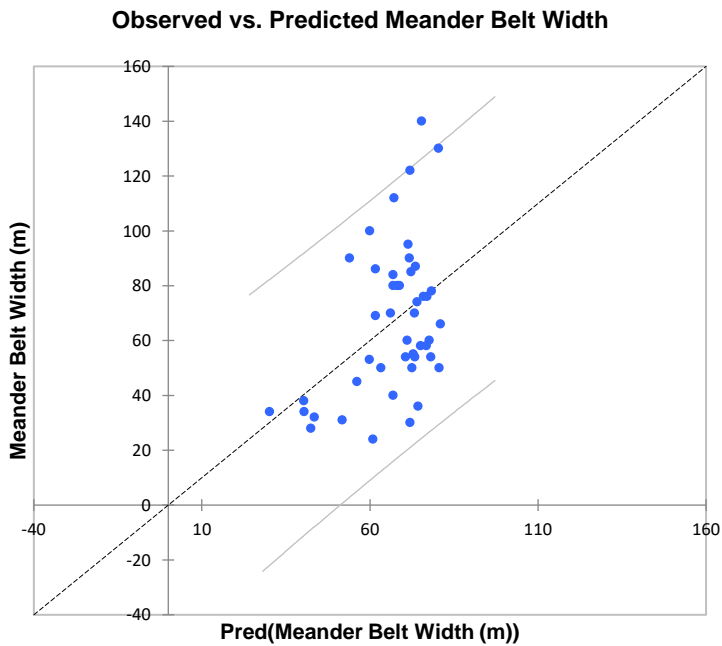
Source	DF	Sum of squares	Mean squares	F	Pr > F
Sinuosity	1	6444.235	6444.235	10.313	0.002

Model parameters (Meander Belt Width (m)):

Source	Value	Standard error	t	Pr > t	Lower bound (95%)	Upper bound (95%)
Intercept	81.652	5.939	13.748	0.0001	69.682	93.621
Sinuosity	-9.614	2.994	-3.211	0.002	-15.647	-3.581

Standardized coefficients (Meander Belt Width (m)):

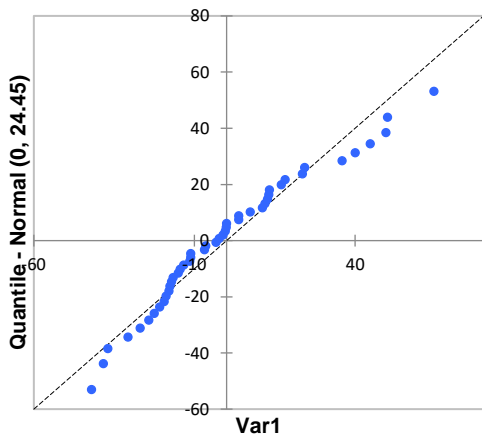
Source	Value	Standard error	t	Pr > t	Lower bound (95%)	Upper bound (95%)
Sinuosity	-0.436	0.136	-3.211	0.002	-0.709	-0.162



Shapiro-Wilk test (Var1):

W	0.956
p-value (Two-tailed)	0.077
alpha	0.05

Q-Q plot (Var1)



Meander Belt Width vs. Valley Gradient

Goodness of fit statistics (Meander Belt Width (m)):

Observations	46.000
Sum of weights	46.000
DF	44.000
R ²	0.103
Adjusted R ²	0.082
MSE	692.083
RMSE	26.307
DW	1.588
Cp	2.000
AIC	302.782

Analysis of variance (Meander Belt Width (m)):

Source	DF	Sum of squares	Mean squares	F	Pr > F
Model	1	3486.085	3486.085	5.037	0.030
Error	44	30451.655	692.083		
Corrected Total	45	33937.739			

Type I Sum of Squares analysis (Meander Belt Width (m)):

Source	DF	Sum of squares	Mean squares	F	Pr > F
Valley Gradient (%)	1	3486.085	3486.085	5.037	0.030

Type III Sum of Squares analysis (Meander Belt Width (m)):

Source	DF	Sum of squares	Mean squares	F	Pr > F
Valley Gradient (%)	1	3486.085	3486.085	5.037	0.030

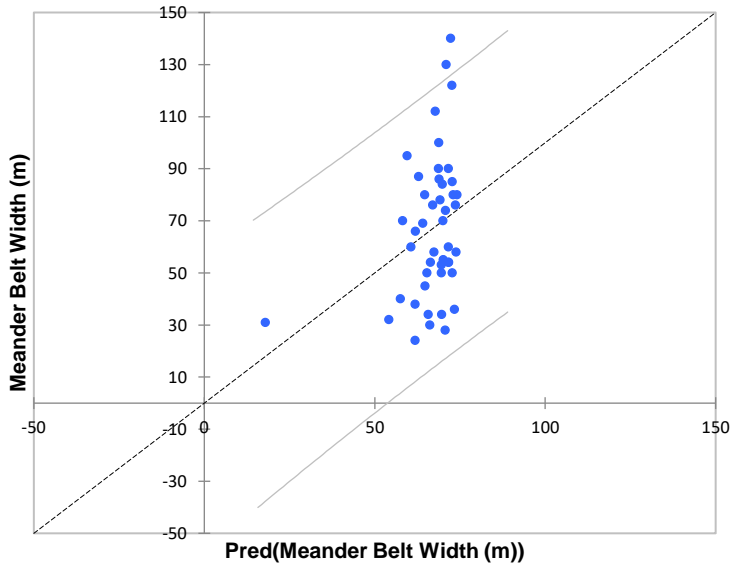
Model parameters (Meander Belt Width (m)):

Source	Value	Standard error	t	Pr > t	Lower bound (95%)	Upper bound (95%)
Intercept	74.397	5.179	14.366	0.0001	63.960	84.833
Valley Gradient (%)	-1188.649	529.619	-2.244	0.030	-2256.027	-121.272

Standardized coefficients (Meander Belt Width (m)):

Source	Value	Standard error	t	Pr > t	Lower bound (95%)	Upper bound (95%)
Valley Gradient (%)	-0.320	0.143	-2.244	0.030	-0.608	-0.033

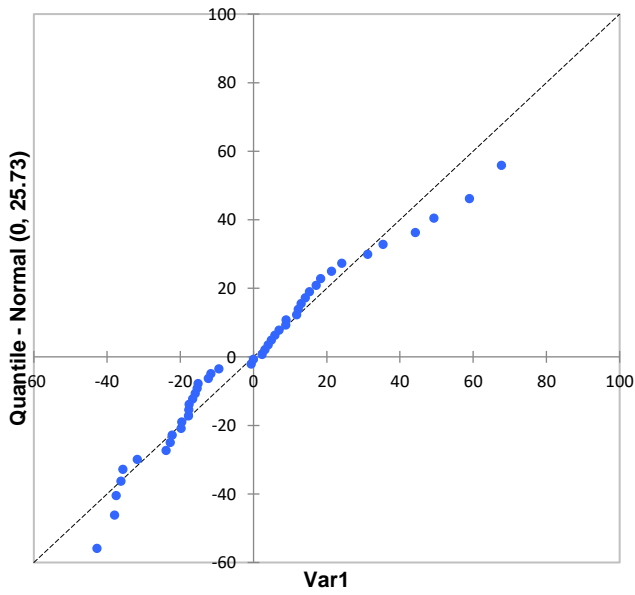
Pred(Meander Belt Width (m)) / Meander Belt Width (m)



Shapiro-Wilk test (Var1):

W	0.961
p-value (Two-tailed)	0.120
alpha	0.05

Q-Q plot (Var1)



Meander Belt Width vs. Total Stream Power

Goodness of fit statistics (Log Meander Belt Width (m)):

Observations	46.000
Sum of weights	46.000
DF	44.000
R ²	0.261
Adjusted R ²	0.244
MSE	0.026
RMSE	0.162
DW	1.956
Cp	2.000
AIC	-165.449

Analysis of variance (Log Meander Belt Width (m)):

Source	DF	Sum of squares	Mean squares	F	Pr > F
Model	1	0.409	0.409	15.555	0.000
Error	44	1.156	0.026		
Corrected Total	45	1.565			

Type I Sum of Squares analysis (Log Meander Belt Width (m)):

Source	DF	Sum of squares	Mean squares	F	Pr > F
Log Stream Power	1	0.409	0.409	15.555	0.000

Type III Sum of Squares analysis (Log Meander Belt Width (m)):

Source	DF	Sum of squares	Mean squares	F	Pr > F
Log Stream Power	1	0.409	0.409	15.555	0.000

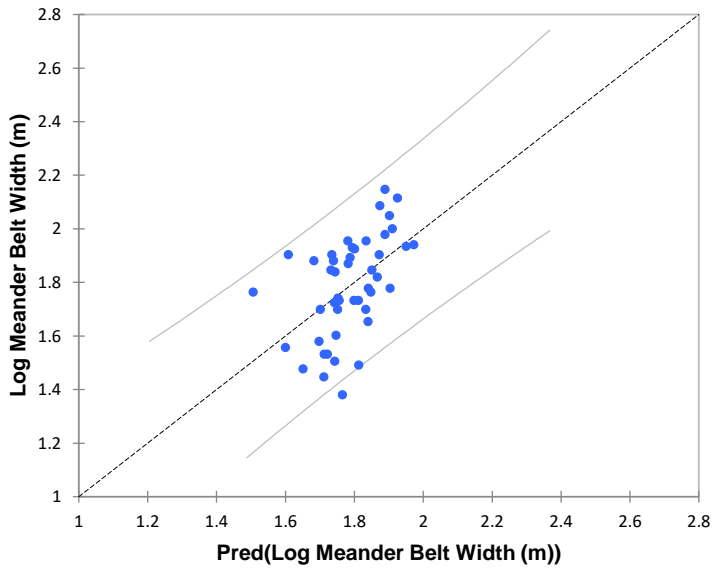
Model parameters (Log Meander Belt Width (m)):

Source	Value	Standard error	t	Pr > t	Lower bound (95%)	Upper bound (95%)
Intercept	1.414	0.097	14.509	0.0001	1.218	1.610
Log Stream Power	0.150	0.038	3.944	0.000	0.073	0.226

Standardized coefficients (Log Meander Belt Width (m)):

Source	Value	Standard error	t	Pr > t	Lower bound (95%)	Upper bound (95%)
Log Stream Power	0.511	0.130	3.944	0.000	0.250	0.772

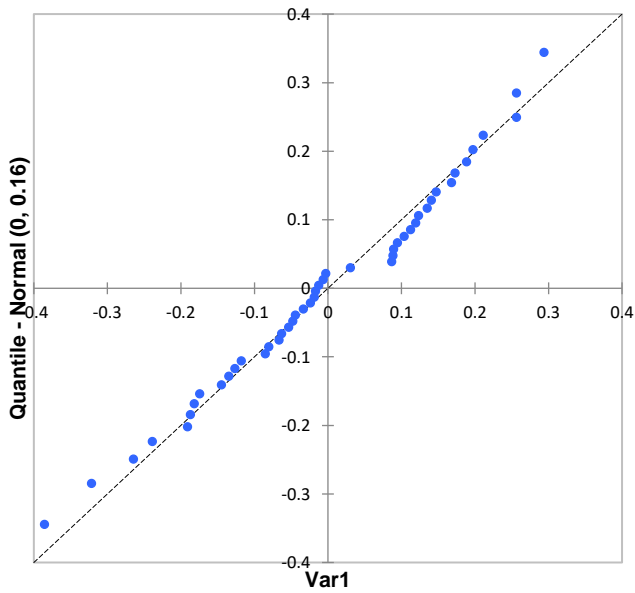
Pred(Log Meander Belt Width (m)) / Log Meander Belt Width (m)



Shapiro-Wilk test (Var1):

W	0.980
p-value (Two-tailed)	0.621
alpha	0.05

Q-Q plot (Var1)



Meander Belt Width vs. Drainage Area

Goodness of fit statistics (Log Meander Belt Width (m)):

Observations	46.000
Sum of weights	46.000
DF	44.000
R ²	0.667
Adjusted R ²	0.659
MSE	0.012
RMSE	0.109
DW	2.010
Cp	2.000
-	-
AIC	202.108

Analysis of variance Log Meander Belt Width (m):

Source	DF	Sum of squares	Mean squares	F	Pr > F
Model	1	1.044	1.044	88.135	< 0.0001
Error	44	0.521	0.012		
Corrected Total	45	1.565			

Type I Sum of Squares analysis (Log Meander Belt Width (m)):

Source	DF	Sum of squares	Mean squares	F	Pr > F
Log Drainage Area (km ²)	1	1.044	1.044	88.135	< 0.0001

Type III Sum of Squares analysis (Log Meander Belt Width (m)):

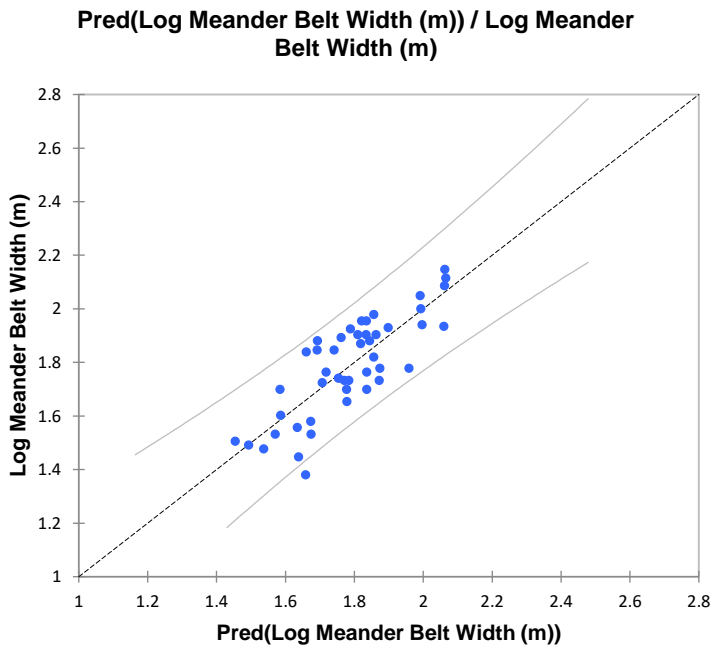
Source	DF	Sum of squares	Mean squares	F	Pr > F
Log Drainage Area (km ²)	1	1.044	1.044	88.135	< 0.0001

Model parameters (Log Meander Belt Width (m)):

Source	Value	Standard error	t	Pr > t	Lower bound (95%)	Upper bound (95%)
Intercept	1.471	0.037	39.448	< 0.0001	1.396	1.546
Log Drainage Area (km ²)	0.225	0.024	9.388	< 0.0001	0.177	0.273

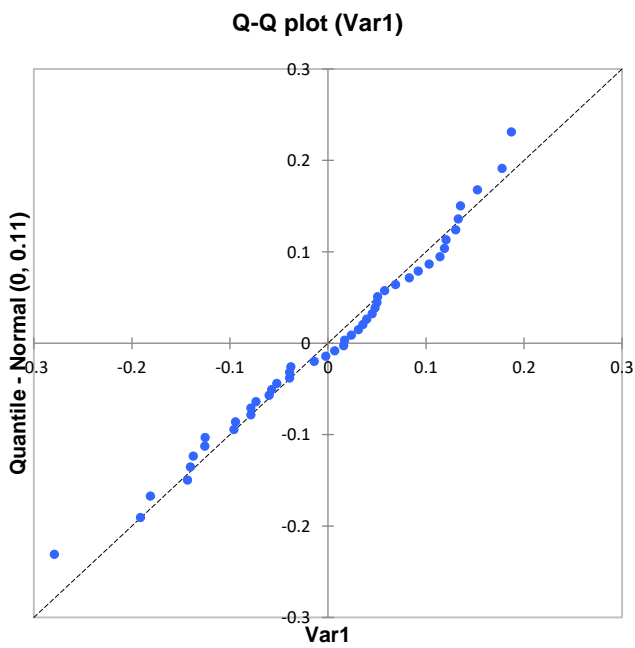
Standardized coefficients (Log Meander Belt Width (m)):

Source	Value	Standard error	t	Pr > t	Lower bound (95%)	Upper bound (95%)
Log Drainage Area (km ²)	0.817	0.087	9.388	< 0.0001	0.641	0.992



Shapiro-Wilk test (Var1):

W	0.978
p-value (Two-tailed)	0.530
alpha	0.05



Meander Belt Width vs. Drainage Area & Stream Power

Goodness of fit statistics (Meander Belt Width (m)):

Observations	46.000
Sum of weights	46.000
DF	44.000
R ²	0.561
Adjusted R ²	0.551
MSE	338.787
RMSE	18.406
DW	2.470
Cp	2.000
AIC	269.922

Analysis of variance (Meander Belt Width (m)):

Source	DF	Sum of squares	Mean squares	F	Pr > F
Model	1	19031.093	19031.093	56.174	< 0.0001
Error	44	14906.647	338.787		
Corrected Total	45	33937.739			

Type I Sum of Squares analysis (Meander Belt Width (m)):

Source	DF	Sum of squares	Mean squares	F	Pr > F
Log SP DA	1	19031.093	19031.093	56.174	< 0.0001

Type III Sum of Squares analysis (Meander Belt Width (m)):

Source	DF	Sum of squares	Mean squares	F	Pr > F
Log SP DA	1	19031.093	19031.093	56.174	< 0.0001

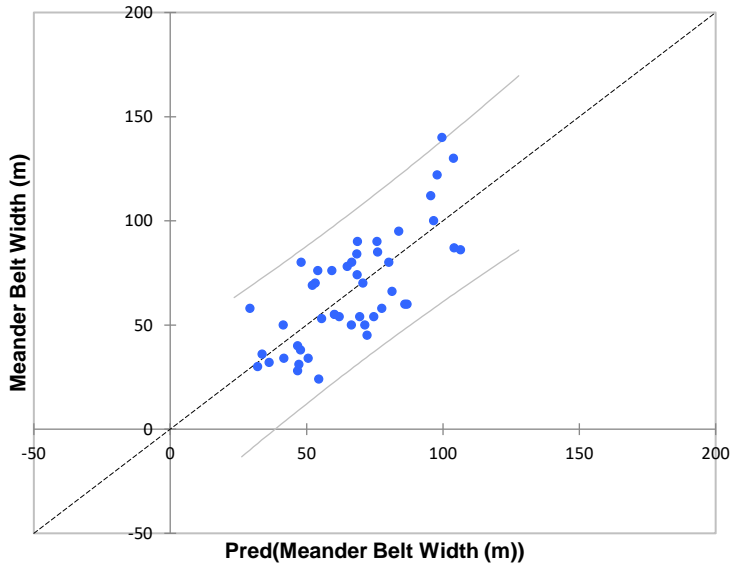
Model parameters (Meander Belt Width (m)):

Source	Value	Standard error	t	Pr > t	Lower bound (95%)	Upper bound (95%)
Intercept	-0.306	9.342	-0.033	0.974	-19.135	18.522
Log SP DA	17.223	2.298	7.495	< 0.0001	12.592	21.854

Standardized coefficients (Meander Belt Width (m)):

Source	Value	Standard error	t	Pr > t	Lower bound (95%)	Upper bound (95%)
Log SP DA	0.749	0.100	7.495	< 0.0001	0.547	0.950

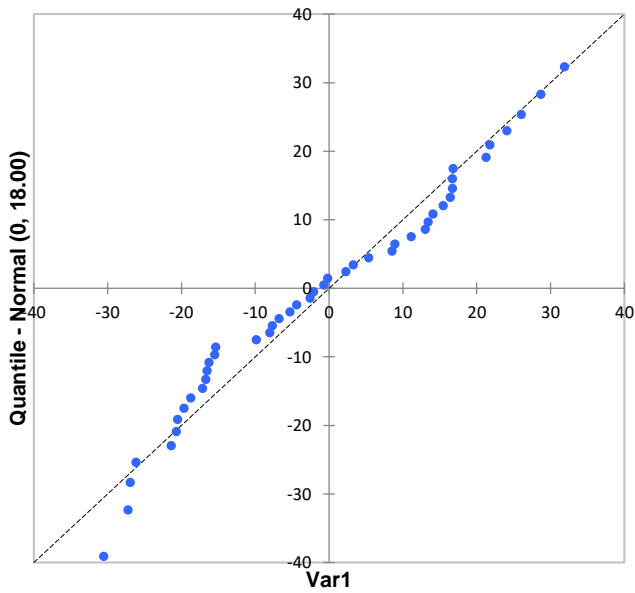
Pred(Meander Belt Width (m)) / Meander Belt Width (m)



Shapiro-Wilk test (Var1):

W	0.965
p-value (Two-tailed)	0.175
alpha	0.05

Q-Q plot (Var1)



Meander Belt Width vs. Discharge

Goodness of fit statistics (Meander Belt Width (m)):

Observations	46.000
Sum of weights	46.000
DF	44.000
R ²	0.650
Adjusted R ²	0.642
MSE	0.012
RMSE	0.111
DW	1.938
Cp	2.000
AIC	-199.869

Analysis of variance (Log Meander Belt Width (m)):

Source	DF	Sum of squares	Mean squares	F	Pr > F
Model	1	1.018	1.018	81.858	< 0.0001
Error	44	0.547	0.012		
Corrected Total	45	1.565			

Type I Sum of Squares analysis (Log Meander Belt Width (m)):

Source	DF	Sum of squares	Mean squares	F	Pr > F
Log Q2 (m3/s)	1	1.018	1.018	81.858	< 0.0001

Type III Sum of Squares analysis (Log Meander Belt Width (m)):

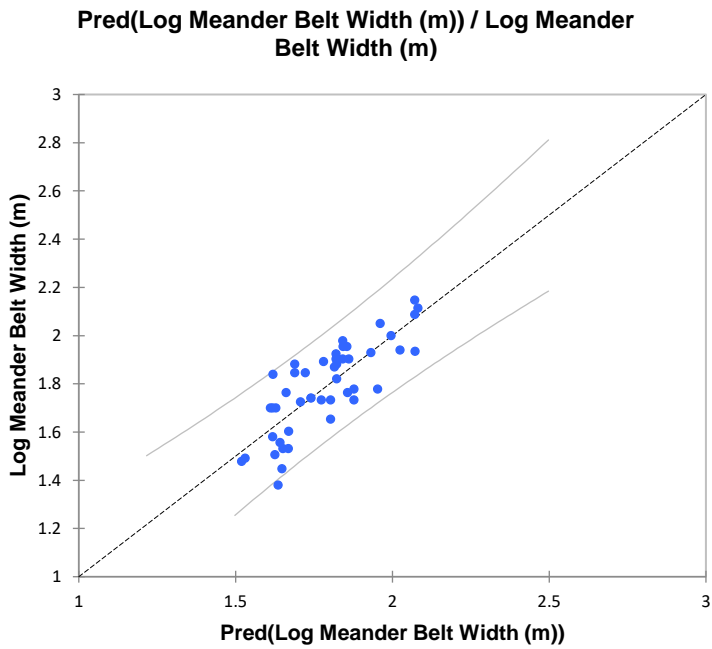
Source	DF	Sum of squares	Mean squares	F	Pr > F
Log Q2 (m3/s)	1	1.018	1.018	81.858	< 0.0001

Model parameters (Log Meander Belt Width (m)):

Source	Value	Standard error	t	Pr > t	Lower bound (95%)	Upper bound (95%)
Intercept	1.545	0.031	49.216	< 0.0001	1.482	1.608
Log Q2 (m3/s)	0.274	0.030	9.048	< 0.0001	0.213	0.335

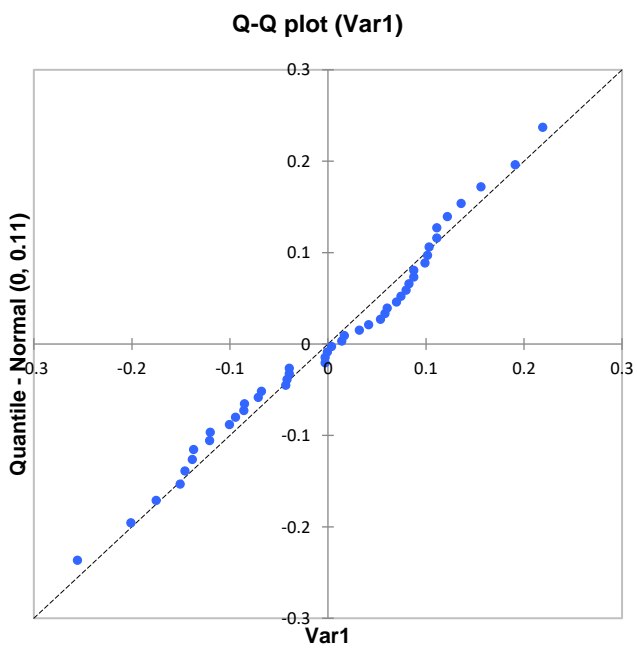
Standardized coefficients (Log Meander Belt Width (m)):

Source	Value	Standard error	t	Pr > t	Lower bound (95%)	Upper bound (95%)
Log Q2 (m3/s)	0.806	0.089	9.048	< 0.0001	0.627	0.986



Shapiro-Wilk test (Var1):

W	0.978
p-value (Two-tailed)	0.543
alpha	0.05



Drainage Area and Discharge

Goodness of fit statistics (Log Q2 (m3/s)):

Observations	46.000
Sum of weights	46.000
DF	44.000
R ²	0.868
Adjusted R ²	0.865
MSE	0.040
RMSE	0.201
DW	1.645
Cp	2.000
AIC	-145.557

Analysis of variance (Log Q2 (m3/s)):

Source	DF	Sum of squares	Mean squares	F	Pr > F
Model	1	11.762	11.762	290.524	< 0.0001
Error	44	1.781	0.040		
Corrected Total	45	13.544			

Type I Sum of Squares analysis (Log Q2 (m3/s)):

Source	DF	Sum of squares	Mean squares	F	Pr > F
Log CVC Drainage Area (km2)	1	11.762	11.762	290.524	< 0.0001

Type III Sum of Squares analysis (Log Q2 (m3/s)):

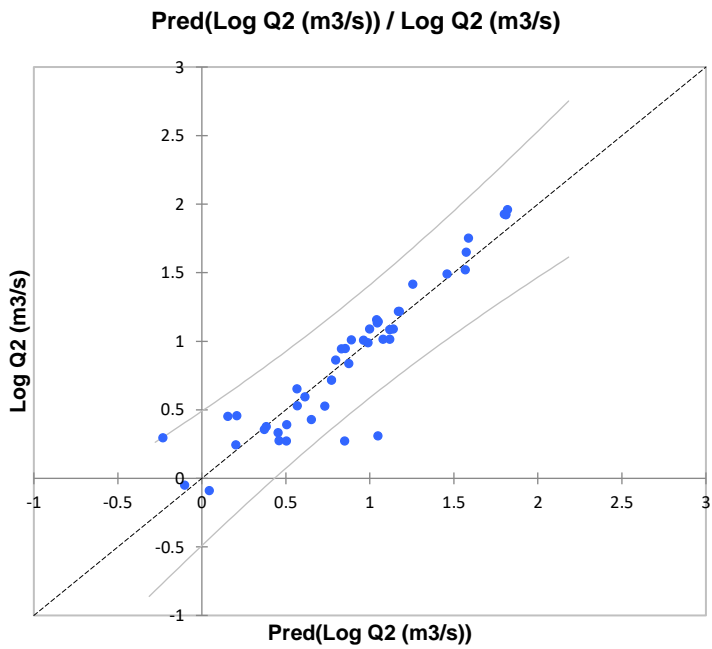
Source	DF	Sum of squares	Mean squares	F	Pr > F
Log CVC Drainage Area (km2)	1	11.762	11.762	290.524	< 0.0001

Model parameters (Log Q2 (m3/s)):

Source	Value	Standard error	t	Pr > t	Lower bound (95%)	Upper bound (95%)
Intercept	-0.178	0.069	-2.584	0.013	-0.317	-0.039
Log CVC Drainage Area (km2)	0.756	0.044	17.045	< 0.0001	0.666	0.845

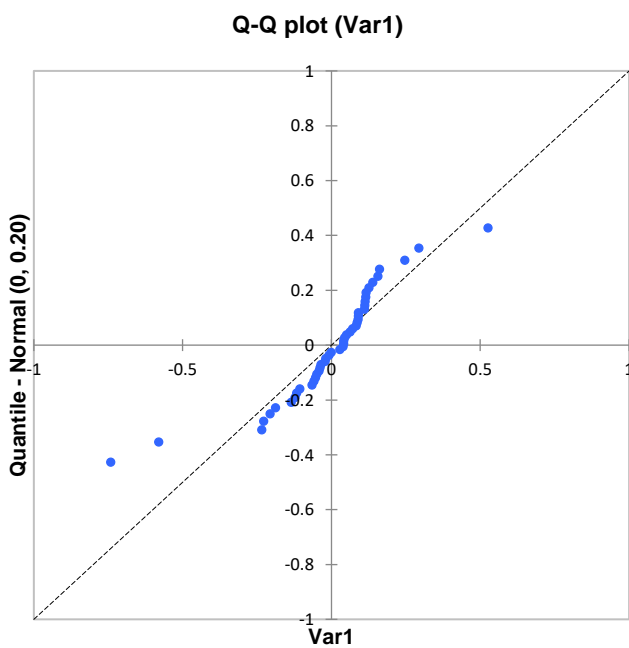
Standardized coefficients (Log Q2 (m3/s)):

Source	Value	Standard error	t	Pr > t	Lower bound (95%)	Upper bound (95%)
Log CVC Drainage Area (km2)	0.932	0.055	17.045	< 0.0001	0.822	1.042



Shapiro-Wilk test (Var1):

W	0.866
p-value (Two-tailed)	< 0.0001
alpha	0.05



Drainage Area and Mean Bankfull Channel Width

Goodness of fit statistics (Log Mean Bankfull Width (m)):

Observations	46.000
Sum of weights	46.000
DF	44.000
R ²	0.794
Adjusted R ²	0.790
MSE	0.019
RMSE	0.139
DW	2.048
Cp	2.000
AIC	-179.586

Analysis of variance (Log Mean Bankfull Width (m)):

Source	DF	Sum of squares	Mean squares	F	Pr > F
Model	1	3.281	3.281	169.789	< 0.0001
Error	44	0.850	0.019		
Corrected Total	45	4.131			

Type I Sum of Squares analysis (Log Mean Bankfull Width (m)):

Source	DF	Sum of squares	Mean squares	F	Pr > F
Log Drainage Area (km2)	1	3.281	3.281	169.789	< 0.0001

Type III Sum of Squares analysis (Log Mean Bankfull Width (m)):

Source	DF	Sum of squares	Mean squares	F	Pr > F
Log Drainage Area (km2)	1	3.281	3.281	169.789	< 0.0001

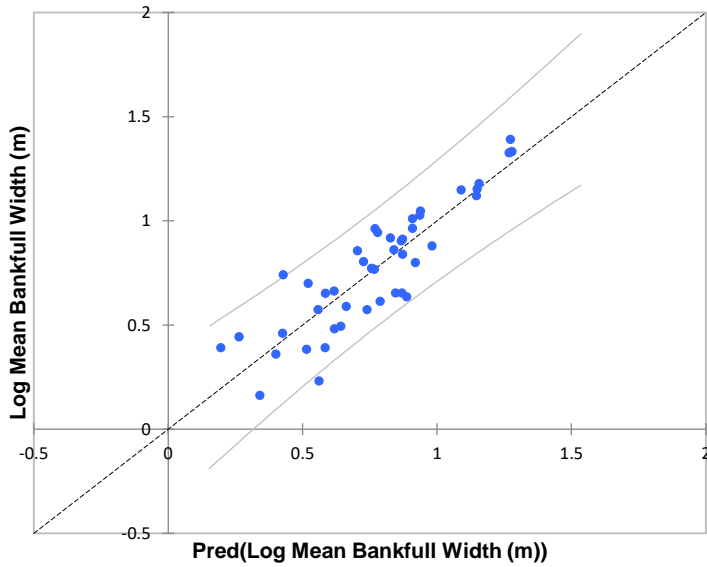
Model parameters (Log Mean Bankfull Width (m)):

Source	Value	Standard error	t	Pr > t	Lower bound (95%)	Upper bound (95%)
Intercept	0.224	0.048	4.701	< 0.0001	0.128	0.320
Log Drainage Area (km2)	0.399	0.031	13.030	< 0.0001	0.337	0.461

Standardized coefficients (Log Mean Bankfull Width (m)):

Source	Value	Standard error	t	Pr > t	Lower bound (95%)	Upper bound (95%)
Log Drainage Area (km2)	0.891	0.068	13.030	< 0.0001	0.753	1.029

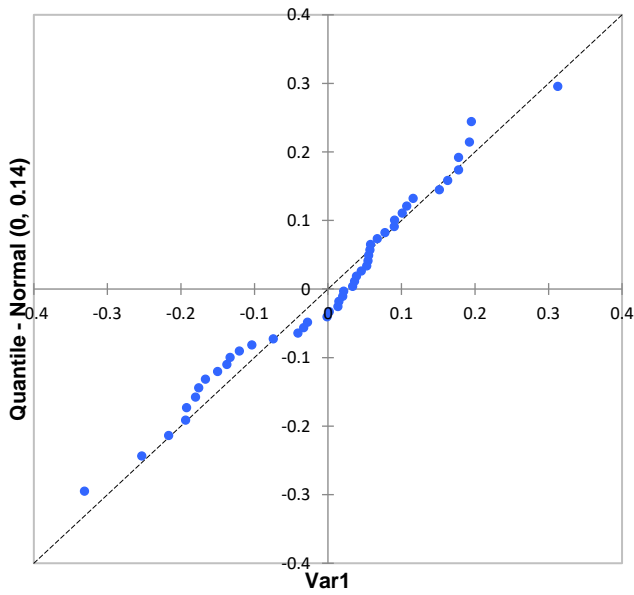
Pred(Log Mean Bankfull Width (m)) / Log Mean Bankfull Width (m)



Shapiro-Wilk test (Var1):

W	0.973
p-value (Two-tailed)	0.345
alpha	0.05

Q-Q plot (Var1)



Drainage Area and Amplitude:

Goodness of fit statistics (Log Amplitude (m)):

Observations	46.000
Sum of weights	46.000
DF	44.000
R ²	0.495
Adjusted R ²	0.484
RMSE	0.157
MAPE	7.863
DW	2.003
Cp	2.000
AIC	-168.096

Analysis of variance (Log Amplitude (m)):

Source	DF	Sum of squares	Mean squares	F	Pr > F
Model	1	1.070	1.070	43.134	< 0.0001
Error	44	1.091	0.025		
Corrected Total	45	2.161			

Type I Sum of Squares analysis (Log Amplitude (m)):

Source	DF	Sum of squares	Mean squares	F	Pr > F
Log Drainage Area (km2)	1	1.070	1.070	43.134	< 0.0001

Type III Sum of Squares analysis (Log Amplitude (m)):

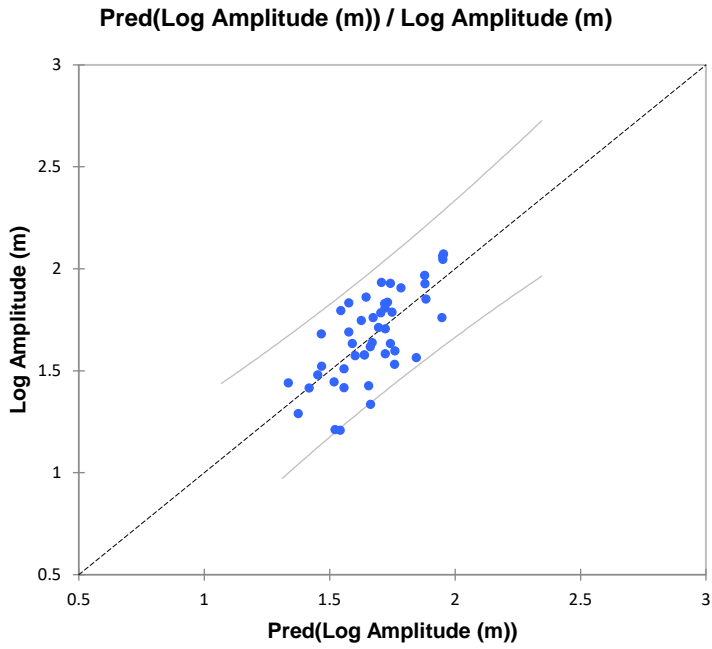
Source	DF	Sum of squares	Mean squares	F	Pr > F
Log Drainage Area (km2)	1	1.070	1.070	43.134	< 0.0001

Model parameters (Log Amplitude (m)):

Source	Value	Standard error	t	Pr > t	Lower bound (95%)	Upper bound (95%)
Intercept	1.352	0.054	25.055	< 0.0001	1.243	1.461
Log Drainage Area (km2)	0.228	0.035	6.568	< 0.0001	0.158	0.298

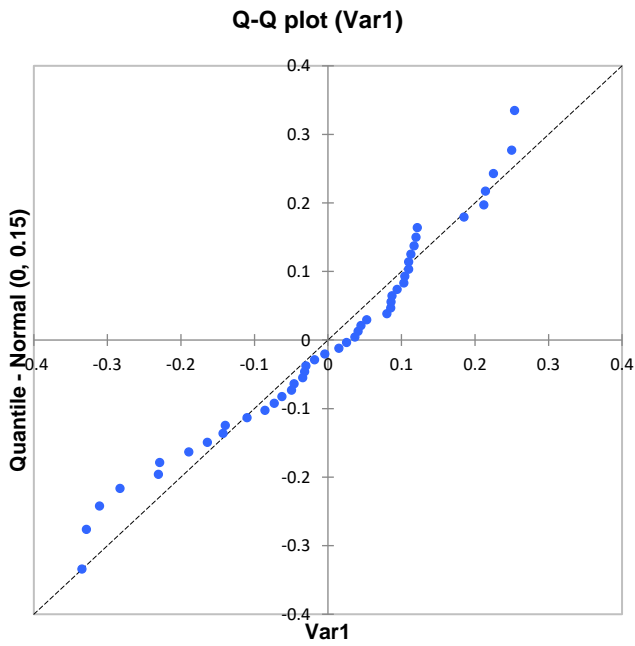
Standardized coefficients (Log Amplitude (m)):

Source	Value	Standard error	t	Pr > t	Lower bound (95%)	Upper bound (95%)
Log Drainage Area (km2)	0.704	0.107	6.568	< 0.0001	0.488	0.919



Shapiro-Wilk test (Var1):

W	0.954
p-value (Two-tailed)	0.069
alpha	0.05



Mean Bankfull Width and Amplitude

Goodness of fit statistics (Log Amplitude):

Observations	46.000
Sum of weights	46.000
DF	44.000
R ²	0.320
Adjusted R ²	0.305
MSE	0.033
RMSE	0.183
DW	1.780
Cp	2.000
AIC	-154.408

Analysis of variance (Log Amplitude):

Source	DF	Sum of squares	Mean squares	F	Pr > F
Model	1	0.692	0.692	20.708	< 0.0001
Error	44	1.470	0.033		
Corrected Total	45	2.161			

Type I Sum of Squares analysis (Log Amplitude):

Source	DF	Sum of squares	Mean squares	F	Pr > F
Log Mean Bankfull Width (m)	1	0.692	0.692	20.708	< 0.0001

Type III Sum of Squares analysis (Log Amplitude):

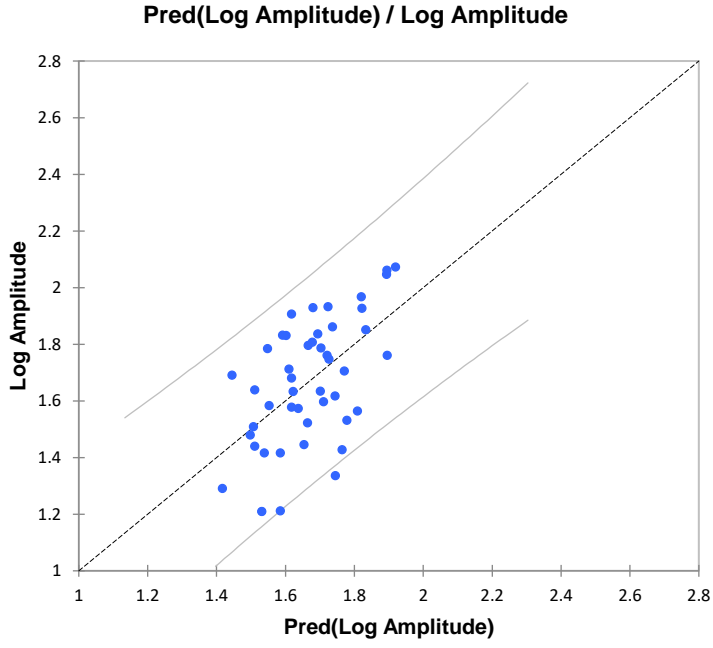
Source	DF	Sum of squares	Mean squares	F	Pr > F
Log Mean Bankfull Width (m)	1	0.692	0.692	20.708	< 0.0001

Model parameters (Log Amplitude):

Source	Value	Standard error	t	Pr > t	Lower bound (95%)	Upper bound (95%)
Intercept	1.351	0.075	17.900	< 0.0001	1.199	1.503
Log Mean Bankfull Width (m)	0.409	0.090	4.551	< 0.0001	0.228	0.590

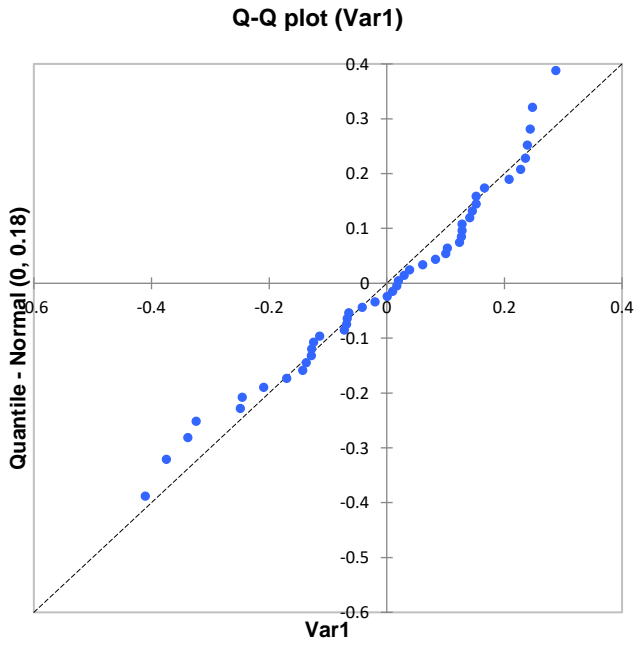
Standardized coefficients (Log Amplitude):

Source	Value	Standard error	t	Pr > t	Lower bound (95%)	Upper bound (95%)
Log Mean Bankfull Width (m)	0.566	0.124	4.551	< 0.0001	0.315	0.816



Shapiro-Wilk test (Var1):

W	0.960
p-value (Two-tailed)	0.111
alpha	0.05



Mean Bankfull Width & Discharge

Goodness of fit statistics (LOG Mean Bankfull Width (m)):

Observations	46.000
Sum of weights	46.000
DF	44.000
R ²	0.788
Adjusted R ²	0.783
MSE	0.020
RMSE	0.141
DW	1.705
Cp	2.000
AIC	-178.159

Analysis of variance (LOG Mean Bankfull Width (m)):

Source	DF	Sum of squares	Mean squares	F	Pr > F
Model	1	3.254	3.254	163.257	< 0.0001
Error	44	0.877	0.020		
Corrected Total	45	4.131			

Type I Sum of Squares analysis (LOG Mean Bankfull Width (m)):

Source	DF	Sum of squares	Mean squares	F	Pr > F
Log Q2 (m3/s)	1	3.254	3.254	163.257	< 0.0001

Type III Sum of Squares analysis (LOG Mean Bankfull Width (m)):

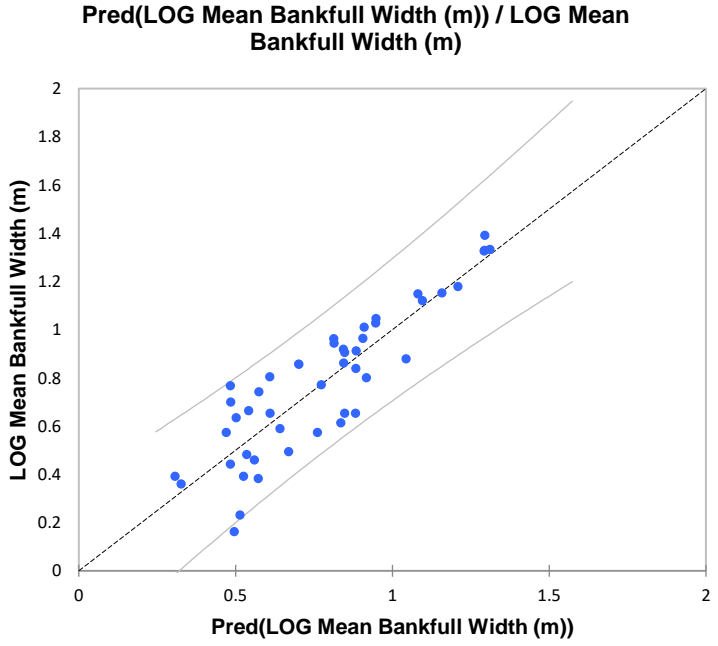
Source	DF	Sum of squares	Mean squares	F	Pr > F
Log Q2 (m3/s)	1	3.254	3.254	163.257	< 0.0001

Model parameters (LOG Mean Bankfull Width (m)):

Source	Value	Standard error	t	Pr > t	Lower bound (95%)	Upper bound (95%)
Intercept	0.351	0.040	8.844	< 0.0001	0.271	0.432
Log Q2 (m3/s)	0.490	0.038	12.777	< 0.0001	0.413	0.567

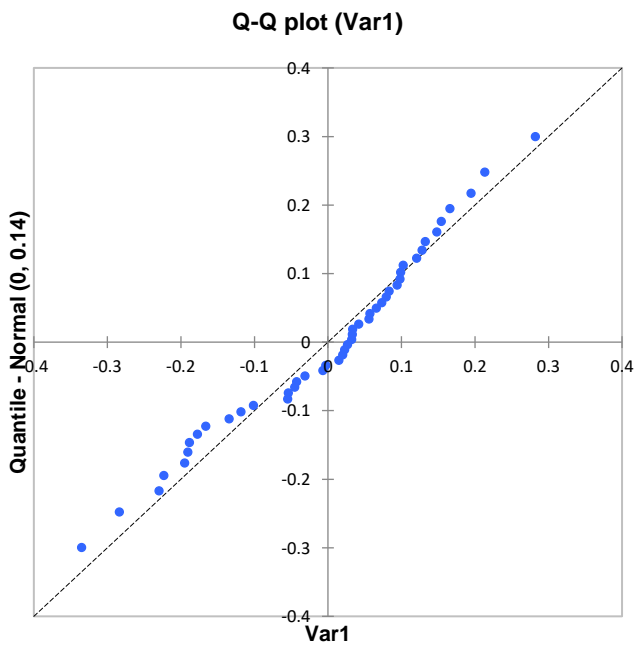
Standardized coefficients (LOG Mean Bankfull Width (m)):

Source	Value	Standard error	t	Pr > t	Lower bound (95%)	Upper bound (95%)
Log Q2 (m3/s)	0.888	0.069	12.777	< 0.0001	0.748	1.028



Shapiro-Wilk test (Var1):

W	0.967
p-value (Two-tailed)	0.207
alpha	0.05



Discharge and Meander Amplitude

Goodness of fit statistics (Log Amplitude (m)):

Observations	46.000
Sum of weights	46.000
DF	44.000
R ²	0.487
Adjusted R ²	0.475
MSE	0.025
RMSE	0.159
DW	2.011
Cp	2.000
AIC	-167.352

Analysis of variance (Log Amplitude (m)):

Source	DF	Sum of squares	Mean squares	F	Pr > F
Model	1	1.052	1.052	41.736	< 0.0001
Error	44	1.109	0.025		
Corrected Total	45	2.161			

Type I Sum of Squares analysis (Log Amplitude (m)):

Source	DF	Sum of squares	Mean squares	F	Pr > F
Log Q2 (m3/s)	1	1.052	1.052	41.736	< 0.0001

Type III Sum of Squares analysis (Log Amplitude (m)):

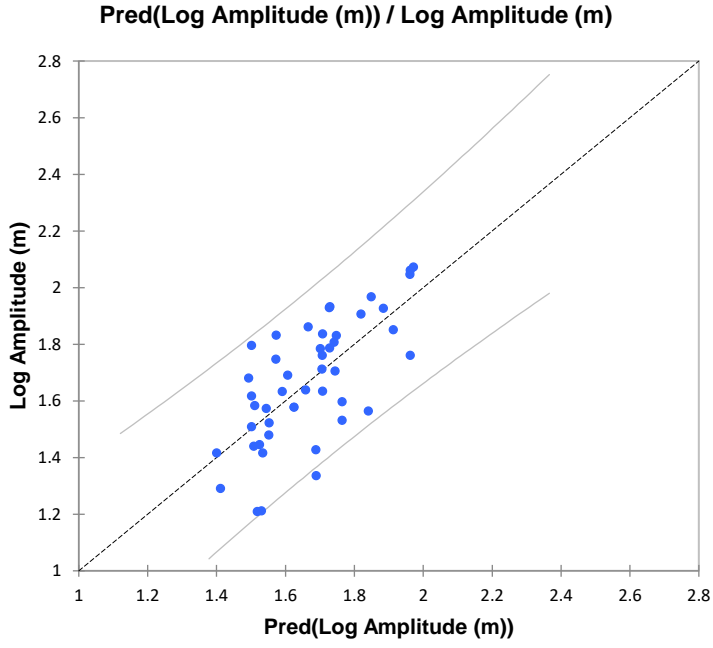
Source	DF	Sum of squares	Mean squares	F	Pr > F
Log Q2 (m3/s)	1	1.052	1.052	41.736	< 0.0001

Model parameters (Log Amplitude (m)):

Source	Value	Standard error	t	Pr > t	Lower bound (95%)	Upper bound (95%)
Intercept	1.426	0.045	31.903	< 0.0001	1.336	1.516
Log Q2 (m3/s)	0.279	0.043	6.460	< 0.0001	0.192	0.366

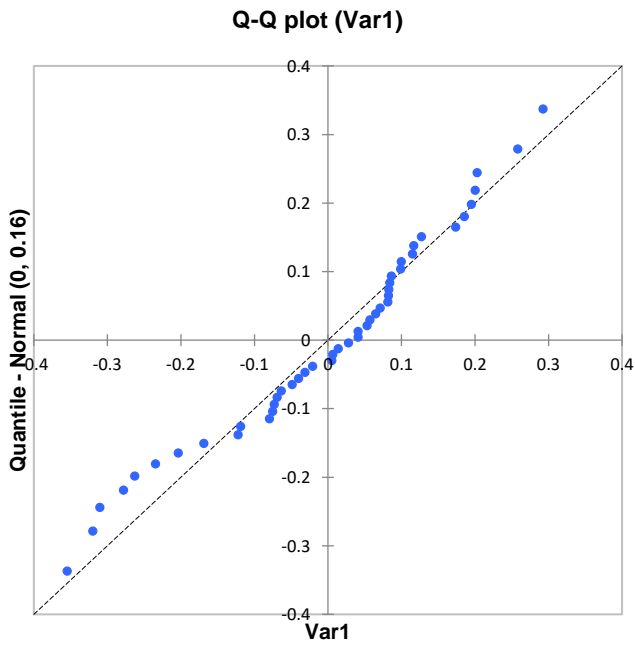
Standardized coefficients (Log Amplitude (m)):

Source	Value	Standard error	t	Pr > t	Lower bound (95%)	Upper bound (95%)
Log Q2 (m3/s)	0.698	0.108	6.460	< 0.0001	0.480	0.915



Shapiro-Wilk test (Var1):

W	0.961
p-value (Two-tailed)	0.121
alpha	0.05



Curriculum Vita

Name: Julia Howett

**Post-secondary
Education and
Degrees:** The University of Western Ontario
London, Ontario, Canada
2011-2015 B.Sc.

The University of Western Ontario
London, Ontario, Canada
2015-[2017] M.Sc.

**Honours and
Awards:** Edward G. Pleva Award for Excellence in Teaching
2016-2017

Edward G. Pleva Fellowship Award
2015-2016

Gold Medal for Highest Academic Achievement – B.Sc. Geography
2015

Certificate of Merit for Academic Excellence
2015

Dean's Honor List
2013-2014, 2014-2015

**Related Work
Experience:** Teaching Assistant
The University of Western Ontario
2015-2017

Publications:

Khan, I., **Howett, J.**, & Ashmore, P. (2016). Meander Belt Width Procedures: Developing a Regional Model for Southern Ontario. Oral presentation at Natural Channel Systems – 5th International Conference, Niagara Falls, Ontario, September 25, 2016.

Howett, J., Ashmore, P., & Khan, I. (2017). Developing a Model for Erodible Corridors in Southern Ontario. Poster presentation at TRIECA Conference, Brampton, Ontario, March 22-23, 2017.

Howett, J., Ashmore, P., & Khan, I. (2017). Meander Belt Width Procedures: Developing a Regional Model for Southern Ontario. Poster presentation at Canadian Geophysical Union Annual Meeting, Vancouver, British Columbia, May 30, 2017.